

# THE PHASES DIFFERENTIAL ASTROMETRY DATA ARCHIVE. I. MEASUREMENTS AND DESCRIPTION

MATTHEW W. MUTERSPAUGH<sup>1, 2</sup>, BENJAMIN F. LANE<sup>3</sup>, S. R. KULKARNI<sup>4</sup>, MACIEJ KONACKI<sup>5, 6</sup>, BERNARD F. BURKE<sup>7</sup>, M. M. COLAVITA<sup>8</sup>, M. SHAO<sup>8</sup>, SLOANE J. WIKTOROWICZ<sup>9</sup>, J. O'CONNELL<sup>1</sup>

*Draft version October 8, 2018*

## ABSTRACT

The Palomar High-precision Astrometric Search for Exoplanet Systems (PHASES) monitored 51 sub-arcsecond binary systems to determine precision binary orbits, study the geometries of triple and quadruple star systems, and discover previously unknown faint astrometric companions as small as giant planets. PHASES measurements made with the Palomar Testbed Interferometer (PTI) from 2002 until PTI ceased normal operations in late 2008 are presented. Infrared differential photometry of several PHASES targets were measured with Keck Adaptive Optics and are presented.

*Subject headings:* astrometry – binaries:close – binaries:visual – techniques:interferometric

## 1. INTRODUCTION

A technique has been developed to obtain high precision ( $35 \mu\text{as}$ ) astrometry of close stellar pairs (separation less than 1 arcsec; Lane and Mutterspaugh 2004) using long-baseline infrared interferometry at the Palomar Testbed Interferometer (PTI; Colavita et al. 1999). This technique was applied to 51 binary systems as the Palomar High-precision Astrometric Search for Exoplanet Systems (PHASES) program during 2002-2008. PHASES science results included precision binary orbits and component masses, studies of the geometries of and physical properties of stars in triple and quadruple star systems, and limits on the presence of giant planet companions to the binaries.

This paper is the first in a series analyzing the final results of the PHASES project as of its completion in late 2008. This paper describes the observing method, sources of measurement uncertainties, limits of observing precisions, derives empirical scaling rules to account for noise sources beyond those predicted by the standard reduction algorithms, and presents the full catalog of astrometric measurements from PHASES. The second paper combines PHASES astrometry, astrometric measurements made by other methods, and radial velocity observations (where available) to determine orbital solutions to several binaries' Keplerian motions, determining

physical properties such as component masses and system distance when possible (Mutterspaugh et al. 2010b). The third paper presents limits on the existence of substellar tertiary companions orbiting either the primary or secondary stars in those systems that are found to be consistent with being simple binaries (Mutterspaugh et al. 2010c). Paper four presents orbital solutions to a known triple star system (63 Gem A = HD 58728) and a newly discovered triple system (HR 2896 = HD 60318) (Mutterspaugh et al. 2010a). Finally, paper five presents candidate substellar companions to PHASES binaries as detected by astrometry (Mutterspaugh et al. 2010d).

Astrometric measurements were made at PTI, which was located on Palomar Mountain near San Diego, CA. It was developed by the Jet Propulsion Laboratory, California Institute of Technology for NASA, as a testbed for interferometric techniques applicable to the Keck Interferometer and other missions such as the Space Interferometry Mission (SIM). It operated in the J ( $1.2\mu\text{m}$ ), H ( $1.6\mu\text{m}$ ), and K ( $2.2\mu\text{m}$ ) bands, and combined starlight from two out of three available 40-cm apertures. The apertures formed a triangle with one 110 and two 87 meter baselines. PHASES observations began in 2002 and continued through 2008 November when PTI ceased routine operations.

## 2. OBSERVATIONS AND DATA PROCESSING

The initial PHASES observing method and data processing algorithm were presented by Lane and Mutterspaugh (2004). Incremental improvements to these procedures were updated in papers from the PHASES science program. The final observing procedure and data processing algorithm is presented in complete form here. All astrometry measurements were reprocessed using the final algorithm presented here. Measurements taken with different instrumental configurations than the standard one presented here (for example, those lacking longitudinal dispersion compensation) are noted in Table 5.

### 2.1. Astrometric Observation Method

#### 2.1.1. Optical Interferometers

In an optical interferometer, light is collected at two or more apertures and brought to a central location where

matthew1@coe.tsuniv.edu, blane@draper.com, maciej@ncac.torun.pl

<sup>1</sup> Department of Mathematics and Physics, College of Arts and Sciences, Tennessee State University, Boswell Science Hall, Nashville, TN 37209

<sup>2</sup> Center of Excellence in Information Systems, Tennessee State University, 3500 John A. Merritt Boulevard, Box No. 9501, Nashville, TN 37209-1561

<sup>3</sup> Draper Laboratory, 555 Technology Square, Cambridge, MA 02139-3563

<sup>4</sup> Division of Physics, Mathematics and Astronomy, 105-24, California Institute of Technology, Pasadena, CA 91125

<sup>5</sup> Nicolaus Copernicus Astronomical Center, Polish Academy of Sciences, Rabianska 8, 87-100 Torun, Poland

<sup>6</sup> Astronomical Observatory, Adam Mickiewicz University, ul. Śloneczna 36, 60-286 Poznań, Poland

<sup>7</sup> MIT Kavli Institute for Astrophysics and Space Research, MIT Department of Physics, 70 Vassar Street, Cambridge, MA 02139

<sup>8</sup> Jet Propulsion Laboratory, California Institute of Technology, 4800 Oak Grove Drive, Pasadena, CA 91109

<sup>9</sup> Department of Astronomy, University of California, Mail Code 3411, Berkeley, CA 94720, USA

the beams are combined and a fringe pattern produced on a detector (at PTI, the detectors were NICMOS and HAWAII infrared arrays, of which only a few pixels were used). For a broadband source of central wavelength  $\lambda$  and optical bandwidth  $\Delta\lambda$  (for PTI  $\Delta\lambda = 0.4\mu\text{m}$ ), the fringe pattern is limited in extent and appears only when the optical paths through the arms of the interferometer are equalized to within a coherence length ( $\Lambda = \lambda^2/\Delta\lambda$ ). For a two-aperture interferometer, neglecting dispersion, the intensity measured at one of the combined beams is given by

$$I(x) = I_0 \left( 1 + V \frac{\sin(\pi x/\Lambda)}{\pi x/\Lambda} \sin(2\pi x/\lambda) \right) \quad (1)$$

where  $V$  is the fringe contrast or “visibility”, which can be related to the morphology of the source, and  $x$  is the optical path difference between arms of the interferometer. More detailed analysis of the operation of optical interferometers can be found in *Principles of Long Baseline Stellar Interferometry* (Lawson 2000).

### 2.1.2. Interferometric Astrometry

The location of the resulting interference fringes is related to the position of the target star and the observing geometry via

$$d = \vec{B} \cdot \vec{S} + \delta_a(\vec{S}, t) + c \quad (2)$$

where  $d$  is the optical path length one must introduce between the two arms of the interferometer to find fringes. This quantity is often called the “delay.”  $\vec{B}$  is the baseline—the vector connecting the two apertures.  $\vec{S}$  is the unit vector in the source direction, and  $c$  is a constant additional scalar delay introduced by the instrument. The term  $\delta_a(\vec{S}, t)$  is related to the differential amount of path introduced by the atmosphere over each telescope due to variations in refractive index. For a 100-m baseline interferometer an astrometric precision of 10  $\mu\text{as}$  corresponds to knowing  $d$  to 5 nm; while difficult, this is achievable for all terms except that related to the atmospheric delay. Atmospheric turbulence, which changes over distances of tens of centimeters and on millisecond timescales, forces one to use very short exposures (to maintain fringe contrast) and limits the sensitivity of the instrument. It also severely limits the astrometric accuracy of a simple interferometer, at least over large sky-angles.

However, in narrow-angle astrometry one is concerned with a close pair of stars, and the observable is a differential astrometric measurement, i.e. one is interested in knowing the angle between the two stars ( $\vec{\Delta}_s = \vec{s}_2 - \vec{s}_1$ ). The atmospheric turbulence is correlated over small angles. If the measurements of the two stars are simultaneous, or nearly so, the atmospheric term cancels out. Hence, it is still possible to obtain high precision “narrow-angle” astrometry.

### 2.1.3. Sub-Arcsecond Differential Astrometry

As illustrated in Figure 1, the light path of the PHASES astrometry program was as follows:

- Light was collected by two of the three siderostats at PTI. The siderostats had diameter 50 cm and

fed 40 cm beam compressing telescopes. These collimated the 40 cm input into a 7.5 cm beam.

- At the siderostat enclosure, a fast steering mirror (FSM) provided tip-tilt correction for low-order adaptive optics improvement. The feedback sensor for the tip-tilt system was located in the beam combining facility (see step (9)), to include both atmospheric and instrumental sources of tip-tilt variations.
- The collimated beams propagated through pipes to the central beam combining building. For the north and south siderostats, the pipes were held at vacuum; for the west siderostat, the pipe was filled with air.
- Each collimated beam was directed to a long delay line (DL) which tracks the sidereal delay rate and receives feedback from the fringe tracking beam combiner for removing some of the atmospheric turbulent delay variations. There were roughly  $\pm 38$  m of optical delay available in the long DLs.
- The collimated beams were recompressed to 2.5 cm collimated beams.
- Each beam passed through a pair of matched prisms. In one arm, one prism was on a linear stage to vary the total glass thickness the starlight passed through. The positions of these prisms were calibrated using fringes from an internal light source to minimize the combined longitudinal dispersion of air path and glass. This calibration also determined the glass-to-air dispersion correction rate. The linear stage was operated in open-loop mode to minimize longitudinal dispersion even as the air path was varied by the long DLs. Some early measurements were made before this dispersion compensator was available, as marked in Table 5.
- The 2.5 cm collimated beams were split  $\sim 70/30$  by plate beam splitters. The reflected  $\sim 30\%$  of the light was directed to the “secondary” beam combiner which made the astrometric science measurement. Red He-Ne LASER metrology signals were injected at these beam splitters and propagated through both beam combiners before being extracted just before the infrared array detectors to monitor path variations.
- The  $\sim 70\%$  transmitted light from each beam was directed through a short DL. These were smaller versions of the long DLs with a few ten’s of centimeters of travel. The short DLs allowed one to set the delay offset between the fringe-tracking and the science beam combiners such that both are near zero optical delay simultaneously. It also introduced the 50-100 Hz sawtooth modulation required for sampling fringes in the fringe tracker, without being in the science camera’s optical path.
- After the short DL, the  $\sim 70\%$  of the original light to be used for fringe tracking was directed to the “primary” beam combiner. I-band light was extracted using a dichroic beamsplitter and focused

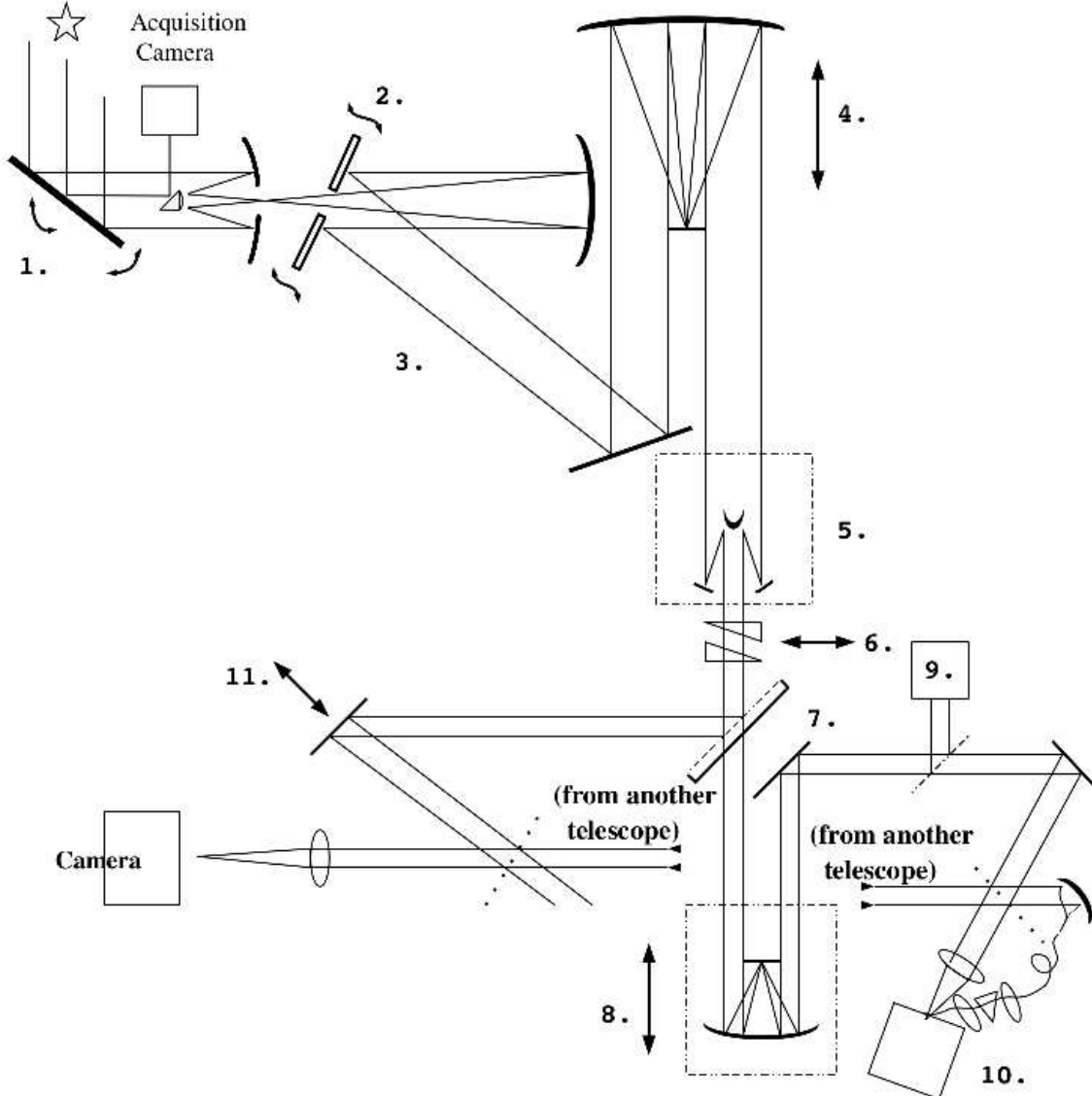


**Figure 1.** Configuration and light path used at PTI for the PHASES experiment is shown in schematic form; the corresponding description is described in Section 2.1.3. Note that the path for only one telescope is shown; light from the second telescope travels a similar path.

- onto quad-cell APD's. The signal was used as feed-back to the fast tip-tilt mirrors in step 2.
10. The longer-wavelength light was combined using a plate beam splitter. Half the light was focused on a single pixel of the NICMOS infrared array for high-signal-to-noise ratio (S/N) phase tracking. The other half passed through a single-mode fiber to improve wavefront quality (and system visibility), then through a low-resolution prism to disperse the light onto  $\sim 5$  pixels for slower group-delay tracking. Phase and group-delay signals were fed to the long DLs to reduce jitter from atmospheric piston motions. This beam combiner was the same as used for PTI's standard visibility mode observations.
  11. The  $\sim 30\%$  of the light redirected to the "secondary" table was used for the astrometric science measurement. The secondary beam combiner was identical to the first with the following exceptions.

- (a) A piezo-driven scanning mirror added up to  $\pm 300 \mu\text{m}$  of optical delay to allow scanning within the arcsecond field of view. The scan was close-loop controlled using the LASER metrology signal.
- (b) No single-mode fiber was used for spatial filtering.
- (c) A HAWAII array was used instead of NICMOS.

The entire optical system was realigned at the beginning of the night and usually updated in the middle of the night, once per night. Alignment drifts from one night to the next were small. Standard detector calibrations (gain, bias and background) were acquired at the beginning of the night for both infrared array detectors; background levels were re-measured with each star acquisition.

The operating sequence began by acquiring the stars and locking star trackers for tip-tilt corrections on both

telescopes. The 50-100 Hz fringe-tracking modulation was applied to the long DLs, which were moved until fringes were found with the “primary” beam combiner. Once fringe lock was made, the long and short DLs were moved simultaneously to maintain primary fringes until fringes were detected on the “secondary” beam combiner. Once fringes were found simultaneously on both beam combiners, (1) the zero-point offset for the short DLs was recorded, (2) the 50-100 Hz fringe tracking modulation was moved from the long to short DLs so that only the “primary” beam combiner was affected by the modulation, (3) the “secondary” detector’s read-out pattern was adjusted from one optimized for fringe tracking to a faster and more evenly spaced one that was better for scanning between fringe packets, and (4) the scanning mirror in the “secondary” beam combiner initiated its  $\sim$ Hz,  $\sim 100 \mu\text{m}$  triangle modulation. The speed and amplitude of the triangle pattern were user-settable according to the predicted projected binary separation. Conservative values were used with larger amplitudes than predicted to ensure good coverage of the fringe packets. Observing a binary when its baseline projected separation ( $\overrightarrow{B} \cdot \Delta \overrightarrow{S}$ ) was of order the interferometric coherence length ( $\Lambda = \lambda^2 / \Delta \lambda \approx 20 \mu\text{m}$ ) or less was avoided due to potential biases associated with an imperfect template fringe packet.

This setup resulted in a special astrometry mode designed to work on pairs of stars separated by no more than  $\sim 1$  arcsec, the diffraction limit of the 40 cm apertures at  $\lambda = 2.2 \mu\text{m}$ . In this mode, the small separation of the binary resulted in both binary components being in the field of view of a single interferometric beam combiner. The fringe positions were measured by modulating the instrumental delay with an amplitude large enough to record both fringe packets. This eliminated the need for a complex internal metrology system to measure the entire optical path of the interferometer, and dramatically reduced the effect of systematic error sources such as uncertainty in the baseline vector (error sources which scale with the binary separation). The same instrumental configuration could be used for double Fourier spectroscopy.

However, since the fringe position measurement of the two stars was no longer truly simultaneous it was possible for the atmosphere to introduce path-length changes (and hence positional error) in the time between measurements of the separate fringes. To reduce this effect a fraction of the incoming starlight was redirected to a separate beam-combiner, as described above. This beam-combiner was used in a “fringe-tracking” mode (Shao and Staelin 1980; Colavita et al. 1999) where it rapidly (10-20 ms) measured the phase of one of the starlight fringes and adjusted the internal delay to keep that phase constant. The fringe tracking data were used both in real-time (operating in a feed-back servo, after which a small—but measurable—residual phase error remained) and in post-processing (the measured residual error was applied to the data as a feed-forward servo). This technique—known as phase referencing—had the effect of stabilizing the fringe measured by the astrometric beam-combiner. For this observing mode, LASER metrology was only required between the two beam combiners through the location of the light split (which

occurred after the optical delay has been introduced), rather than throughout the entire array. This greatly reduced system complexity and increased the percentage of time on-sky. Extra efforts in system reliability and automation allowed most PHASES measurements to be acquired by a single night assistant with high (> 90%, not counting weather) on-sky efficiency.

In making an astrometric measurement the optical delay was modulated in a triangle-wave pattern around the stabilized fringe position, while measuring the intensity of the combined starlight beams. The range of the delay sweep was set to include both fringe packets; typically this required a scan amplitude on the order of  $150 \mu\text{m}$ . Typically one such “scan” was obtained every second, consisting of up to 1000 intensity samples (the scan rate was limited by the source brightness and the requirement that > 2 samples are made per fringe modulation period). A double fringe packet based on Equation 1 was then fit to the data, and the differential optical path between fringe packets was measured.

## 2.2. Astrometric Data Reduction Algorithm

The intensity versus delay position measurements produced by the interferometer were processed into astrometric measurements as follows.

1. Detector calibrations (gain, bias, and background) were applied to the intensity measurements.
2. The residual phase errors from the primary fringe tracker were converted to delay and applied to the data. Note that while the intensity measurements were spaced regularly in time, and the delay scanned linearly in time, the variable amount of delay correction applied from the fringe tracker resulted in the intensity measurements being unevenly spaced in delay. This somewhat complicated the downstream processing, in that FFT-based algorithms could not be used.
3. The data were broken up into “scans” either when the delay sweep changed direction or when the fringe tracker lost lock. Only scans for which at least 90% of the scan was continuously recorded (without fringe lock loss) were used in processing.
4. For each scan, a power spectrum was calculated using a Lomb-Scargle algorithm (Scargle 1982; Press et al. 1992). This spectrum provided an S/N estimate based on the ratio of the power in and out of the instrument bandpass. Only the scans with an S/N greater than unity were kept.
5. For a range of values of differential optical delays between fringe packets, a model of a double-fringe packet was calculated and compared to the observed scan to derive a  $\chi^2$  value versus differential delay.
6. A two-dimensional grid in differential R.A. and decl. over which to search was constructed (in ICRS 2000.0 coordinates). For each point in the search grid the expected differential delay was calculated based on the interferometer location, baseline geometry, and time of observation for each scan.

These conversions were simplified using the routines from the Naval Observatory Vector Astrometry Subroutines C Language Version 2.0 (NOVAS-C; see Kaplan et al. (1989)). The value of  $\chi^2$  for the grid point's differential delay as determined by the previous step was co-added to an R.A./decl.  $\chi^2$  grid.

7. After co-adding the R.A./decl  $\chi^2$  over all the scans in one night, all resulting values of  $\chi^2$  within  $4\sigma$  of the minimum point were used to fit a two-dimensional quadratic function to interpolate the location of the best minimum  $\chi^2$  value as the final astrometric solution, and the widths of the quadratics determined the formal uncertainties as discussed in detail below. The final product was a measurement of the apparent vector between the stars and associated uncertainty ellipse. Because the data were obtained with a single-baseline instrument, the resulting error contours are very elliptical, with aspect ratios at times  $\geq 10$ .

Sample illustrations of several of these stages are plotted in Figure 2.

In previous data reductions, the scans were optionally digitally bandpass filtered before being processed for astrometry. This resulted in astrometric measurements that differed from those derived without filtering by much less than the measurement uncertainties. In this final analysis, the scans were not bandpass filtered.

### 2.2.1. Probability Distribution Function Sidelobes

One potential complication with fitting a fringe to the data was that there were many local minima spaced at multiples of the operating wavelength. If one were to fit a fringe model to each scan separately and average (or fit an astrometric model to) the resulting delays, one would be severely limited by this fringe ambiguity (for a 110-m baseline interferometer operating at  $2.2\mu\text{m}$ , the resulting positional ambiguity is  $\sim 4.1$  mas). However, by using the  $\chi^2$ -surface approach, and co-adding the probabilities associated with all possible delays for each scan, the ambiguity disappeared. This was due to two things, the first being that co-adding simply improved the S/N. Second, since the observations usually lasted for an hour or even longer, the associated baseline change due to Earth rotation also had the effect of “smearing” out all but the true global minimum. The final  $\chi^2$ -surfaces did have dips separated by  $\sim 4.1$  mas from the true location, but any data sets for which these showed up at the  $4\sigma$  level were rejected. The  $4\sigma$  region is that for which the properly normalized  $\chi^2$  function has a value less than the number of degrees of freedom plus 19.33, the latter being the value appropriate for two-dimensional  $\chi^2$  distributions. The final astrometry measurement and related uncertainties were derived by fitting only the  $4\sigma$  region of the surface.

### 2.2.2. Residual Unmonitored Phase Noise

Unmonitored system phase noise can affect the  $\chi^2$  surface in two ways. First, components of the phase noise that operated at frequencies faster than the scan rate caused the two fringe packets to be smeared an extra amount, and to first order this appeared as extra noise in the intensity measurements. This affected the width

of the  $\chi^2$  fit for each individual scan (which is designated as  $\sigma_m$ , the “measurement” noise), and thus appeared directly in the co-added  $\chi^2$  contour.

If instead the instrumental noise was much slower than an individual scan, it was essentially “frozen into” the scan—for the duration of that scan, the stars really did appear to have a different separation than their true separation. The  $\chi^2$  surface for the fit to an individual scan takes the form

$$f(d - d_j) = \frac{(d - d_j)^2}{\sigma_m^2} + n \quad (3)$$

where  $d_j$  is the value of the star separation that minimizes  $f = \chi^2$ , and  $n$  is the number of degrees of freedom of the fit (typical values for  $n$  are 400–1000; for this derivation, it suffices to assume a one-dimensional  $\chi^2$  surface as it has no curvature in the direction perpendicular to the sky-projected baseline—only Earth-rotation synthesis lifts this degeneracy). The low-frequency components of the phase noise cause  $d_j$  to vary from  $d_o$ , the true star separation, by more than one expects from measurement noise alone. By taking many such scans, one can determine this instrumental scatter (which is designated as  $\sigma_i$ , the “instrument” noise for an individual scan) and add (in quadrature) the instrumental noise to the measurement noise as

$$F(d - d_o) = \frac{(d - d_o)^2}{(\sigma_m^2 + \sigma_i^2)/N} + nN \quad (4)$$

where  $N$  is the number of scans ( $N$  was typically hundreds to thousands).

Consider a function  $f(d - d_{o_j})$  with position of the minimum at  $d_{o_j}$ ; this centroid position is distributed with probability

$$P(d_{o_j}) = \frac{e^{-(d_o - d_{o_j})^2/2\sigma_i^2}}{\sqrt{2\pi}\sigma_i}. \quad (5)$$

One may naively hope that summing several instances of this function with variable  $d_{o_j}$  together would properly add the instrumental and measurement noises in quadrature. However, the summation results in

$$\sum_{j=0}^N f(d - d_{o_j}) = N \int_{-\infty}^{\infty} f(d - x) P(x) dx \quad (6)$$

$$= \frac{(d - d_o)^2}{(\sigma_m^2)/N} + nN + N \frac{\sigma_i^2}{\sigma_m^2} \quad (7)$$

$$\neq \frac{(d - d_o)^2}{(\sigma_m^2 + \sigma_i^2)/N} + nN. \quad (8)$$

Even if one renormalizes so that the additive term equals  $nN$  (i.e. multiply by  $n/(n + \sigma_i^2/\sigma_m^2)$ ), this is still:

$$\sum_{j=0}^N f(d - d_{o_j}) = \frac{(d - d_o)^2}{(\sigma_m^2 + \sigma_i^2/n)/N} + nN. \quad (9)$$

Note the extra factor of  $n$  dividing  $\sigma_i^2$ ; this effectively underestimates the scan-to-scan instrumental noise by a very large amount—roughly  $20\times$  for typical PHASES data.

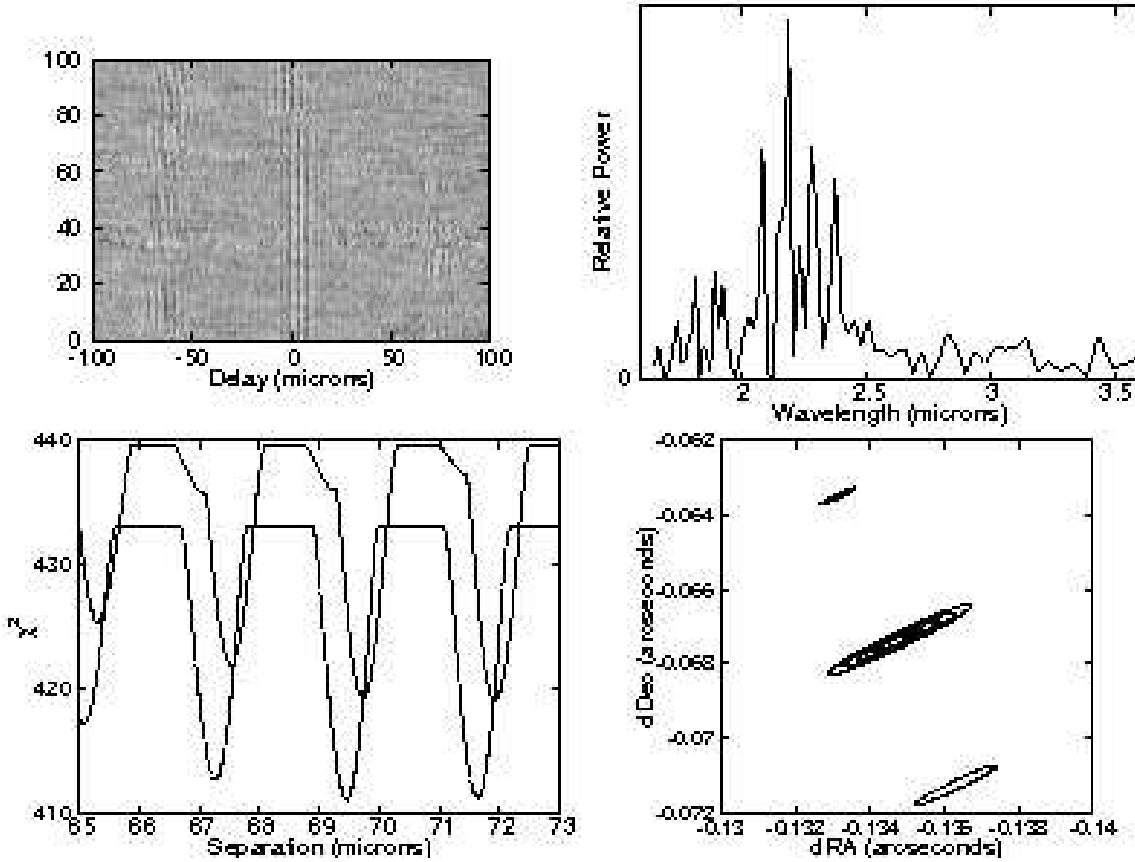


**Figure 2.** Several steps of the data processing pipeline are shown for an observation of HD 13872 (21 Ari) from MJD 54385.33270. Upper left: raw interferograms show two distinct fringe packets, one from each star in the over-resolved binary. One star was found near zero delay, the other at  $\sim 70 \mu\text{m}$ . The flipping from side-to-side was a result of the fringe tracker first tracking on one star for some scans, then the other. Upper right: the periodogram of one scan, used to evaluate the fringe S/N within the optical passband used (K-band, 2.0–2.4  $\mu\text{m}$ ). The power in the passband is not flat, but rather oscillates, a result of the object being a binary star (visibility changes with wavelength). Lower left: the likelihood metric  $\chi^2$  as a function of delay separation of the binaries, for two scans. Note there are multiple minima separated by the fringe modulation period, and the noise is large enough to prevent high confidence identification of the correct local minimum. Lower right: The coadded  $\chi^2$  surface in differential R.A./decl., with contours corresponding to 1-, 2-, 3-, and 4- $\sigma$  confidence regions. Note that in this case sidelobes appeared at the 4- $\sigma$  confidence level, so the measurement was rejected as ambiguous.

Instead, the appropriate way to determine the scan-to-scan fit is by noticing that the minimum value of the co-added  $\chi^2$  surface is greater than the total number of degrees of freedom  $nN$  by the amount:

$$N \frac{\sigma_i^2}{\sigma_m^2}. \quad (10)$$

The quantity  $\sigma_m$  was measured directly from the shape of the surface, which remained unchanged, and the number of scans  $N$  was known. Thus, one could derive  $\sigma_i$  and apply it to the formal uncertainties. For all observations the average value of  $\sigma_i^2/\sigma_m^2$  was 1.29; values ranged from 0.0042 (for bright sources and good weather conditions) to 7.2.

Phase-referencing was used to decrease the amount of unmonitored phase noise during narrow-angle astrometry observations (see Section 3.1), but some residual phase noise remained, so the correction outlined here had to be applied to the astrometric data. Synthetic data were constructed both with and without unmonitored phase noise of the actual spectrum observed, and the data reduction algorithm determined measurement uncertainties consistent with the actual scatters in the measurements between multiple synthetic data sets. With-

out the additional phase-noise correction outlined here, the formal uncertainties significantly underestimated the scatter in the results.

### 3. EXPECTED PERFORMANCE

The expected astrometric performance of the PHASES observing mode was determined by several factors contributing measurement uncertainties and biases. These can be subdivided into three broad categories:

1. observational noise terms, which are fundamental to atmospheric turbulence and finite source brightness;
2. instrumental noise terms, which result from the design of the interferometer and the method in which the measurements were obtained;
3. astrophysical noise terms, which result from the astrometric stability of the stars themselves.

The size of each noise source is summarized in Table 1. The details of a few of these terms were described by Lane and Mutterspaugh (2004); here, a more complete summary of the PHASES error budget is presented.

**Table 1**  
Astrometric Noise Sources

Source	Section	Typical Magnitude ( $\mu\text{as}$ )
Temporal decoherence	3.1.1	$\sim 5$
Anisoplanatism	3.1.2	0.2
Photon noise	3.1.3	3
Differential dispersion	3.2.1	$\sim 30$
Baseline errors	3.2.2	$< 10$
Fringe template	3.2.3	1
Scan rate	3.2.4	1
Beam walk	3.2.5	1
Global astrometry	3.2.6	$\ll 1$
Star spots	3.3.1	$< 8$
Stellar granulation	3.3.2	$< 3$

**Note.** — Sources of astrometric noise vary in magnitude from tens of micro-arcseconds to sub-microarcsecond levels. Differential dispersion depends on color difference between binary components; for many targets, this is nearly zero, but for extreme color differences, this can be hundreds of microarcseconds. This is not the case for any of the PHASES targets. Photometric variability accompanies star spots, of a magnitude that is easily detected for astrometric signatures of  $8 \mu\text{as}$  or larger.

### 3.1. Astrometric Observational Noise

In calculating the expected astrometric performance three major sources of error were taken into account: errors caused by fringe motion during the delay sweep between fringes (loss of coherence with time), errors caused by differential atmospheric turbulence (loss of coherence with sky angle, i.e., anisoplanatism), and measurement noise in the fringe position. Each is quantified in turn below, and the expected measurement precision is the root-sum-squared of the terms.

#### 3.1.1. Loss of Temporal Coherence

The power spectral density of the fringe phase of a source observed through the atmosphere has a power-law dependence on frequency; at high frequencies typically

$$A(f) \propto f^{-\alpha} \quad (11)$$

where  $\alpha$  is usually in the range 2.5–2.7. The effect of phase-referencing is to high-pass filter this atmospheric phase noise. For PHASES, the servo was an integrating servo with finite processing delays and integration times, with the residual phase error “fed forward” to the second beam combiner (Lane and Colavita 2003). The response of this system to an input atmospheric noise can be written in terms of frequency as

$$H(f) = \frac{1 - 2\text{sinc}(\pi f T_s) \cos(2\pi f T_d) + \text{sinc}^2(\pi f T_s)}{1 - 2\frac{f_c}{f} \text{sinc}(\pi f T_s) \sin(2\pi f T_d) + \left(\frac{f_c}{f}\right)^2 \text{sinc}^2(\pi f T_s)} \quad (12)$$

where  $\text{sinc}(x) = \sin(x)/x$ ,  $f_c$  is the closed-loop bandwidth of the fringe-tracker servo (for PHASES  $f_c = 10$  Hz or 5 Hz),  $T_s$  is the integration time of the phase sample (in standard mode, 6.75 ms), and  $T_d$  is the delay between measurement and correction (done in post-processing, effectively 5 ms). The phase noise superimposed on the double fringe measured by the astrometric beam combiner has a spectrum given by  $A(f)H(f)$ .

The sampling of the double fringe packet took a finite amount of time, first sampling one fringe, then the other. In the time domain the sampling function can be represented as a “top-hat” function convolved with a pair of

delta functions (one positive, one negative). The width of the top-hat is equal to the time taken to sweep through a single fringe, while the separation between the delta functions is equal to the time to sweep between fringes. In the frequency domain, this sampling function becomes

$$S(f) = \sin^2(2\pi f \tau_p) \text{sinc}^2(\pi f \tau_*), \quad (13)$$

where  $\tau_p$  is the time taken to move the delay between stars,  $\Delta d/v_s$ , and  $\tau_*$  is the time to sweep through a single stellar fringe,  $\Lambda/v_s$ .  $v_s$  is the delay sweep rate.

The resulting error in the astrometric measurement, given in radians by  $\sigma_{tc}$ , can be found from

$$\sigma_{tc}^2 = \left(\frac{\lambda}{2\pi B}\right)^2 \frac{1}{N} \int_0^\infty A(f) H(f) S(f) df \quad (14)$$

where  $N$  is the number of measurements. It is worth noting that if phase-referencing was not used to stabilize the fringe, i.e.  $H(f) = 1$ , the atmospheric noise contribution increases by a factor of  $\approx 10^2$ – $10^3$ . For  $\sim$ Hz scanning, the corresponding error is less than  $10 \mu\text{as}$ .

#### 3.1.2. Anisoplanatism

The performance of a simultaneous narrow-angle astrometric measurement has been thoroughly analyzed by Shao and Colavita (1992). Here the primary result for the case of typical seeing at a site such as Palomar Mountain is restated, with the astrometric error in arcseconds due to anisoplanatism ( $\sigma_a$ ) is given by

$$\sigma_a = 540 B^{-2/3} \theta t^{-1/2} \quad (15)$$

where  $B$  is the baseline (in meters),  $\theta$  is the angular separation of the stars (in radians), and  $t$  is the integration time in seconds. This assumes a standard (Lindegren 1980) atmospheric turbulence profile; it is likely that particularly good sites will have somewhat (factor of two) better performance. For  $\theta = 5 \times 10^{-7} \sim 100$  mas, and 1 hr of integration, this term is roughly a fifth of a microarcsecond.

#### 3.1.3. Photon Noise

The astrometric error due to photon-noise ( $\sigma_p$ ) is given in radians as

$$\sigma_p = \frac{\lambda}{2\pi B} \frac{1}{\sqrt{N}} \frac{1}{\text{S/N}}, \quad (16)$$

where  $N$  is the number of fringe scans, and  $\text{S/N}$  is the signal-to-noise ratio of an individual fringe. For typical PHASES targets and PTI’s throughput ( $N \sim 2000$ ,  $\text{S/N} \sim 10$ ), this was of order a few microarcseconds.

### 3.2. Astrometric Instrumental Noise

There were several effects internal to the instrument that could contribute noise terms or biases to the astrometric measurements. Some could potentially vary on night-to-night timescales as the optical alignments vary on roughly these timescales. Others resulted from properties of the measurement design.

#### 3.2.1. Differential Dispersion

The path compensation for the geometric delay at PTI was done with DLs in air. At near-infrared wavelengths,

air introduces a wavelength-dependent index of refraction given by Cox (2000)

$$n = 1 + \left( \frac{pT_s}{p_s T} \right) \left( 6.4328 \times 10^{-5} + \frac{0.029498}{146 - 1/\lambda^2} + \frac{2.554 \times 10^{-4}}{41 - 1/\lambda^2} \right) - 4.349 \times 10^{-5} (1 - 7.956 \times 10^{-3}/\lambda^2) \frac{p_w}{p_s} \quad (17)$$

where  $\lambda$  is the vacuum wavelength in  $\mu\text{m}$ ,  $p$  is the air pressure,  $p_w$  is the partial pressure of water vapor,  $p_s = 1.01325 \times 10^5 \text{ Pa}$ ,  $T$  is the temperature, and  $T_s = 288.15 \text{ K}$ . The fringe packets of astrophysical sources were dispersed by an amount that depends on the difference in air paths between arms of the interferometer; this changed the shape and overall location of the fringe packets; see Figure 3. If two stars were in the same beam and identical in color, the change in location was common to both and canceled; similarly, the distortions of the fringe packets are common and canceled to first order in a differential measurement. Simulated data and reanalysis of real data with modified fringe templates showed that higher order terms in the fringe packet shape are negligible at the microarcsecond level.

If, however, the two stars were of differing colors, each would be dispersed by a slightly different amount, and their apparent separation would be biased. The shift in the apparent position of each star's fringes can be approximated by evaluating the dispersion at the effective average wavelength of the star in the passband. The effective average wavelength was calculated by multiplying the instrumental bandpass by the stellar spectrum. For an order-of-magnitude estimate of the effect of differential dispersion, one can model the instrumental bandpass as a tophat function passing wavelengths  $2 - 2.4\mu\text{m}$  (nominal K-band) and the stellar spectra as blackbodies. The shifts in apparent positions for several spectral types over 40 m of differential air path (a maximum amount for PTI) are given in Table 2. Note that for G5-K5 binaries, the amount is  $35.8 \mu\text{as}$  and for B5-A5 it is  $30.6 \mu\text{as}$ . For much more extreme color ratios, the effect can be as large as  $150.6 \mu\text{as}$  for B5-M5 binaries; the PHASES sample did not include such systems, as their high contrast ratios prevented observation.

Because the stars were often observed at the same hour angles from one night to the next (and thus the delay positions are relatively common between nights), this effect introduced a much smaller scatter than that listed in the table. However, it may have introduced biases in the stellar separations and introduced scatter between observations taken in multiple baselines (for which the delay positions differed). These biases and scatters were of order the amounts given in Table 2.

The binaries in the PHASES sample were generally of components with equal brightnesses and thus similar colors. No hour-angle dependent biases significant on the level of the precision of the observations were observed. This effect is likely to be important for traditional narrow angle astrometry methods at the Keck Interferometer or Very Large Telescope Interferometer, which aim to use field stars as astrometric references for nearby stars, and reference and target will often have very different colors. The effect is largely reduced if one uses a spectrometer to measure the group delay positions of the fringes.

Starting in 2005, the longitudinal dispersion compen-

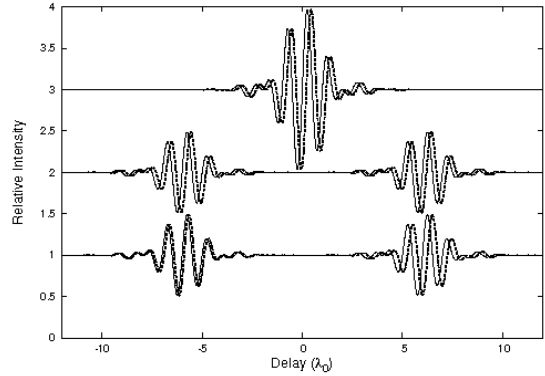


**Figure 3.** Schematic of the shift in fringe positions due to dispersion (the effect has been exaggerated for clarity). The vacuum (no dispersion) interferograms are plotted with solid lines; those dispersed by air with dotted lines. Top: dispersion shifts the point of zero optical path difference for a star, due to different amounts of air path in each arm of the interferometer (the effective optical path difference measured as if in vacuum). Middle: the dispersion shifts for stars of equal colors were equal and canceled; the measured separation is the same. Bottom: stars of unequal colors are shifted by slightly different amounts by dispersion, and the resulting measured separation is different. For very extreme color differences, the shift can be hundreds of microarcseconds. Not shown are the shape distortions to interferograms.

sator addressed this potential systematic. The measurements acquired with this correction are flagged in Table 5.

### 3.2.2. Baseline Errors

The baseline vector used in the differential delay equation to determine astrometric quantities was derived by inversion of the delay equation from the fringe locations of point-like sources with known global astrometric positions. Uncertainties and variability of the baseline vector were sources of differential astrometry uncertainties via the differential delay equation. An incorrect baseline model would show up as an hour-angle dependent error term that would potentially increase night-to-night scatter beyond that predicted by the formal uncertainties; this was tested by dividing data sets within single nights into multiple sets by hour-angle range and the results were self-consistent.

No evidence of hour-angle dependent error terms was seen in the PHASES data, supporting evidence that the baseline models are correct. As shown in Figure 4, except for a few outliers (likely due to using point sources with poor global astrometry values or a night's observation only covering a small range of hour angles or declinations) the night-to-night drift in baseline model solutions were less than 1 mm in north-south and east-west directions for the two primary baselines used for PHASES observations (NS and SW). The up-down dimension was stable to a few millimeters in both cases; this scatter was likely due to limited measurement precision rather than actual baseline variability, implying that it could be improved by averaging several nights' values.

The amount by which a baseline error of  $\vec{\sigma}_B$  affects a differential astrometry measurement  $\vec{\Delta S}$  was determined as follows. To maintain the same observed differential delay between stars, the differential delay equation requires that

$$\vec{B} \cdot \vec{\Delta S} = (\vec{B} + \vec{\sigma}_B) \cdot (\vec{\Delta S} + \vec{\sigma}_{\Delta S}) \quad (18)$$

**Table 2**  
Differential Dispersion

Spectral Type	Effective Temperature (K)	Effective K-band Wavelength ( $\mu\text{m}$ )	$(n - 1) \times 10^4$	$(n - n_{F5}) \times 10^9$	$(n - n_{F5}) \times 38\text{m} [\text{nm}]$	Error vs. F5 [ $\mu\text{as}$ ]
O5	44500	2.1763	2.729232	0.93	35.4	73
B5	15400	2.1772	2.729229	0.66	25.0	51
A5	8200	2.1785	2.729225	0.25	9.7	20
F5	6440	2.1794	2.729223	0.00	0.0	0
G5	5770	2.1799	2.729221	-0.14	-5.4	11
K5	4350	2.1815	2.729217	-0.61	-23.3	48
M5	3240	2.1839	2.729210	-1.32	-50.3	103

**Note.** — Effect of color-dependent differential dispersion. Stellar temperatures are for dwarf stars, from Carroll and Ostlie (1996). All numbers are for zero water vapor pressure,  $p_w = 0$ . Increasing water vapor pressure to  $p_w = p_s$  increases the astrometric effect by a factor of roughly 20%.

where  $\overrightarrow{\sigma_{\Delta S}}$  is the astrometric error caused by baseline error  $\overrightarrow{\sigma_B}$ . Canceling like terms and assuming  $\overrightarrow{\sigma_{\Delta S}} \cdot \overrightarrow{\sigma_B}$  is less than the other terms simplifies this to

$$\overrightarrow{\sigma_B} \cdot \overrightarrow{\Delta S} = -\overrightarrow{B} \cdot \overrightarrow{\sigma_{\Delta S}}. \quad (19)$$

The vector  $\overrightarrow{\Delta S}$  was tangent to the celestial sphere; only that component which was not perpendicular to the baseline was actually measured (this measured component of the separation is referred to as  $\delta S$ ) and only its uncertainty ( $\sigma_{\delta S}$ ) was thus applicable. The angle between these measured components and the baseline vector is given by the target's zenith angle  $z$ ; this was always kept to less than  $45^\circ$ . Of course, the baseline uncertainty vector  $\overrightarrow{\sigma_B}$  need not be oriented with  $\overrightarrow{B}$  itself; its components  $\sigma_{Bx}$  and  $\sigma_{By}$  tangent to and  $\sigma_{Bz}$  normal to the Earth (also referred to as the “U” or “Up” component) are introduced. Substituting into Equation 19 gives the relationship between baseline error and astrometric error as

$$\delta S ((\sigma_{Bx} \cos \phi + \sigma_{By} \sin \phi) \cos z + \sigma_{Bz} \sin z) = -|B| \sigma_{\delta S} \cos z, \quad (20)$$

where  $\phi$  is an angle determined by the hour angle and declination of the target. On rearranging terms, the fractional astrometric measurement uncertainty due to baseline uncertainties was

$$\frac{\sigma_{\delta S}}{\delta S} = -\frac{\sigma_{Bx} \cos \phi + \sigma_{By} \sin \phi + \sigma_{Bz} \tan z}{|B|}. \quad (21)$$

For  $|B| = 100$  m and  $z < 45^\circ$ , baseline uncertainties of 2 mm cause 10  $\mu\text{as}$  errors in the astrometry for a binary with projected separation  $\delta S = 0.5$  arcsec. Though the measured component of  $\Delta S$  continually varies as the Earth rotates the baseline vector, the above derivation is true at any given instant. Earth rotation causes errors to appear in both astrometric dimensions.

A slightly more subtle baseline effect was that there can be differences between the wide-angle (“astrometric”) and narrow-angle (“imaging”) baselines. When determining the baseline vector via the delay positions for stars with known global astrometry solutions spread across the sky, the siderostats are repointed for each observation to place the target star on-axis. Thus, one was measuring the vector between the pivot points of the siderostats, about which the siderostats were repointed for each target. When measuring the separations between two stars in a single field with a single pointing of the telescopes, at least one of the stars would be off

axis; one instead desired to know the separations between the corresponding points on the surfaces of the two siderostats to get the proper delay scale. Through careful optical design, PTI was built to minimize differences between the astrometric and imaging baselines in order that the original narrow angle astrometry mode would function at the 100  $\mu\text{as}$  level for binaries with separations of tens of arcseconds. Because errors due to baseline uncertainty scale with binary separation, the effect was negligible at the level of a few microarcseconds for subarcsecond binaries in the PHASES sample.

### 3.2.3. Fringe Template

Because the astrometric measurements were differential between two stars, they were relatively insensitive to the model fringe template. The fringe model used in the astrometric analysis was determined by observing interferograms of single stars. An effective bandpass was constructed from an incoherent averaging of the periodograms of many such interferograms, and used to recompute a standard interferogram template, to be applied to the data. This effective bandpass was only an approximation for most stars, as there were variations in source temperature and spectra. However, reanalysis with several different fringe models showed variations only at the single microarcsecond level.

### 3.2.4. Scan Rate and Earth Rotation

Earth rotation caused variable projection of the binary separation on the interferometer baseline vector. The details of the variability depend of the observatory location, sky position of the target binary, and the orientation of the baseline vector, but for order-of-magnitude estimations, can be approximated as a sinusoid with period of 1 day and amplitude equal to the total binary separation  $a$ :

$$\Delta s \approx a \times \cos(2\pi t/\text{day}). \quad (22)$$

The differential delay rate was given by the first derivative of this equation with respect to time, converted from sky angle to delay length by the interferometer’s resolution. For  $a \sim 500$  mas, this differential delay rate is about  $20 \text{ nm s}^{-1}$ , or 5 nm (10  $\mu\text{as}$ ) in the (typically) 250 ms required to scan between the fringe packets. Roughly an equal number of scans were obtained in each scan direction (to within 10%), and this effect canceled to first order (to the same level, 10% or 1  $\mu\text{as}$ ). However, curvature in the differential delay motion does not cancel; it is given by the second time derivative of the projected

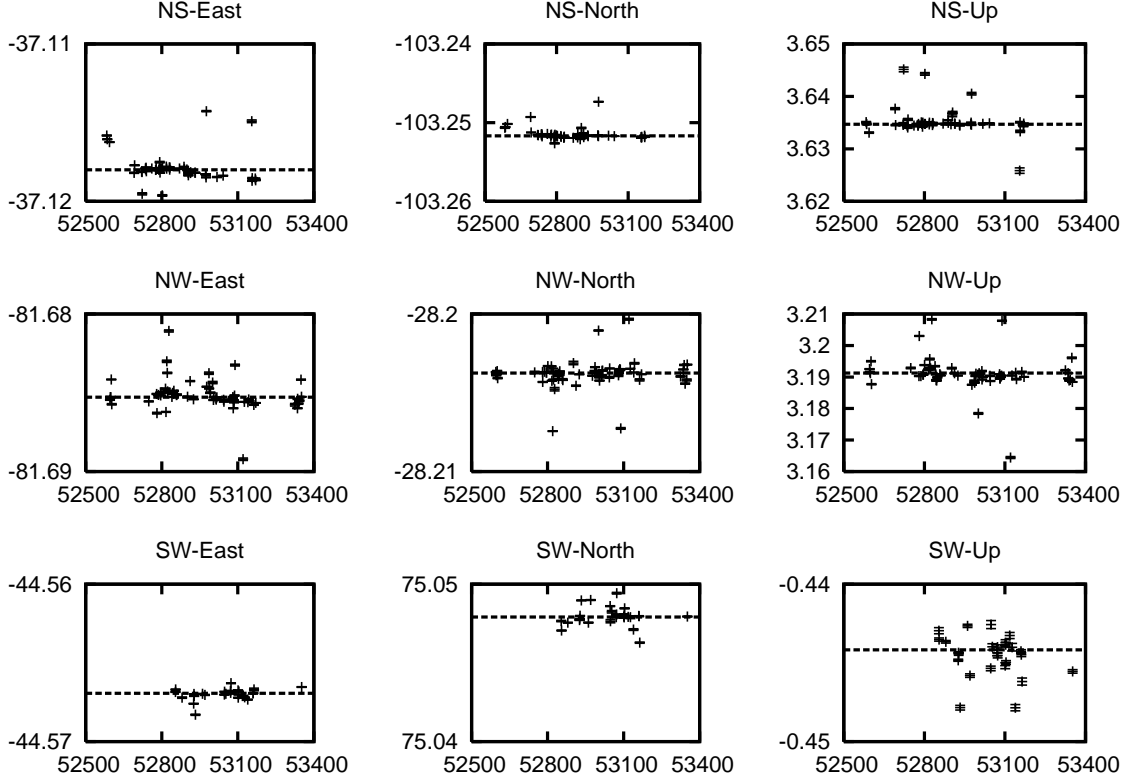


**Figure 4.** Solutions for the three PTI baseline vectors. The three baselines at PTI were named “NS”, “NW”, and “SW” due to their rough orientations. Each was a three dimensional vector, which was given by components in the “East” (east-west), “North” (north-south), and “Up” (up-down) directions (the first two were tangent to the Earth, the last was perpendicular). Horizontal axes are time in modified Julian Days (MJD), vertical axes are baseline length in meters. Lines represent average baseline fits used for data reduction presented in this paper; points with error bars represent a given night’s baseline solution. The baseline solutions were derived from the observed delay positions of single-star sources with known global astrometric positions via inversion of Equation 2. The y-axis tick marks in each plot are all 10 mm. Note that the scatter in the “Up” dimension was much larger than the other dimensions; this was due to preferential observing of targets overhead, for which the “Up” component is highly covariant with the constant term in the delay equation. The baseline solution used for data analysis was a weighted average of the solutions plotted.

separation and was roughly  $1.4 \times 10^{-3} \text{ nm s}^{-2}$  (less than 3 nano-arcseconds  $s^{-2}$ ). Thus the differential delay rate was small enough, and the measurement rate fast enough, that the finite measurement rate did not contribute significant uncertainties.

### 3.2.5. Beam Walk

The interferometer telescopes imaged a sky field and then recollimated the light. Through this process, light from two stars separated on the sky by angle  $\alpha$  was partially sheared with respect to each other and proceeded to illuminate slightly different parts of the optics that guide the light to the detector. Starlight in a recollimated beam that originated from different sky positions also developed relative shear equal to the path traveled multiplied by their angular separation (see Figure 5). To the extent that the optics were imperfect (had rough surfaces), the light from each star traveled slightly different path-lengths from telescope to detector. This process is known as beam walk.

Colavita (2009) determined the extent to which beam walk introduces astrometric errors. That approximate stochastic analysis yielded an rms pathlength error  $\epsilon$  given by

$$\epsilon \sim w \left( \frac{\delta}{q} \right) \left( \frac{q}{z} \right)^{1/4}, \quad \delta \ll q,$$

where  $w$  is the rms wavefront error over an optic of diameter  $z$ ,  $q$  is the diameter of the starlight footprint, and  $\delta$  is the linear beamwalk. For optics with a surface quality of  $\lambda/20$  peak-to-valley (like those used at PTI), the wavefront rms is  $w \simeq \lambda/40$ . The actual error is  $\sim \sqrt{2}$  larger than this due to the presence of two telescopes in the interferometer.

The first place where beam walk could occur was within the telescope itself. The beam was collimated at the telescope primary, focused by the primary, and recollimated to a  $q = 0.075$  m beam by a  $z = 0.1$  m diameter mirror to be fed to the “Fast Steering Mirror” (FSM; this mirror corrected for tip-tilt wavefront errors across the telescope, providing low-order adaptive optics). The distance from primary mirror to this mirror was the sum of their focal lengths, 4.75 m. The beam walk over 0.1 arcsec ( $4.8 \times 10^{-7}$  rad) was thus  $\delta = 2.3 \mu\text{m}$ . Beam walk on the FSM thus contributed an astrometric error of 0.001  $\mu\text{as}$  and was negligible.

The relative angles of starlight in the recollimated beam were increased by a factor of the ratio of the primary mirror and FSM focal lengths (5.33), thus light from sky locations separated by 0.1 arcsec had a differential angle of 0.533 arcsec ( $2.6 \times 10^{-6}$  rad). This recollimated beam from the FSM traveled through light pipes to the beam combining laboratory, where mov-

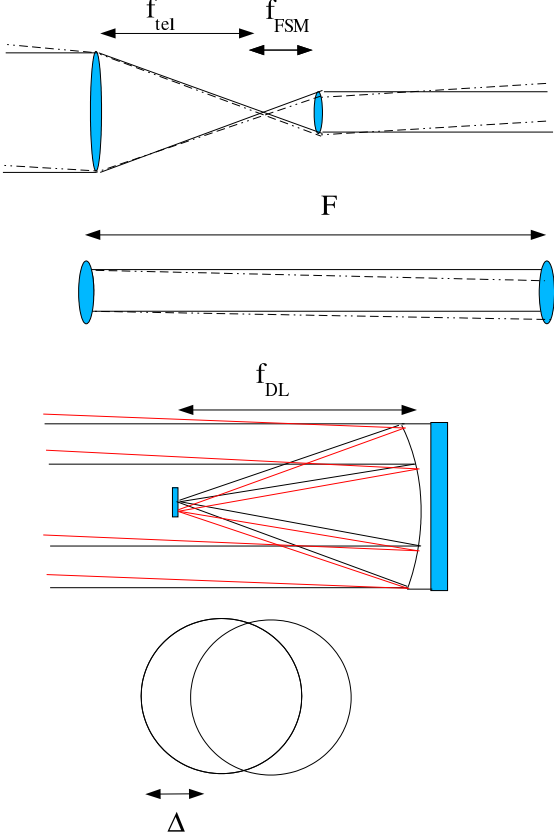


**Figure 5.** Three instances where beam walk could occur, causing stars at slightly different sky angles to illuminate different parts of optical elements. Top: shear introduced at the telescope by focusing and recollimating the beam. “FSM” stands for the “Fast Steering Mirror”, which provided tip-tilt corrections (first-order adaptive optics) and recollimated the light after the telescope. Second from top: shear within a collimated beam over large optical paths. Second from bottom: shear at focus of DL optics (the movable mirrors that provide optical delays). Bottom: the shear of two beams by amount  $\Delta$ , causing only partial overlap.

able mirrors added a variable amount of delay. This total travel is of order 50 m; the mirrors are typically  $z = 0.1$  m diameter. The beam walk over 0.533 arcsec was  $\delta = 130 \mu\text{m}$ , which contributed an astrometric error of  $0.07 \mu\text{as}$ . There were a few mirrors along this path, and the total astrometric error would be determined by considering the optical qualities of all optics and adding the effects in quadrature. Because this beam walk was so small, the sum total of these remained negligible.

The movable mirrors were comprised of a parabolic mirror of focal length 1.07 m and a small ( $z \approx 0.01$  m) flat mirror located near its focus. Collimated light was directed to one side of the parabola, focused onto the flat mirror, then recollimated by the parabola’s other side. On the flat mirror, the (diffraction-limited) beam diameter was only  $q \sim \lambda f/d = 31 \mu\text{m}$  where  $\lambda$  is the operating wavelength of light,  $f$  is the parabola’s focal length, and  $d$  is the collimated beam diameter (0.075 m). The beam walk was  $2.8 \mu\text{m}$ . The flat mirrors contributed an astrometric error of  $0.9 \mu\text{as}$  from beam walk. It is concluded that beam walk did not contribute significant measurement errors.

### 3.2.6. Global Astrometry Errors

Uncertainty in the global position of a target binary on the celestial sphere was coupled into the differential astrometric measurement. Errors in right ascension were equivalent to measurement timing errors; declination uncertainties had similar effects. The order of magnitude of this effect can be derived as follows: the fractional error in global astrometry (error in arcseconds divided by total number of arcseconds around a quarter circle) is roughly equal to the fractional error in differential astrometry separation vector (astrometric error divided by binary separation). A 1 arcsec global astrometry error caused differential astrometric errors of less than  $3 \mu\text{as}$  for binaries of separation 1 arcsec or less. Typical uncertainties in global astrometry were much less than an arcsecond, with 10 mas being a much more common value. Effects such as stellar aberration (20 arcsec) were accounted for in the PHASES data reduction software; if ignored, these could cause significant differential astrometry uncertainties.

### 3.3. Astrometric Astrophysical Noise

There were potential sources of apparent astrometric motion in the target stars due to processes within the stars themselves. These included star spots and stellar granulation.

#### 3.3.1. Star Spots

As previously presented by Mutterspaugh et al. (2006), the maximum shift in the center-of-light of a star caused by star spots can be evaluated with a model comprised of a uniform stellar disk (radius  $R$ ) except for a zero-temperature (non-emitting) circular region of radius  $r$  tangent to the edge of the stellar disk (i.e. centered at  $x = R - r$ ,  $y = 0$ ). The center of light is displaced by:

$$\frac{x_c}{R} = \frac{\int_{-R}^R \int_{-\sqrt{R^2-x^2}}^{\sqrt{R^2-x^2}} x dy dx - \int_{R-2r}^R \int_{-\sqrt{r^2-(x-R+r)^2}}^{\sqrt{r^2-(x-R+r)^2}} x dy dx}{R \pi (R^2 - r^2)} \\ = -\frac{r^2/R^2}{1 + r/R}. \quad (23)$$

The presence of star spots can be confirmed through photometric measurements simultaneous with astrometric observations. The non-emitting spots in this model would cause photometric variations proportional to the fractional area of the stellar disk covered:

$$\frac{F}{F_o} = 1 - \frac{r^2}{R^2} \quad (24)$$

where  $F_o$  is the star’s flux when no spots are present. Equations 23 and 24 provide a relationship between the apparent astrometric and photometric shifts caused by star spots.

The largest possible astrometric shift by a star spot is given by evaluating a slightly different model. In this case, the star spot fills the (non-circular) area from the star’s edge to a chord at distance  $x_o$  from the star’s true center. The astrometric shift is

$$\frac{x_c}{R} = \frac{\int_{-R}^{x_o} \int_{-\sqrt{R^2-x^2}}^{\sqrt{R^2-x^2}} x dy dx}{R \int_{-R}^{x_o} \int_{-\sqrt{R^2-x^2}}^{\sqrt{R^2-x^2}} dy dx}$$

$$= -\frac{2 \left(1 - \frac{x_o^2}{R^2}\right)^{3/2}}{3 \left(\frac{\pi}{2} + \arcsin \frac{x_o}{R} + \frac{x_o}{R} \left(1 - \frac{x_o^2}{R^2}\right)^{1/2}\right)} \quad (25)$$

with corresponding photometric variations of

$$\frac{F}{F_o} = \frac{1}{\pi} \left( \frac{\pi}{2} + \arcsin \frac{x_o}{R} + \frac{x_o}{R} \left(1 - \frac{x_o^2}{R^2}\right)^{1/2} \right). \quad (26)$$

For stars of typical radius 1 mas, the simplified model gives a roughly linear relationship of 0.8  $\mu$ as of astrometric shift per milli-magnitude of photometric variability, see Figure 6. Only stars with diameters smaller than PTI’s resolution of  $\sim 4$  mas were observed by PHASES. Photometric variations of these scales can be monitored by small ground-based telescopes. The timescale of these variations is on order the rotation rate of a star (days to weeks). Lanza et al. (2008) re-evaluated the effects of spots with a model that includes stellar limb darkening and lower spot contrast (“warm” spots rather than the completely non-emitting spots assumed above) and found this reduces the astrometric effect by  $\sim 40\%$ .

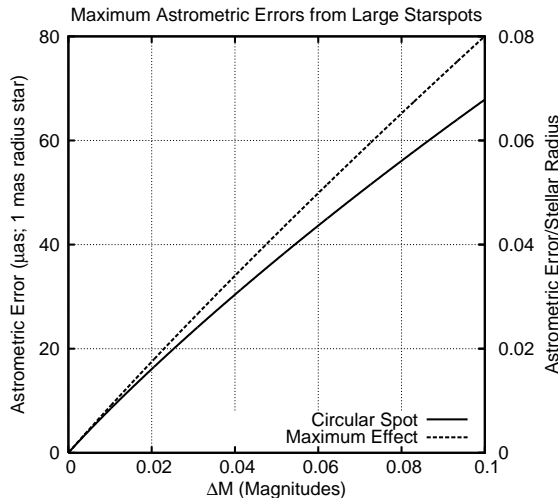


**Figure 6.** Maximum effect of star spots on astrometric measurements vs. the photometric variations they cause.

### 3.3.2. Stellar Granulation

Stellar granulation causes photometric variability of subsections of a star’s surface. Averaged over the whole of the stars surface, these photometric variations can cancel to large extent and the intrinsic variability of the star remains small, though with a large astrometric uncertainty. Svensson and Ludwig (2005) showed that the effects of stellar granulation are independent of a star’s radius but are strongly correlated with surface gravity, and provide values for the astrometric effects in white light.

For stars with very low surface gravities (i.e. red giants), astrometric perturbations can be quite large—as much as  $300 \mu$ as/ $D$  [pc]. Red giants within 100 pc were overresolved by PTI and could not be observed, thus even for these stars this effect was negligible. For main-sequence stars, the effect was closer to  $0.1 \mu$ as/ $D$  [pc].

## 4. EMPIRICAL ERROR BAR SCALING RULES

The formal uncertainty ellipses derived with the procedure outlined in Section 2.2 were found to underestimate the actual scatter of the measurements to an orbital model. Two reasonable approaches to correct this are to find a multiplicative scale factor by which to increase the formal uncertainties, or a noise floor to be added-in-quadrature to the formal uncertainties. Unfortunately, no single multiplicative factor nor noise floor was found that could bring the measurement uncertainties and fit residuals into satisfactory agreement for a majority of the stars. The instrumental changes made in 2005 to introduce a longitudinal dispersion compensator (discussed in Section 3.2.1) and an automated alignment system further complicate this effort. However, upon dividing the measurements into two subsets according to whether or not the instrumental changes were implemented (the subset without the upgrades will be referred to as subset 1, that with the upgrades will be referred to as subset 2), and allowing for different scaling or noise floor factors in each subset, again no single solution was obtained.

Recognizing that both multiplicative factors and noise floors might be present, and could affect the major and minor axes of the uncertainty ellipses in different ways, a solution was sought to incorporate parameters for both types of terms, allowing for different values in the two axes and in the two subsets. This finally produced a single satisfactory solution. The procedure used to find the solution and the final values obtained were as follows.

Of the 51 star systems observed by PHASES, 33 had 10 or more measurements. Six of those 33 had been previously discovered to be triple or quadruple star systems, and a seventh (HR 2896 = HD 60318) was discovered by PHASES to be a triple system; for simplicity of analysis, the effort to derive the uncertainty scaling rules was limited to binaries. Three more systems had too few measurements in one or both subsets 1 and 2, and were not included in the analysis. Of the remaining 23 binaries, 15 ( $\sim 2/3$ ) were selected for evaluation; the other  $\sim 1/3$  of the systems were not included allowing for the possibility that their increased levels of scatter were the result of astrophysical phenomena; however, the empirical scaling rules have been found to work satisfactorily on many of these as well, as a check of the rules’ validities.

The size of the major and minor axes of each measurement was resized by the formula

$$\sigma_{(i,j),c}^2 = f_{(i,j)}^2 \sigma_{(i,j),\text{raw}}^2 + \sigma_{(i,j),q}^2$$

where  $i = 1, 2$  indicates the subset number,  $j = 1, 2$  indicates whether it is the uncertainty ellipse major (1) or minor (2) axis,  $\sigma_{(i,j),c}$  is the “corrected” 1- $\sigma$  uncertainty,  $f_{(i,j)}$  is a multiplicative scaling factor,  $\sigma_{(i,j),\text{raw}}$  is the formal 1- $\sigma$  uncertainty, and  $\sigma_{(i,j),q}$  is a noise floor added in quadrature.

An iterative procedure was used to optimize the values of the eight parameters  $f_{(i,j)}$  and  $\sigma_{(i,j),q}$  in order to produce the most statistically reasonable set of uncertainty ellipses to represent the observed scatter about Keplerian models for the 15 stars. The constraints for optimizing those eight parameters were: (1) within each subset, for each axis, the  $\chi_r^2$  goodness-of-fit statistics computed along that axis should have minimal variance among the binaries (i.e. all the binaries being evaluated should have

similarly good fits in a given axis), (2) averaged over all the binaries, the  $\chi_r^2$  statistic computed within each subset/axis combinations should be equal to the other subset/axis (and unity; i.e. fit residuals should equally distributed among the various subsets and axes), and (3) the fits for as many binaries as possible should have  $\chi_r^2$  as close to unity as possible.

The eight parameters  $f_{(i,j)}$  and  $\sigma_{(i,j),q}$  were given nominal values, and the 15 binaries' PHASES measurements were fit to Keplerian models using the replacement uncertainty ellipses. The correction parameters were varied one at a time, each step recalculating the Keplerian models, until the variance of the  $\chi_r^2$  among the binaries on the affected subset/axis was minimized (criterion 1). This was repeated over the eight parameters, after which the average  $\chi_r^2$  was calculated in each of the four subset/axis combinations, and the parameters affecting each subset/axis combination were renormalized to force the average  $\chi_r^2 = 1$  for that combination (criterion 2). This procedure was then iterated, varying the parameters individually to minimize  $\chi_r^2$  variance followed by renormalizing to  $\chi_r^2 = 1$  for each axis, until the parameter values converged.

The final parameter values that produced the best universal uncertainty scaling rules were found to be:

- $f_{(1,1)} = 1.3$  (original instrument configuration, major axis);
- $f_{(1,2)} = 3.8$  (original instrument configuration, minor axis);
- $f_{(2,1)} = 1.3$  (revised instrument configuration, major axis);
- $f_{(2,2)} = 1.0$  (revised instrument configuration, minor axis);
- $\sigma_{(1,1),q} = 140 \mu\text{as}$  (original instrument configuration, major axis);
- $\sigma_{(1,2),q} = 35 \mu\text{as}$  (original instrument configuration, minor axis);
- $\sigma_{(2,1),q} = 140 \mu\text{as}$  (revised instrument configuration, major axis);
- $\sigma_{(2,2),q} = 35 \mu\text{as}$  (revised instrument configuration, minor axis).

Only four non-trivial parameters end up being needed to correct the measurement uncertainties: a single multiplicative factor of 1.3 for the major axis (independent of subset), a multiplicative factor of 3.8 for the minor axis of data that lacked the dispersion compensator and/or automatic alignment system ( $f_{(2,2)} = 1$  is a trivial value representing no correction is needed), and noise floors of 140 and 35  $\mu\text{as}$  to be added in quadrature to the major and minor axes, respectively (independent of subset). These values are not entirely surprising: a large multiplicative factor for the minor axis before the instrument revisions disappeared as those changes made the instrument more stable and increased path monitoring. A noise floor of 35  $\mu\text{as}$  in the minor axis, regardless of subset,

**Table 3**  
Binaries Evaluated Using Empirical Uncertainty Ellipse Scaling Laws

HD Number	Nights Observed	$\chi_r^2$	*
17904	46	0.53	*
26690	20	0.75	
44926	23	0.62	*
76943	16	1.10	
114378	24	1.24	*
137107	51	1.22	*
137391	23	0.59	*
137909	73	0.85	*
140159	15	1.15	*
171779	54	1.04	*
187362	10	0.97	
202275	69	0.91	*
207652	50	0.58	*
214850	53	0.87	*
5286	18	4.71	
6811	20	2.16	
13872	89	0.46	*
77327	47	0.44	*
81858	12	2.27	
129246	17	1.86	*
140436	43	1.82	*
155103	10	0.21	
176051	66	4.43	
196524	73	2.68	
202444	39	3.52	
221673	99	8.01	

**Note.** — Column 1 is the star's HD Catalog Number, Column 2 is the total number of nights the star was observed, and Column 3 is the value of  $\chi_r^2$  calculated for a Keplerian model. An asterisk appears in the fourth column of stars used to evaluate the uncertainty ellipse scaling rules.

is reasonably expected from the many noise sources described in Section 3. The root-sum-square of the errors in Table 1 is 15  $\mu\text{as}$ . Given that some of the simple arguments presented were designed to provide error estimates at only the factor of 2 level, the resulting 35  $\mu\text{as}$  noise floor is not unreasonable. In addition, it is possible some differential dispersion persisted even with the dispersion compensator in place, though it certainly reduced the amount. Because the major axis represents a direction perpendicular to that at which the interferometer baseline was oriented at the average measurement time, the measurement along that axis is slow to build via Earth-rotation synthesis, and it is not surprising to find a small multiplicative factor and larger noise floor in that direction.

After applying these corrections to the measurement uncertainties, the  $\chi_r^2$  statistic was calculated for Keplerian fits to the data of all 26 binaries having more than 10 observations. Fourteen of the 26 (54%) evaluate to  $0.5 < \chi_r^2 < 1.5$ , and an additional two just miss the cut-off (with values of 0.44 and 0.46; including these would bring the total to 62%). Furthermore, four of the systems with too-large values of  $\chi_r^2$  are much better modeled by a double Keplerian model, indicating an additional component may be present; see Paper V. The 26 binaries, number of observations, the fits'  $\chi_r^2$  metrics, and which binaries were used to evaluate the scaling rules are listed in Table 3.

## 5. DISTRIBUTION OF FIT RESIDUALS

To use the PHASES measurements for orbit fitting and companion searches, it was important to establish the statistical properties of the measurement residuals to determine whether they are Gaussian. Using uncertainties derived from the process outlined in Section 4, Keplerian orbits were fit for 19 of the 20 binaries presented in Paper II (HD 202444 has been omitted, since there is some evidence to suggest it hosts a substellar companion; see Paper V), as well as  $\delta$  Equ (HD 202275), which has previously been studied at length (Muterspaugh et al. 2005, 2008). The fits included all the non-PHASES and radial velocity measurements as listed in Paper II, rather than just the PHASES measurements, to ensure the residuals represented the best known binary motions. The PHASES measurement residuals along the minor axes of the error ellipses for these 20 binaries were normalized by their minor axis measurement uncertainties and combined into a joint residual distribution; a similar distribution was made for the major axis residuals. Histograms and continuous distribution functions (the latter being the integral of the histogram, which has the advantage of avoiding misinterpretation of the statistics caused by the granularity of bin size used in the histograms, though at the expense of being a less-familiar distribution), of the minor- and major-axis residuals are presented in Figure 7, along with the theoretical distributions one would obtain from unit-deviation distribution (a Gaussian and an error function, respectively). The distributions agree quite well with the theoretical distributions, though there might be a slight excess number in the distribution wings. However, any excess is small, and Gaussian statistics are a reasonable approximation for orbit-fitting and companion search applications.

## 6. SUMMARY OF PHASES MEASUREMENTS

The 1332 PHASES measurements are presented in Table 5. All have been processed with the standard pipeline described in Section 2.2. In total, 51 binaries were observed on 443 nights. An average of 1983 scans was used for each measurement, and the average formal minor-axis uncertainty is  $13 \mu\text{as}$ . After the scaling laws from §4 were applied, the average minor- and major-axis uncertainties were  $53 \mu\text{as}$  and  $486 \mu\text{as}$ , respectively.

## 7. SUPPORTING MEASUREMENTS

Infrared differential photometry between the primary and secondary components of several PHASES targets were obtained using Keck Adaptive Optics on MJD 53227. The differential photometries were measured in the  $K_p$  filter for faint systems, and a narrow band  $H_2$  2-1 filter centered at  $2.2622 \mu\text{m}$  for brighter binaries. Six systems of moderate brightness were measured with both filters. Differential magnitudes for the 20 binaries observed with Keck AO are presented in Table 4.

Though it has no impact on the current study, as an astrometry team we could not resist pointing out that—due to precession—PHASES target HD 149630 ( $\sigma$  Her) was the pole star around 8250 BC. PHASES benefits from the efforts of the PTI collaboration members who have each contributed to the development of an extremely reliable observational instrument. Without this outstanding engineering effort to produce a solid foundation, advanced

**Table 4**  
Keck AO Differential Photometry Measurements

HD	HJD-2453227.5	Filter	$\Delta m$	$\sigma$
5286	0.49	$H_2$	0.442	0.002
6811	0.49	$H_2$	1.426	0.002
13872	0.50	$H_2$	0.137	0.002
17904	0.51	$K_p$	1.218	0.003
17904	0.54	$H_2$	1.206	0.003
40932	0.63	$H_2$	0.002	0.005
41116	0.64	$H_2$	2.043	0.008
44926	0.64	$H_2$	0.215	0.004
137107	0.33	$K_p$	0.185	0.001
140436	0.35	$K_p$	0.936	0.001
165908	0.40	$H_2$	2.063	0.002
165908	0.40	$K_p$	1.909	0.001
171745	0.40	$K_p$	0.278	0.001
171745	0.41	$H_2$	0.272	0.001
171779	0.42	$K_p$	0.167	0.002
171779	0.42	$H_2$	0.163	0.003
176051	0.43	$H_2$	1.308	0.001
176051	0.43	$K_p$	1.235	0.001
196524	0.46	$H_2$	1.096	0.002
196867	0.46	$H_2$	1.587	0.004
202275	0.47	$H_2$	0.066	0.004
206901	0.44	$H_2$	0.188	0.001
207652	0.48	$K_p$	0.740	0.004
213973	0.44	$K_p$	0.293	0.003
221673	0.45	$H_2$	0.570	0.003

**Note.** — Column 1 is the star’s HD catalog number. Column 2 is the heliocentric Julian date offset by the day of observations. Column 3 is the filter used during the observation ( $K_p$  or  $H_2$ ). Columns 5 and 6 are the differential photometry and uncertainty measurements in units of magnitudes.

phase-referencing techniques would not have been possible. We thank PTI’s night assistant Kevin Rykoski for his efforts to maintain PTI in excellent condition and operating PTI in phase-referencing mode every week. Part of the work described in this paper was performed at the Jet Propulsion Laboratory under contract with the National Aeronautics and Space Administration. Interferometer data were obtained at the Palomar Observatory with the NASA Palomar Testbed Interferometer, supported by NASA contracts to the Jet Propulsion Laboratory. This publication makes use of data products from the Two Micron All Sky Survey, which is a joint project of the University of Massachusetts and the Infrared Processing and Analysis Center/California Institute of Technology, funded by the National Aeronautics and Space Administration and the National Science Foundation. This research has made use of the Simbad database, operated at CDS, Strasbourg, France. M.W.M. acknowledges support from the Townes Fellowship Program, Tennessee State University, and the state of Tennessee through its Centers of Excellence program. Some of the software used for analysis was developed as part of the SIM Double Blind Test with support from NASA contract NAS7-03001 (JPL 1336910). PHASES is funded in part by the California Institute of Technology Astronomy Department, and by the National Aeronautics and Space Administration under Grant No. NNG05GJ58G issued through the Terrestrial Planet Finder Foundation Science Program. This work was supported in part by the National Science Foundation through grants AST 0300096, AST 0507590, and AST 0505366. MK is supported by the Foundation for Polish Science through a FOCUS grant and fellowship, by the Polish Ministry of

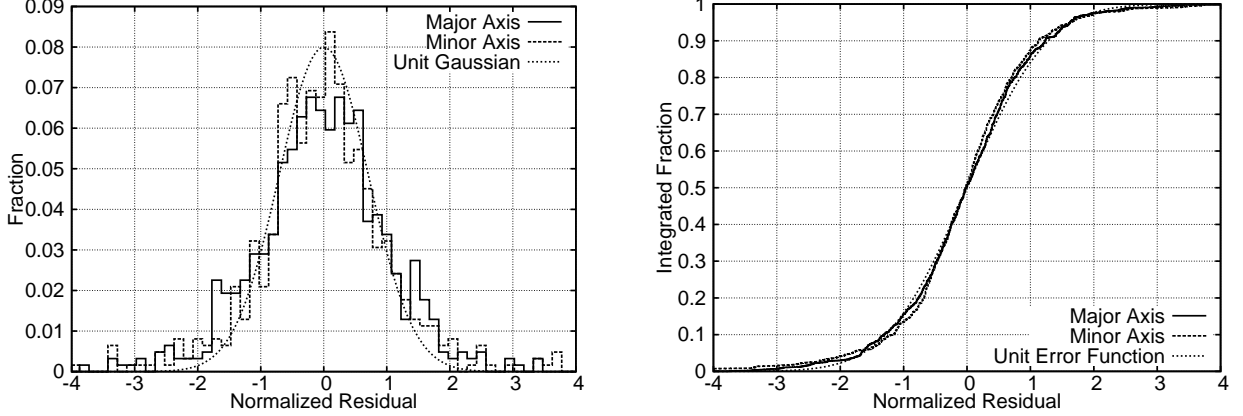


**Figure 7.** Distributions of normalized residuals for two-body Keplerian fits to 20 binaries, in major and minor axes. On the left is the histogram of the residuals and unit-width Gaussian for comparison, while on the right is the continuous distribution function, with the theoretical distribution for Gaussian noise (the error function).

Science and Higher Education through grant N203 3020 35.

*Facilities:* PO:PTI, Keck I

## REFERENCES

- B. W. Carroll and D. A. Ostlie. *An introduction to modern astrophysics*. Reading, MA: Addison-Wesley, —c1996, 1996.
- M. M. Colavita. Adverse effects in dual-feed interferometry. *NAR*, 53:344–352, November 2009.  
doi:10.1016/j.newar.2010.07.004.
- M. M. Colavita, J. K. Wallace, B. E. Hines, Y. Gursel, F. Malbet, D. L. Palmer, X. P. Pan, M. Shao, J. W. Yu, A. F. Boden, P. J. Dumont, J. Gubler, C. D. Koresko, S. R. Kulkarni, B. F. Lane, D. W. Mobley, and G. T. van Belle. The Palomar Testbed Interferometer. *ApJ*, 510:505–521, January 1999.
- A. N. Cox. *Allen's astrophysical quantities*. Allen's astrophysical quantities, 4th ed. Publisher: New York: AIP Press; Springer, 2000. Edited by Arthur N. Cox. ISBN: 0387987460, 2000.
- G. H. Kaplan, J. A. Hughes, P. K. Seidelmann, C. A. Smith, and B. D. Yallop. Mean and apparent place computations in the new IAU system. III - Apparent, topocentric, and astrometric places of planets and stars. *AJ*, 97:1197–1210, April 1989.
- B. F. Lane and M. M. Colavita. Phase-referenced Stellar Interferometry at the Palomar Testbed Interferometer. *AJ*, 125:1623–1628, March 2003.
- B. F. Lane and M. W. Mutterspaugh. Differential Astrometry of Subarcsecond Scale Binaries at the Palomar Testbed Interferometer. *ApJ*, 601:1129–1135, February 2004.
- A. F. Lanza, C. De Martino, and M. Rodonò. Astrometric effects of solar-like magnetic activity in late-type stars and their relevance for the detection of extrasolar planets. *New Astronomy*, 13:77–84, February 2008.  
doi:10.1016/j.newast.2007.06.009.
- P. R. Lawson, editor. *Principles of Long Baseline Stellar Interferometry*, 2000.
- L. Lindegren. Atmospheric limitations of narrow-field optical astrometry. *A&A*, 89:41–47, September 1980.
- M. W. Mutterspaugh, B. F. Lane, M. Konacki, B. F. Burke, M. M. Colavita, S. R. Kulkarni, and M. Shao. PHASES High-Precision Differential Astrometry of δ Equulei. *AJ*, 130:2866–2875, December 2005.
- M. W. Mutterspaugh, B. F. Lane, M. Konacki, B. F. Burke, M. M. Colavita, S. R. Kulkarni, and M. Shao. PHASES differential astrometry and the mutual inclination of the V819 Herculis triple star system. *A&A*, 446:723–732, February 2006.
- M. W. Mutterspaugh, B. F. Lane, F. C. Fekel, M. Konacki, B. F. Burke, S. R. Kulkarni, M. M. Colavita, M. Shao, and S. J. Wiktorowicz. Masses, Luminosities, and Orbital Coplanarities of the μ Orionis Quadruple-Star System from Phases Differential Astrometry. *AJ*, 135:766–776, March 2008.  
doi:10.1088/0004-6256/135/3/766.
- M. W. Mutterspaugh, F. C. Fekel, B. F. Lane, W. I. Hartkopf, S. R. Kulkarni, M. Konacki, B. F. Burke, M. M. Colavita, M. Shao, and M. Williamson. The PHASES Differential Astrometry Data Archive IV: The Triple Star Systems 63 Gem A and HR 2896. *Submitted to AJ*, 2010a.
- M. W. Mutterspaugh, W. I. Hartkopf, B. F. Lane, J. O'Connell, M. Williamson, S. R. Kulkarni, M. Konacki, B. F. Burke, M. M. Colavita, M. Shao, and S. J. Wiktorowicz. The PHASES Differential Astrometry Data Archive II: Updated Binary Star Orbits and a Long Period Eclipsing Binary. *Submitted to AJ*, 2010b.
- M. W. Mutterspaugh, B. F. Lane, S. R. Kulkarni, M. Konacki, B. F. Burke, M. M. Colavita, and M. Shao. The PHASES Differential Astrometry Data Archive III: Limits to Tertiary Companions. *Submitted to AJ*, 2010c.
- M. W. Mutterspaugh, B. F. Lane, S. R. Kulkarni, M. Konacki, B. F. Burke, M. M. Colavita, M. Shao, W. I. Hartkopf, A. P. Boss, and M. Williamson. The PHASES Differential Astrometry Data Archive V: Candidate Substellar Companions. *Submitted to AJ*, 2010d.
- W. H. Press, S. A. Teukolsky, W. T. Vetterling, and B. P. Flannery. *Numerical recipes in C: The art of scientific computing*. Cambridge: University Press, —c1992, 2nd ed., 1992.
- J. D. Scargle. Studies in astronomical time series analysis. II - Statistical aspects of spectral analysis of unevenly spaced data. *ApJ*, 263:835–853, December 1982.
- M. Shao and M. M. Colavita. Potential of long-baseline infrared interferometry for narrow-angle astrometry. *A&A*, 262:353–358, August 1992.
- M. Shao and D. H. Staelin. First fringe measurements with a phase-tracking stellar interferometer. *Appl. Opt.*, 19:1519–1522, May 1980.
- F. Svensson and H.-G. Ludwig. Hydrodynamical simulations of convection-related stellar micro-variability. *560:979–*, March 2005.

**Table 5**  
PHASES Astrometry Measurements

HD Number	HJD- 2400000.5	$\delta\text{RA}$ (mas)	$\delta\text{Decl}$ (mas)	$\sigma_{\min}$ ( $\mu\text{as}$ )	$\sigma_{\text{maj}}$ ( $\mu\text{as}$ )	$\phi_e$ (deg)	$\sigma_{\text{RA}}$ ( $\mu\text{as}$ )	$\sigma_{\text{Dec}}$ ( $\mu\text{as}$ )	$\frac{\sigma_{\text{RA},\text{Decl}}^2}{\sigma_{\text{RA}} \sigma_{\text{Decl}}}$	$\sigma_{\min,c}$ ( $\mu\text{as}$ )	$\sigma_{\text{maj},c}$ ( $\mu\text{as}$ )	$\sigma_{\text{RA},c}$ ( $\mu\text{as}$ )	$\sigma_{\text{Decl},c}$ ( $\mu\text{as}$ )	$\frac{\sigma_{\text{RA},\text{Decl}}^2}{\sigma_{\text{RA}} \sigma_{\text{Decl}}}$
4934	54004.36328	-57.0674	-179.9978	27.8	416.4	161.61	395.3	134.0	-0.97578	44.7	559.1	530.8	181.4	-
5286	52894.31345	-681.5589	665.6299	17.8	1360.0	146.08	1128.5	759.1	-0.99960	76.2	1773.5	1472.3	991.7	-
5286	52896.29389	-681.5838	665.5458	19.6	549.6	144.35	446.7	320.8	-0.99717	82.3	728.1	593.6	429.6	-
5286	52897.28803	-681.9351	665.8532	16.4	382.3	144.32	310.7	223.4	-0.99590	71.5	516.3	421.5	306.7	-
5286	53198.45485	-676.2609	690.8888	3.9	213.7	143.53	171.9	127.1	-0.99928	38.0	311.1	251.2	187.4	-
5286	53215.43340	-675.9374	692.1281	7.2	273.5	146.42	227.9	151.4	-0.99838	44.4	382.1	319.3	214.6	-
5286	53222.39706	-676.3939	693.0688	4.1	217.5	144.05	176.1	127.7	-0.99921	38.3	315.5	256.4	187.8	-
5286	53229.40966	-674.7178	692.6724	17.9	1669.5	148.35	1421.2	876.3	-0.99971	76.5	2174.9	1851.8	1143.1	-
5286	53235.41932	-675.2293	693.4864	6.3	197.6	152.60	175.4	91.1	-0.99699	42.4	292.6	260.5	139.8	-
5286	53250.34592	-675.1408	694.9482	13.0	133.2	148.22	113.4	71.0	-0.97667	60.5	222.7	192.0	128.1	-
5286	53578.49345	-667.5496	720.3887	10.6	239.7	155.25	217.7	100.8	-0.99324	53.4	341.6	311.0	151.0	-
5286	53585.41899	-667.3132	720.7603	21.9	1887.5	146.03	1565.4	1054.8	-0.99969	90.3	2457.7	2038.9	1375.3	-
5286	53600.39059	-667.0935	721.9211	20.9	273.1	148.09	232.1	145.4	-0.98558	86.8	381.6	327.2	214.8	-
5286	53632.29638	-666.8551	724.8877	14.2	150.3	146.28	125.3	84.3	-0.97936	64.3	240.4	203.1	143.8	-
5286	53636.28795	-667.6554	725.7109	9.6	98.1	147.56	82.9	53.2	-0.97721	50.6	189.4	162.1	110.2	-
5286	53691.15757	-666.0233	729.6058	7.5	85.8	150.80	75.0	42.3	-0.97949	45.1	179.0	157.8	95.8	-
5286	53957.40057	-659.8107	749.8176	5.1	57.2	147.73	48.5	30.9	-0.98055	35.4	158.5	135.4	89.8	-
5286	53970.37137	-659.5338	750.6116	3.8	44.9	147.90	38.1	24.1	-0.98252	35.2	151.7	129.8	85.9	-
5286	53971.35704	-660.2025	751.1008	6.9	97.3	145.40	80.2	55.5	-0.98873	35.7	188.7	156.6	111.1	-
6811	52894.40088	422.2735	-280.2728	25.9	811.8	159.74	761.6	282.1	-0.99521	104.5	1064.6	999.4	381.4	-
6811	52895.40411	422.3082	-280.3050	19.6	376.1	160.62	354.8	126.1	-0.98635	82.3	508.6	480.5	185.8	-
6811	52896.40601	411.4655	-275.8378	30.4	395.5	158.80	368.9	145.8	-0.97461	120.7	532.9	498.7	223.2	-
6811	52897.38891	422.7105	-280.3014	26.7	998.1	158.42	928.2	367.9	-0.99694	107.3	1305.1	1214.2	490.3	-
6811	53222.50651	426.1493	-277.4293	5.2	118.3	161.03	111.9	38.8	-0.98974	40.2	208.0	197.1	77.6	-
6811	53228.48820	424.8371	-276.7571	16.5	621.1	160.37	585.1	209.3	-0.99647	71.8	819.5	772.2	283.5	-
6811	53263.39025	426.2968	-276.7695	9.9	263.6	159.41	246.7	93.1	-0.99351	51.4	370.2	347.0	138.8	-
6811	53271.37223	426.4827	-276.6943	10.1	126.2	160.62	119.1	42.9	-0.96867	51.9	215.7	204.2	86.7	-
6811	53313.25700	427.3890	-276.3916	22.3	270.8	160.25	255.0	93.9	-0.96777	91.7	378.9	357.9	154.4	-
6811	53636.36731	430.7551	-273.1652	15.8	592.3	158.72	551.9	215.5	-0.99690	69.5	782.6	729.7	291.3	-
6811	53663.36469	424.8200	-272.0314	26.9	1466.0	175.11	1460.7	127.9	-0.97740	108.0	1910.9	1904.0	195.3	-
6811	53687.19475	431.4921	-272.0317	27.4	230.6	22.43	213.4	91.5	0.94638	109.8	330.9	308.7	162.0	-
6811	53972.46365	433.3682	-269.1288	16.5	400.9	163.19	383.8	117.0	-0.98914	38.7	539.6	516.7	160.4	-
6811	54003.36229	434.3438	-269.0321	12.5	556.2	158.67	518.1	202.6	-0.99782	37.2	736.5	686.2	270.1	-
6811	54006.35815	433.6679	-268.6007	24.4	414.3	159.97	389.4	143.8	-0.98361	42.7	556.5	523.0	194.8	-
6811	54008.35403	433.9942	-268.7999	8.5	110.9	159.82	104.1	39.1	-0.97295	36.0	201.0	189.0	77.1	-
6811	54341.44154	437.0441	-264.9185	17.3	361.7	160.07	340.1	124.4	-0.98896	74.5	490.6	461.9	181.3	-
6811	54350.42520	437.1835	-264.9587	8.6	124.5	161.89	118.4	39.5	-0.97365	47.9	214.0	203.9	80.6	-
6811	54357.40553	437.5387	-264.8896	18.4	314.6	161.36	298.2	102.0	-0.98180	78.2	432.3	410.4	156.8	-
6811	54769.28217	441.7437	-260.4480	35.0	1055.9	162.13	1005.0	325.8	-0.99359	49.5	1379.8	1313.3	426.0	-
11636	53638.46558	24.8811	-10.4154	10.6	313.6	39.98	240.4	201.7	0.99764	53.4	431.0	332.1	280.0	-
13872	52868.45994	-134.4324	4.9165	19.5	2025.3	149.53	1745.7	1027.0	-0.99976	82.0	2636.6	2272.9	1338.9	-
13872	53215.50012	-144.8076	-14.6601	28.0	1083.3	148.43	923.1	567.7	-0.99832	112.0	1415.2	1207.2	747.1	-
13872	53222.46534	-143.9341	-15.6965	5.5	212.2	145.90	175.8	119.1	-0.99845	40.8	309.4	257.2	176.7	-
13872	53234.45075	-144.5008	-16.2052	16.8	179.2	149.25	154.2	92.7	-0.97750	72.8	271.8	236.5	152.4	-
13872	53249.46019	-144.8697	-17.0067	6.2	49.3	157.43	45.6	19.8	-0.93981	42.2	154.0	143.1	70.8	-
13872	53250.46337	-144.6809	-17.1576	31.6	488.9	159.08	456.8	177.1	-0.98155	125.1	650.8	609.5	260.1	-
13872	53263.40075	-145.2831	-17.7597	6.3	51.7	153.42	46.4	23.8	-0.95598	42.4	155.3	140.2	79.2	-
13872	53271.38426	-145.3640	-18.2781	5.5	45.8	154.32	41.4	20.5	-0.95411	40.8	152.1	138.2	75.5	-
13872	53312.30383	-146.5058	-20.3929	2.7	31.5	160.49	29.7	10.8	-0.96334	36.5	145.9	138.0	59.6	-
13872	53313.28343	-147.1579	-20.1609	10.7	417.5	156.00	381.4	170.1	-0.99761	53.6	560.5	512.5	233.2	-
13872	53333.23983	-146.8661	-21.5534	8.8	231.2	158.14	214.6	86.5	-0.99400	48.4	331.6	308.3	131.4	-
13872	53334.25787	-148.3531	-21.1557	18.4	1427.2	162.48	1361.0	430.0	-0.99899	78.2	1860.6	1774.5	565.1	-
13872	53340.19672	-147.4399	-21.7883	20.1	960.2	153.66	860.5	426.5	-0.99862	84.0	1256.1	1126.3	562.4	-
13872	53341.24624	-147.7720	-21.7435	25.5	1154.0	164.19	1110.4	315.4	-0.99646	103.0	1506.7	1450.0	422.3	-
13872	53358.47779	-151.6375	-34.5213	21.7	690.1	146.43	575.1	382.0	-0.99768	89.6	908.0	758.2	507.6	-
13872	53586.47768	-151.4689	-34.7058	9.9	121.5	147.59	102.7	65.7	-0.98387	51.4	211.1	180.3	121.2	-
13872	53599.45344	-152.3887	-34.8899	19.7	979.5	148.68	836.8	509.4	-0.99898	82.6	1281.0	1095.2	669.6	-
13872	53606.44225	-151.5573	-35.3871	9.0	275.7	150.03	238.8	137.9	-0.99716	48.9	384.8	334.2	196.8	-
13872	53607.43452	-151.2101	-36.0727	12.4	422.4	149.08	362.4	217.3	-0.99778	58.7	566.7	487.1	295.5	-
13872	53613.41692	-151.9164	-35.9521	23.1	826.9	148.91	708.2	427.5	-0.99800	94.5	1084.0	929.6	565.6	-
13872	53614.41517	-151.7623	-36.2031	26.2	1064.2	148.83	910.6	551.3	-0.99846	105.5	1390.5	1191.0	725.3	-
13872	53639.35205	-151.7435	-37.6653	20.2	1070.3	149.46	921.8	544.2	-0.99907	84.4	1398.4	1205.2	714.3	-
13872	53670.28242	-151.3679	-39.3993	38.5	1039.2	151.85	916.5	491.4	-0.99605	150.4	1358.2	1199.6	654.4	-
13872	53691.18919	-152.6309	-39.7322	14.6	118.9	148.36	101.5	63.6	-0.96314	65.6</td				

**Table 5**  
PHASES Astrometry Measurements

13872	53935.47952	-151.9327	-51.4370	21.3	896.2	141.49	701.4	558.2	-0.99881	41.0	1173.4	918.6	731.3
13872	53936.48606	-151.7695	-51.6402	7.1	195.4	142.94	156.0	117.9	-0.99718	35.7	290.0	232.5	177.1
13872	53937.48724	-151.9168	-51.5570	4.4	116.0	143.48	93.2	69.1	-0.99684	38.8	205.8	167.0	126.4
13872	53951.44870	-151.7068	-52.1619	15.7	351.3	143.26	281.7	210.5	-0.99565	38.4	477.7	383.5	287.4
13872	53956.48858	-151.5248	-52.5074	4.3	48.8	152.38	43.3	23.0	-0.97759	35.3	153.7	137.2	77.8
13872	53957.44792	-151.3560	-52.6303	7.2	125.5	145.75	103.8	70.9	-0.99248	35.7	215.0	178.8	124.5
13872	53958.48472	-151.5132	-52.5578	8.8	72.8	152.17	64.5	34.9	-0.95903	36.1	169.0	150.4	85.1
13872	53963.46233	-151.5164	-52.7090	30.3	292.0	150.43	254.4	146.5	-0.97146	46.3	404.6	352.6	203.7
13872	53965.50072	-151.5046	-52.8522	4.9	59.3	158.31	55.2	22.4	-0.97196	35.3	159.8	149.1	67.6
13872	53970.40460	-151.2200	-53.1663	6.6	114.1	143.60	91.9	67.9	-0.99263	35.6	204.0	165.5	124.4
13872	53971.49071	-150.9509	-53.2562	15.3	84.3	157.82	78.3	34.9	-0.88075	38.2	177.8	165.3	75.9
13872	53972.40215	-150.9837	-53.4119	10.3	152.6	144.73	124.7	88.5	-0.98973	36.5	242.8	199.4	143.3
13872	53977.40389	-150.9146	-53.6256	8.1	233.8	146.35	194.7	129.7	-0.99716	35.9	334.6	279.3	187.8
13872	53978.44990	-151.3107	-53.4354	7.2	45.9	154.75	41.6	20.6	-0.92351	35.7	152.2	138.5	72.5
13872	53979.48348	-151.3883	-53.4012	18.7	362.6	161.35	343.6	117.3	-0.98576	39.7	491.7	466.1	161.7
13872	53985.43797	-151.6481	-53.5143	9.6	239.1	155.73	218.0	98.6	-0.99429	36.3	340.9	311.1	144.0
13872	53986.38174	-150.7794	-53.9608	26.9	451.2	147.18	379.5	245.6	-0.99149	44.1	603.0	507.3	328.9
13872	53996.32588	-151.1242	-54.0624	8.3	117.1	142.31	92.8	71.9	-0.98925	36.0	206.8	165.1	129.6
13872	54003.37200	-150.7523	-54.5566	8.4	46.6	153.62	41.9	22.0	-0.90585	36.0	152.5	137.6	75.1
13872	54004.32755	-150.7397	-54.5913	14.3	75.8	145.35	62.9	44.7	-0.92271	37.8	171.2	142.5	102.2
13872	54005.38271	-150.9772	-54.4755	12.7	71.8	157.90	66.7	29.5	-0.88566	37.2	168.3	156.5	72.1
13872	54006.38793	-150.5945	-54.7009	11.3	78.5	158.98	73.4	30.1	-0.91518	36.8	173.2	162.3	71.0
13872	54007.40917	-150.4264	-54.8060	6.0	167.7	161.80	159.4	52.7	-0.99280	35.5	259.1	246.4	87.7
13872	54008.36643	-150.7097	-54.7213	6.6	74.6	154.63	67.5	32.5	-0.97412	35.6	170.3	154.6	79.8
13872	54009.33295	-150.6374	-54.7549	16.1	70.2	147.98	60.2	39.7	-0.88013	38.5	167.1	143.2	94.4
13872	54010.43151	-150.6045	-54.8265	37.0	249.7	168.10	244.5	62.9	-0.80000	50.9	353.5	346.1	88.3
13872	54029.25388	-150.1810	-55.6599	16.0	125.1	144.61	102.4	73.6	-0.96399	38.5	214.6	176.4	128.2
13872	54031.35220	-150.3564	-55.7080	27.5	296.3	162.81	283.2	91.4	-0.94929	44.5	409.8	391.8	128.4
13872	54032.28753	-150.1185	-55.8089	26.2	122.2	152.72	109.3	60.6	-0.87580	43.7	211.7	189.3	104.5
13872	54055.29473	-149.6837	-56.6572	10.5	75.3	168.50	73.8	18.2	-0.80786	36.5	170.8	167.6	49.4
13872	54056.27674	-149.6402	-56.7221	9.8	84.1	161.60	79.9	28.1	-0.93069	36.3	177.6	168.9	65.8
13872	54061.26736	-149.6525	-56.9097	23.2	214.0	161.51	203.1	71.4	-0.93932	42.0	311.4	295.7	106.5
13872	54075.19906	-149.2366	-57.4598	11.9	66.8	157.71	62.0	27.6	-0.88510	37.0	164.7	153.1	71.2
13872	54083.18848	-148.7537	-57.8983	33.6	271.4	157.82	251.6	107.1	-0.94091	48.5	379.6	352.0	150.2
13872	54084.15457	-148.7872	-57.9119	28.1	237.5	153.46	212.8	109.0	-0.95781	44.9	339.0	303.9	156.7
13872	54306.50056	-140.2172	-65.2065	10.3	236.8	146.72	198.1	130.3	-0.99550	36.5	338.2	283.4	188.1
13872	54320.50160	-139.5456	-65.4951	7.2	184.2	152.76	163.8	84.6	-0.99540	44.4	277.4	247.5	133.0
13872	54321.48036	-140.1975	-65.0709	26.4	1400.9	149.35	1205.3	714.4	-0.99007	106.3	1826.5	1572.3	935.6
13872	54335.47793	-138.5053	-65.9154	10.1	106.6	155.70	97.2	44.8	-0.96914	51.9	197.0	180.8	93.9
13872	54336.47475	-138.5287	-65.9115	7.1	87.3	155.45	79.5	36.8	-0.97763	44.2	180.2	165.0	85.0
13872	54341.39967	-138.9760	-65.4734	22.5	865.2	145.33	711.7	492.5	-0.99846	92.4	1133.4	933.7	649.2
13872	54348.40089	-137.5612	-66.3738	15.2	312.9	148.94	268.1	162.0	-0.99400	67.5	430.2	370.2	229.4
13872	54350.42515	-137.4713	-66.3429	9.4	69.0	154.52	62.4	30.9	-0.94159	50.0	166.3	151.6	84.6
13872	54356.42061	-137.2160	-66.4234	6.3	61.1	155.82	55.8	25.7	-0.96365	42.4	161.0	147.9	76.4
13872	54357.35796	-136.6772	-66.6918	19.8	700.8	145.41	577.1	398.2	-0.99817	83.0	921.7	760.3	527.7
13872	54370.39212	-136.2901	-66.7839	7.7	89.3	157.78	82.7	34.5	-0.97087	45.6	181.9	169.2	80.7
13872	54376.32513	-136.3925	-66.5157	30.9	920.9	148.30	783.7	484.6	-0.99719	122.5	1205.3	1027.5	641.9
13872	54377.39723	-135.9560	-66.7954	24.3	84.5	160.67	80.1	36.1	-0.70637	98.8	178.0	171.1	110.2
13872	54419.26390	-132.8213	-67.6774	10.5	131.4	158.73	122.5	48.6	-0.97272	53.1	220.9	206.7	94.2
13872	54685.47397	-103.8655	-67.3995	10.8	145.4	148.45	124.0	76.6	-0.98619	36.6	235.2	201.4	127.0
13872	54695.48895	-102.5878	-66.9776	18.7	283.4	155.34	257.7	119.5	-0.98513	39.7	394.1	358.6	168.3
13872	54713.46790	-99.9635	-66.4378	24.6	442.3	160.83	417.8	147.1	-0.98415	42.8	591.8	559.1	198.5
13872	54740.39294	-95.4755	-65.4747	15.9	90.1	160.30	85.0	33.9	-0.86767	38.4	182.5	172.3	71.4
13872	54763.34251	-91.4004	-64.5013	10.9	68.1	161.32	64.6	24.1	-0.87997	36.7	165.6	157.4	63.4
13872	54769.34859	-90.4781	-64.1907	15.0	71.9	167.92	70.4	21.0	-0.68485	38.1	168.3	164.8	51.3
13872	54794.26958	-85.6181	-62.9320	19.3	80.1	162.77	76.7	30.0	-0.74244	40.0	174.5	167.1	64.3
16234	53242.45987	47.2253	-57.0737	21.9	147.4	22.05	136.8	58.9	0.91675	90.3	237.3	222.6	122.2
16234	53272.50347	48.6455	-53.4479	12.4	303.0	176.11	302.3	24.0	-0.85551	58.7	418.0	417.1	65.1
16234	53284.34866	50.1017	-51.6841	26.4	269.7	22.53	249.4	106.2	0.96310	106.3	377.5	351.1	174.8
16234	53986.48518	50.5112	-50.5456	12.6	133.1	161.93	126.6	43.0	-0.95139	37.2	222.6	211.9	77.6
16234	54003.45071	50.2442	-47.4788	9.9	51.1	162.07	48.7	18.3	-0.82398	36.4	155.0	147.9	58.9
16739	53243.52050	31.6286	-43.4840	15.8	332.3	33.41	277.5	183.4	0.99466	69.5	454.1	381.0	256.7
16739	54447.20268	-19.2362	-37.7102	32.3	242.8	156.55	223.1	101.1	-0.93761	47.6	345.3	317.3	144.2
16739	54763.30273	-22.8473	-26.1662	4.3	133.5	150.40	116.1	66.0	-0.99721	35.3	223.0	194.7	114.3
17904	52868.49771	-54.7748	193.1608	15.1	252.1	151.25	221.2	122.0	-0.98995	67.2	356.4	314.1	181.3
17904	52895.47559	-56.0072	192.9863	15.0	332.0	161.33	314.6	107.2	-0.98899	66.9	453.7	430.4	158.5
17904	52896.45244	-56.9743	193.4265	24.7	1125.4	156.97	1035.8	440.8	-0.99814	100.2	1469.7	1353.1	582.3
17904	52915.44772	-56.7591	192.9154	25.0	542.2	166.40	527.1	129.8	-0.98012	101.2	718.6	698.9	195.5
17904	52919.38659	-57.1669	192.9632	23.9	673.6	156.02	615.6	274.6	-0.99546	97.3	886.8	811.2	371.2
17904	52951.32546	-59.0320	192.9003	26.3	934.3	161.49	886.0	297.7	-0.99566	105.9	1222.6	1159.9	400.9
17904	52979.24870	-59.2207	192.5059	24.6	496.9	160.95	469.7	163.8	-0.98734	99.8	661.0	625.6	235.5</

**Table 5**  
PHASES Astrometry Measurements

17904	53263.49057	-72.1259	190.7931	14.7	393.5	166.40	382.5	93.6	-0.98685	65.9	530.4	515.7	140.2
17904	53284.42312	-72.7156	190.3493	16.4	145.5	33.77	121.3	82.0	0.97089	71.5	235.3	199.6	143.7
17904	53285.36332	-72.4170	190.4805	21.0	201.7	22.00	187.2	78.0	0.95683	87.1	297.2	277.5	137.6
17904	53312.38452	-74.6204	190.2752	13.3	367.1	171.53	363.1	55.7	-0.97047	61.5	497.3	492.0	95.2
17904	53333.27871	-75.3351	190.1275	28.2	1597.9	160.94	1510.3	522.5	-0.99837	112.7	2082.0	1968.2	688.2
17904	53334.28896	-74.9998	189.9412	16.1	210.9	162.09	200.8	66.7	-0.96714	70.5	307.8	293.7	116.0
17904	53593.48089	-85.6820	186.4908	15.5	239.9	12.96	233.9	55.9	0.95883	68.5	341.9	333.5	101.7
17904	53599.50102	-85.7398	186.2555	13.2	247.3	152.42	219.3	115.1	-0.99157	61.2	350.7	312.1	171.2
17904	53670.34114	-88.3975	185.1358	15.1	210.6	156.85	193.7	84.0	-0.98080	67.2	307.5	284.0	135.8
17904	53676.29680	-88.0306	184.5033	26.4	863.3	152.18	763.6	403.5	-0.99726	106.3	1131.0	1001.5	536.1
17904	53687.21628	-90.5435	184.9247	19.6	115.9	11.09	113.8	29.4	0.73496	82.3	205.7	202.5	89.9
17904	53705.23989	-90.1875	184.6091	30.9	261.5	158.62	243.8	99.6	-0.94297	122.5	367.6	345.3	176.0
17904	53746.19958	-91.0840	183.8636	24.5	432.5	172.21	428.6	63.5	-0.92075	99.5	579.4	574.2	126.0
17904	53957.50712	-100.2106	180.0509	5.9	129.9	150.03	112.5	65.1	-0.99459	35.5	219.4	190.9	113.8
17904	53971.47164	-100.8707	179.7833	18.3	382.4	150.06	331.5	191.5	-0.99392	39.5	516.5	448.0	260.0
17904	53977.45176	-101.1291	179.6746	9.7	248.0	149.59	214.0	125.8	-0.99600	36.3	351.5	303.7	180.7
17904	53978.46943	-100.9825	179.5559	10.6	112.7	152.21	99.9	53.4	-0.97436	36.6	202.6	180.1	99.9
17904	54003.41510	-101.8039	179.0073	12.4	70.4	154.36	63.7	32.4	-0.90678	37.1	167.3	151.6	79.7
17904	54075.21871	-104.4772	177.4768	19.3	153.1	156.32	140.5	64.0	-0.94421	40.0	243.3	223.4	104.4
17904	54321.51425	-113.3554	171.5662	9.5	282.9	150.83	247.1	138.1	-0.99690	50.3	393.5	344.5	196.8
17904	54335.50232	-114.1699	171.3764	7.7	88.7	156.89	81.6	35.5	-0.97185	45.6	181.4	167.8	82.6
17904	54336.49358	-114.0004	171.2792	6.5	63.1	154.18	56.9	28.1	-0.96614	42.8	162.3	147.2	80.5
17904	54343.45469	-114.3753	171.1791	6.9	189.5	150.41	164.8	93.8	-0.99640	43.7	283.4	247.3	145.0
17904	54349.44708	-114.4152	170.9166	8.3	89.3	151.16	78.3	43.7	-0.97633	47.1	181.9	160.9	97.0
17904	54356.41519	-114.8098	170.8137	7.5	238.5	149.43	205.4	121.5	-0.99742	45.1	340.2	293.8	177.3
17904	54370.41375	-115.3712	170.5431	7.4	43.1	155.51	39.3	19.1	-0.90458	44.9	150.8	138.5	74.7
17904	54385.35724	-115.5743	170.0673	32.9	254.8	150.95	223.3	127.0	-0.95533	129.8	359.6	320.6	208.3
17904	54419.26027	-116.7572	169.0748	14.3	215.0	151.68	189.4	102.8	-0.98748	64.6	312.6	276.9	158.8
17904	54713.47536	-126.7889	161.1280	21.0	173.5	157.37	160.4	69.5	-0.94508	40.8	265.5	245.5	108.9
17904	54740.40809	-127.8307	160.4343	24.9	173.7	157.78	161.1	69.6	-0.92237	43.0	265.7	246.5	108.1
17904	54763.34405	-129.1195	159.9749	22.3	300.2	156.05	274.5	123.6	-0.98026	41.5	414.6	379.3	172.5
17904	54769.33578	-128.8847	159.5838	23.6	247.6	157.51	229.0	97.2	-0.96477	42.2	351.0	324.7	139.8
17904	54794.26290	-129.6028	158.8408	22.4	281.1	157.05	259.0	111.5	-0.97603	41.6	391.3	360.7	157.3
19356	54468.24107	-33.3272	17.2516	14.2	148.6	172.17	147.2	24.6	-0.81447	37.8	238.6	236.4	49.6
26690	52895.52618	-60.6904	111.7775	30.8	1059.7	158.16	983.7	395.2	-0.99647	122.2	1384.7	1286.1	527.5
26690	52896.49745	-61.1543	111.9381	29.2	1768.6	153.09	1577.1	800.9	-0.99916	116.3	2303.4	2054.7	1047.7
26690	52951.36244	-50.4678	105.9390	13.4	397.7	155.40	361.6	166.0	-0.99603	61.8	535.6	487.7	229.9
26690	53620.53066	57.4978	-81.3535	23.8	698.3	156.26	639.3	281.9	-0.99575	97.0	918.5	841.7	380.3
26690	53663.40922	53.3058	-87.0778	6.9	115.2	155.27	104.7	48.6	-0.98759	43.7	205.0	187.1	94.5
26690	53676.35969	50.6665	-83.1246	24.6	833.9	152.41	739.1	386.8	-0.99742	99.8	1093.1	969.9	513.9
26690	53691.31987	50.0569	-89.9745	9.9	95.1	153.81	85.5	42.9	-0.96616	51.4	186.8	169.1	94.5
26690	53732.22590	43.9410	-92.1914	13.9	248.4	155.52	226.1	103.7	-0.98914	63.4	352.0	321.4	156.8
26690	53977.50681	0.4743	-81.3542	9.2	270.6	148.49	230.8	141.7	-0.99710	36.2	378.6	323.3	200.3
26690	53979.52302	-0.8235	-80.5741	24.8	950.6	151.80	837.8	449.7	-0.99804	42.9	1243.7	1096.3	588.9
26690	54003.41073	-5.8826	-77.3104	18.0	2195.5	145.06	1799.7	1257.5	-0.99985	39.4	2857.6	2342.6	1636.9
26690	54075.26912	-18.5487	-68.1538	7.9	86.1	153.16	76.9	39.5	-0.97436	35.9	179.2	160.8	87.0
26690	54342.51646	-64.3062	-21.2231	11.8	251.1	149.79	217.1	126.8	-0.99416	56.9	355.2	308.3	185.4
26690	54343.50565	-64.2432	-21.1709	4.7	135.5	148.57	115.7	70.8	-0.99699	39.3	225.0	193.1	122.0
26690	54348.52167	-64.6958	-20.2642	13.9	259.8	153.69	233.0	115.8	-0.99096	63.4	365.6	328.9	171.7
26690	54356.47952	-66.1069	-18.6432	7.4	260.7	149.84	225.4	131.1	-0.99787	44.9	366.7	317.8	188.3
26690	54369.45682	-67.8037	-16.2381	14.3	330.3	152.04	291.8	155.4	-0.99455	64.6	451.6	400.1	219.3
26690	54370.45481	-68.7716	-15.5673	6.4	148.2	151.88	130.7	70.1	-0.99460	42.6	238.2	211.0	118.4
26690	54376.43547	-69.5418	-14.5283	13.1	300.9	151.37	264.1	144.6	-0.99467	60.9	415.5	365.8	206.1
26690	54425.27913	-76.2399	-5.0107	23.6	796.7	147.61	672.8	427.3	-0.99787	96.3	1045.1	884.0	565.7
28307	54468.21255	-28.9516	24.9986	15.7	147.4	152.73	131.2	68.9	-0.96662	38.4	237.3	211.7	114.0
29140	52979.33952	-32.1749	-101.5914	8.3	191.2	163.71	183.5	54.2	-0.98733	47.1	285.3	274.1	91.9
29140	53034.13427	-40.3178	-91.5427	5.6	124.7	152.78	111.0	57.3	-0.99394	41.0	214.2	191.4	104.5
29140	53250.50243	-65.6824	-53.5439	16.1	710.2	147.24	597.3	384.5	-0.99876	70.5	933.8	786.2	508.8
29140	53263.53075	-68.2378	-50.0532	5.0	119.6	158.10	111.0	44.9	-0.99268	39.8	209.2	194.7	86.3
29140	53271.46792	-70.0370	-48.2688	6.6	267.9	150.15	232.4	133.5	-0.99836	43.1	375.4	326.3	190.5
29140	53291.40263	-71.5816	-44.8765	35.3	703.7	148.37	599.5	370.3	-0.99371	138.6	925.5	791.3	499.5
29140	53294.47732	-71.0249	-44.6002	12.9	680.3	164.09	654.2	186.9	-0.99742	60.2	895.4	861.3	252.2
29140	53312.38161	-74.1286	-40.9474	3.1	27.2	154.15	24.5	12.2	-0.95879	36.9	144.4	130.9	71.2
29140	53320.33469	-74.5083	-39.6051	16.1	830.4	150.23	720.8	412.6	-0.99899	70.5	1088.6	945.5	543.9
29140	53334.32195	-76.1005	-36.8198	8.5	333.3	154.46	300.8	143.9	-0.99785	47.6	455.3	411.4	201.0
29140	53340.29375	-77.4849	-35.5086	7.3	86.1	152.98	76.7	39.6	-0.97862	44.7	179.2	161.0	90.6
29140	53341.28189	-77.5106	-35.2744	6.9	220.6	150.70	192.4	108.1	-0.99734	43.7	319.1	279.1	160.8
29140	53605.52839	-104.7430	15.6169	7.3	382.6	147.65	323.2	204.8	-0.99911	44.7	516.7	437.2	279.0
29140	53606.51646	-106.5086	16.8979	6.3	389.0	146.14	323.0	216.8	-0.99939	42.4	524.7	436.4	294.5
29140	53613.51062	-105.2544	17.0220	9.3	312.5	147.80	264.5	166.7	-0.99781	49.7	429.7	364.6	232.8
29140	53614.50772	-105.6802	17.1894	10.2	309.4	147.94	262.3						

**Table 5**  
PHASES Astrometry Measurements

29140	54055.38704	-136.2414	98.5399	19.2	348.0	161.74	330.5	110.6	-0.98318	39.9	473.6	449.9	153.1
29140	54061.37315	-136.6954	99.4920	6.5	120.8	163.08	115.6	35.7	-0.98164	35.6	210.4	201.5	70.1
29140	54075.33237	-136.8559	101.6153	5.4	99.8	162.18	95.0	31.0	-0.98298	35.4	190.9	182.0	67.4
29140	54083.30631	-137.8506	103.1454	12.6	275.5	161.39	261.1	88.7	-0.98863	37.2	384.5	364.6	127.7
29140	54084.31264	-136.7974	103.1035	25.5	696.6	163.11	666.6	203.8	-0.99139	43.3	916.3	876.9	269.4
29140	54103.25527	-137.6727	106.3288	17.1	404.7	162.34	385.7	123.8	-0.98949	39.0	544.4	518.9	169.3
29140	54138.15393	-139.3240	112.2447	11.4	183.2	161.39	173.6	59.5	-0.97917	36.8	276.3	262.1	94.8
29140	54349.52640	-143.0809	143.4811	5.7	127.3	152.85	113.3	58.3	-0.99386	41.2	216.8	193.8	105.5
29140	54384.45472	-142.3448	147.7776	14.6	453.7	156.65	416.6	180.4	-0.99612	65.6	606.2	557.2	247.7
30090	54007.52586	-48.9471	51.9661	18.7	268.0	165.19	259.2	70.8	-0.96217	39.7	375.5	363.1	103.4
30090	54008.52179	-48.2120	51.8597	13.1	228.3	164.52	220.1	62.2	-0.97575	37.4	328.2	316.4	94.7
30090	54356.52411	-58.9350	79.8443	15.2	368.1	155.47	334.9	153.4	-0.99407	67.5	498.6	454.5	215.9
40932	53271.50038	59.1469	105.9933	5.2	281.6	146.70	235.4	154.7	-0.99918	40.2	391.9	328.3	217.8
40932	53285.47135	61.8963	110.1620	8.5	217.9	19.95	204.8	74.8	0.99273	47.6	316.0	297.5	116.7
40932	53290.47993	62.4497	112.0044	22.9	1175.7	151.07	1029.0	569.1	-0.99894	93.8	1534.8	1344.0	747.0
40932	53312.46235	66.0452	119.6805	3.0	62.6	158.79	58.3	22.8	-0.98982	36.8	161.9	151.6	67.9
40932	53334.41285	69.4570	127.2486	6.7	136.0	160.77	128.4	45.2	-0.98775	43.3	225.5	213.4	84.8
40932	53340.38026	70.2143	128.6950	8.7	95.5	157.63	88.4	37.2	-0.96792	48.1	187.1	174.0	84.0
40932	53341.34797	70.4710	129.3401	7.7	84.7	153.15	75.7	38.9	-0.97538	45.6	178.1	160.2	90.2
40932	53639.51369	104.4656	211.4485	9.4	131.0	149.61	113.1	66.8	-0.98653	50.0	220.5	191.8	119.6
40932	53663.47710	106.2449	217.1611	6.0	70.2	153.87	63.0	31.4	-0.97702	41.8	167.1	151.2	82.6
40932	53698.43976	110.2453	225.7801	27.1	516.9	37.76	409.0	317.2	0.99417	108.8	686.4	546.7	429.0
40932	53705.34728	108.6099	226.3862	32.5	1039.0	151.29	911.5	499.9	-0.99724	128.4	1357.9	1192.6	662.0
40932	53732.29770	111.8056	231.4895	11.6	108.3	156.29	99.3	44.8	-0.95961	56.3	198.5	183.2	95.0
40932	53753.23345	113.4811	235.7264	25.3	200.4	158.08	186.2	78.4	-0.93783	102.3	295.8	277.0	145.6
40932	53789.18175	117.7651	244.3028	27.4	1326.5	36.86	1061.4	796.1	0.99908	109.8	1730.1	1385.8	1041.5
40932	54056.41997	131.6216	287.8565	20.5	161.6	159.05	151.1	60.9	-0.93262	40.6	252.5	236.2	97.9
40932	54061.42509	132.3700	288.4524	17.8	335.4	161.71	318.5	106.6	-0.98450	39.3	457.9	435.0	148.5
40932	54103.32274	134.6930	294.9206	25.9	616.3	163.89	592.2	172.8	-0.98779	43.5	813.3	781.5	229.5
40932	54376.53421	143.7491	326.7842	16.1	246.3	156.47	225.9	99.4	-0.98427	70.5	349.5	321.6	153.8
40932	54384.53862	144.3181	327.8358	19.1	398.7	161.42	378.0	128.3	-0.98766	80.6	536.9	509.5	187.3
40932	54391.50585	144.4388	328.8837	32.3	584.0	158.22	542.5	218.7	-0.98730	127.6	772.0	718.5	310.0
41116	52979.30446	-66.3021	-208.2956	26.8	1525.0	147.21	1282.2	826.1	-0.99926	107.7	1987.4	1671.8	1080.1
41116	53294.53873	-88.2656	-155.7271	4.6	92.1	166.41	89.6	22.1	-0.97711	39.1	184.2	179.3	57.6
41116	53333.48253	-89.7805	-148.6646	8.9	131.9	177.46	131.8	10.7	-0.54724	48.7	221.4	221.2	49.6
41116	53340.45440	-90.9105	-146.6141	6.0	59.9	172.85	59.4	9.5	-0.77520	41.8	160.2	159.0	46.0
41116	53341.40117	-91.1426	-146.4472	5.5	34.1	164.67	32.9	10.5	-0.83856	40.8	146.9	142.0	55.3
41116	53446.17307	-95.9927	-125.5838	21.1	546.1	178.11	545.8	27.7	-0.64874	87.5	723.6	723.2	90.6
41116	53632.51409	-101.1302	-86.5536	5.7	79.0	148.68	67.6	41.4	-0.98712	41.2	173.6	149.9	96.9
41116	53637.49803	-101.6928	-84.5006	17.0	325.4	148.11	276.4	172.5	-0.99325	73.5	445.6	380.3	243.5
41116	53639.48943	-101.3809	-84.4832	5.2	77.6	148.27	66.1	41.1	-0.98900	40.2	172.6	148.3	97.0
41116	53648.46693	-102.0040	-82.1033	3.8	85.2	147.36	71.8	46.1	-0.99514	37.9	178.5	151.7	101.4
41116	53676.48593	-102.6684	-75.5939	7.6	56.0	164.94	54.1	16.3	-0.87684	45.4	157.8	152.8	60.0
41116	53690.37578	-101.8137	-73.7882	16.0	163.8	150.02	142.1	83.0	-0.97506	70.2	254.8	223.5	141.1
41116	53725.40629	-103.4052	-64.3701	7.3	97.8	177.25	97.7	8.7	-0.53915	44.7	189.1	188.9	45.5
41116	53747.28929	-102.5682	-60.3672	11.4	85.1	164.11	81.9	25.8	-0.88779	55.7	178.4	172.3	72.5
41116	53753.26569	-103.5685	-57.7633	7.2	45.9	162.23	43.8	15.6	-0.87561	44.4	152.2	145.6	62.8
41116	53760.26558	-102.6124	-57.0295	16.2	99.3	172.39	98.4	20.8	-0.61596	70.8	190.4	189.0	74.6
41116	53992.52332	-101.7159	0.4800	6.2	174.8	147.52	147.5	94.0	-0.99692	35.5	266.9	226.0	146.4
41116	53993.53718	-100.2397	-0.1331	23.6	1190.0	150.05	1031.2	594.4	-0.99895	42.2	1553.3	1346.1	776.3
41116	54005.50485	-100.2658	2.5738	3.8	43.1	150.77	37.7	21.3	-0.97876	35.2	150.8	132.7	79.8
41116	54009.51223	-98.3076	2.6117	6.0	252.9	152.70	224.8	116.1	-0.99831	35.5	357.3	318.0	166.9
41116	54029.41661	-96.2216	11.4119	28.7	593.7	146.39	494.7	329.5	-0.99454	45.3	784.4	653.8	435.8
41116	54369.52002	-74.6987	86.9307	3.0	47.4	152.01	41.8	22.4	-0.98862	36.8	153.0	136.2	78.8
41116	54376.47755	-76.0054	85.0768	6.6	321.9	147.82	272.4	171.5	-0.99897	43.1	441.3	374.2	237.8
41116	54384.49380	-72.3091	89.5548	6.0	147.2	154.26	132.6	64.1	-0.99463	41.8	237.1	214.3	109.6
41116	54391.44955	-71.4185	90.3825	9.5	192.7	150.78	168.3	94.4	-0.99329	50.3	287.0	251.7	146.8
41116	54420.45604	-67.5093	95.7218	4.9	42.3	163.49	40.6	12.9	-0.91879	39.6	150.4	144.7	57.2
41116	54425.41497	-68.4678	98.1220	6.2	54.9	159.19	51.3	20.3	-0.94612	42.2	157.1	147.7	68.4
41116	54524.18054	-53.7486	112.9393	3.9	23.1	165.35	22.4	6.9	-0.81735	35.2	143.2	138.8	49.7
41116	54769.46872	-10.4299	127.9161	7.5	125.2	157.83	116.0	47.8	-0.98567	35.8	214.7	199.3	87.5
41116	54794.41053	-5.2193	125.9489	8.3	152.4	160.44	143.7	51.6	-0.98533	36.0	242.6	228.9	88.0
44926	52979.39500	-35.2577	119.9384	7.8	330.6	160.82	312.3	108.9	-0.99709	45.9	452.0	427.2	154.7
44926	53034.23459	-34.8746	119.6472	5.8	139.7	158.68	130.2	51.1	-0.99265	41.4	229.3	214.1	91.8
44926	53250.53134	-32.0356	117.5082	25.0	2606.9	142.49	2067.8	1587.6	-0.99980	101.2	3391.9	2691.3	2066.9
44926	53271.53548	-33.7021	118.8737	4.8	167.3	150.71	146.0	82.0	-0.99778	39.5	258.7	226.4	131.1
44926	53272.54422	-33.0730	118.5858	17.3	2086.3	152.61	1852.4	959.9	-0.99979	74.5	2715.8	2411.6	1251.1
44926	53284.49457	-33.8095	118.8309	13.8	138.0	18.94	130.6	46.7	0.95010	63.0	227.6	216.2	94.9
44926	53312.51677	-33.8413	118.8095	2.7	66.5	168.42	65.2	13.6	-0.97877	36.5	164.5	161.4	48.7
44926	53334.45165	-33.6514	118.7316	5.3	208.1	167.00	202.8	47.1	-0.99319	40.4	304.6	296.9	79.0
44926	53340.45995	-33.9078	118.7351	7.2	265.4	172.71	263.3	34.4	-0.97730	44.4	372.3	369.4	

**Table 5**  
PHASES Astrometry Measurements

44926	54006.51469	-29.8046	115.3735	9.0	215.1	149.25	184.9	110.2	-0.99545	36.1	312.7	269.4	162.9
44926	54056.44638	-29.6302	115.1160	12.9	105.6	160.48	99.6	37.3	-0.93095	37.3	196.1	185.2	74.4
44926	54075.40339	-29.4892	115.0714	6.5	120.3	162.27	114.6	37.2	-0.98294	35.6	209.9	200.2	72.4
44926	54350.53105	-28.1189	113.5520	10.3	619.4	143.81	499.9	365.8	-0.99939	52.5	817.3	660.3	484.4
44926	54483.24948	-26.6224	112.3288	21.5	180.3	156.77	165.9	73.8	-0.94874	41.1	273.0	251.4	114.1
44926	54524.16706	-26.8294	112.2227	5.2	78.0	160.66	73.7	26.3	-0.97785	35.4	172.9	163.5	66.3
44926	54748.50946	-25.6082	110.7129	17.0	250.0	154.50	225.7	108.7	-0.98490	38.9	353.9	319.8	156.3
44926	54762.44298	-25.9496	110.8420	17.9	358.2	149.17	307.7	184.2	-0.99358	39.3	486.3	418.0	251.5
58728	53034.27303	-21.7671	69.7307	10.8	343.2	157.37	316.8	132.4	-0.99611	53.9	467.6	432.1	186.7
58728	53648.52545	-24.0983	102.0803	7.5	201.5	147.85	170.7	107.4	-0.99662	45.1	297.0	252.6	162.6
58728	53663.52313	-23.5607	100.7802	5.9	64.3	154.41	58.0	28.3	-0.97280	41.6	163.1	148.2	79.8
58728	53705.41371	-23.6320	94.8323	10.9	70.3	152.52	62.6	33.9	-0.93234	54.2	167.2	150.4	90.9
58728	53727.33588	-21.9527	89.4581	25.8	1204.1	150.55	1048.6	592.4	-0.99875	104.1	1571.6	1369.5	778.0
58728	53732.39012	-22.6217	88.7557	8.1	101.0	162.58	96.4	31.2	-0.96273	46.6	191.9	183.7	72.7
58728	53739.31549	-22.1496	86.7264	12.2	326.7	152.77	290.5	149.9	-0.99580	58.1	447.2	398.5	211.0
58728	53746.29719	-22.4211	85.1343	9.6	66.3	153.84	59.7	30.5	-0.93716	50.6	164.4	149.2	85.5
58728	53747.35674	-22.3286	84.7353	21.7	406.3	165.65	393.7	102.9	-0.97597	89.6	546.4	529.8	160.9
58728	53779.20452	-20.3576	74.4071	21.2	132.5	150.45	115.7	67.9	-0.93377	87.8	222.0	197.9	133.5
58728	53790.20966	-18.9168	70.5481	27.2	239.3	30.76	206.1	124.6	0.96737	109.1	341.1	298.4	198.1
58728	54174.16806	-8.6169	42.2071	8.0	74.3	160.67	70.2	25.7	-0.94447	35.9	170.1	160.9	65.7
58728	54370.52780	-23.7857	103.1992	8.0	277.9	144.91	227.4	159.9	-0.99814	46.4	387.4	318.1	225.9
58728	54383.51155	-24.4379	103.4596	31.0	689.9	147.56	582.5	371.0	-0.99510	122.9	907.7	768.9	497.8
58728	54420.47609	-24.1552	101.3020	8.4	84.6	157.90	78.4	32.7	-0.96108	47.4	178.0	165.9	80.1
58728	54425.46497	-24.8721	101.1027	17.2	163.6	158.05	151.8	63.2	-0.95604	74.1	254.6	237.8	117.4
58728	54483.33279	-23.4139	91.0054	18.0	123.0	164.37	118.5	37.4	-0.86616	39.4	212.5	204.9	68.7
58728	54503.23719	-22.0842	85.5832	25.9	519.3	155.69	473.3	215.1	-0.99124	43.5	689.5	628.6	286.6
58728	54524.19366	-21.4321	79.3948	9.0	174.0	157.34	160.6	67.6	-0.98945	36.1	266.0	245.9	107.8
58728	54526.16985	-21.0047	78.5180	36.3	1269.6	154.42	1145.2	549.2	-0.99731	50.4	1656.4	1494.2	716.6
58728	54529.16654	-17.9140	76.3879	16.1	898.3	155.39	816.8	374.3	-0.99888	38.5	1176.2	1069.4	491.0
60318	52948.54661	50.6805	-59.5074	3.5	62.2	165.74	60.3	15.7	-0.97250	37.4	161.7	157.0	53.9
60318	52952.49909	51.4400	-59.6509	7.6	203.3	157.89	188.4	76.9	-0.99427	45.4	299.1	277.6	120.2
60318	52979.49138	51.1041	-58.3711	10.8	481.2	171.72	476.2	70.1	-0.98787	53.9	641.0	634.4	106.6
60318	53034.32232	49.0157	-55.6260	3.9	109.6	166.98	106.8	25.0	-0.98703	38.0	199.8	194.8	58.3
60318	53284.53247	45.2897	-47.1859	3.4	40.7	17.46	38.9	12.7	0.95873	37.3	149.7	143.2	57.3
60318	53312.55639	45.0879	-46.9776	1.7	37.6	166.79	36.6	8.8	-0.97880	35.6	148.3	144.6	48.5
60318	53333.53712	45.3627	-46.7988	7.6	258.7	175.88	258.0	20.1	-0.92495	45.4	364.3	363.4	52.3
60318	53334.53365	45.7510	-46.7960	3.5	132.4	175.23	131.9	11.5	-0.95181	37.4	221.9	221.1	41.6
60318	53340.52090	44.7072	-46.6276	3.0	66.0	175.72	65.8	5.7	-0.85574	36.8	164.2	163.8	38.7
60318	53341.51946	44.5720	-46.6507	3.7	35.7	176.05	35.7	4.4	-0.54756	37.7	147.5	147.2	39.0
60318	53466.17741	43.6811	-44.8996	5.0	53.1	176.16	53.0	6.1	-0.57727	39.8	156.1	155.8	41.1
60318	53473.16554	43.3236	-44.7518	3.7	60.6	178.48	60.6	4.1	-0.39431	37.7	160.6	160.6	37.9
60318	53687.49497	40.5353	-37.8723	4.4	47.0	29.60	40.9	23.5	0.97657	38.8	152.8	134.2	82.6
75470	54175.21628	264.5539	58.6260	9.8	83.5	159.86	78.4	30.2	-0.93862	36.3	177.2	166.8	69.9
76943	54083.45907	-243.2769	491.0586	7.3	155.3	156.07	141.9	63.3	-0.99203	35.8	245.7	225.0	104.9
76943	54084.47707	-243.4674	490.7196	9.4	111.8	161.34	105.9	36.8	-0.96344	36.2	201.8	191.5	73.1
76943	54090.44605	-245.6274	488.8202	21.1	371.2	158.36	345.2	138.3	-0.98646	40.9	502.5	467.3	189.1
76943	54103.38879	-249.1727	484.6900	11.6	137.6	152.86	122.6	63.6	-0.97871	36.9	227.2	202.8	108.7
76943	54138.28852	-259.1432	473.1842	29.0	462.9	152.45	410.6	215.7	-0.98842	45.5	617.8	548.2	288.6
76943	54174.18725	-268.1380	460.6022	11.1	299.7	152.26	265.3	139.8	-0.99598	36.7	414.0	366.8	195.4
76943	54179.20791	-270.1570	459.0538	26.1	318.2	159.43	298.1	114.4	-0.97001	43.7	436.7	409.2	158.8
76943	54194.15600	-273.3613	453.6365	14.0	264.6	156.59	242.9	105.9	-0.98962	37.7	371.4	341.1	151.6
76943	54420.54028	-329.5905	369.6534	14.2	437.5	158.11	406.0	163.6	-0.99561	64.3	585.7	544.0	226.4
76943	54433.49036	-332.4642	364.4549	23.9	339.7	155.17	308.5	144.3	-0.98328	42.4	463.3	420.8	198.3
76943	54483.34004	-344.5220	345.1646	19.1	806.1	151.75	710.2	381.9	-0.99838	39.9	1057.2	931.5	501.6
76943	54526.29870	-353.8186	327.4686	33.6	1083.4	167.11	1056.1	243.9	-0.98994	48.5	1415.4	1379.7	319.3
76943	54529.34042	-354.0925	326.1132	22.5	147.0	178.82	147.0	22.7	-0.12997	41.6	236.9	236.8	41.9
76943	54530.24857	-353.8025	325.6138	24.9	165.4	158.46	154.2	65.0	-0.91158	43.0	256.6	239.2	102.3
76943	54538.23460	-355.8054	322.5258	7.9	70.7	161.27	67.0	23.9	-0.93774	35.9	167.5	159.0	63.6
76943	54544.24148	-357.0549	319.9628	12.4	92.5	164.91	89.4	26.9	-0.87857	37.1	184.6	178.5	59.9
77327	52979.53035	-110.2675	85.2636	10.4	275.0	167.10	268.0	62.2	-0.98530	52.8	383.9	374.4	100.0
77327	53033.37609	-114.2128	86.1745	12.4	401.5	164.98	387.8	104.8	-0.99248	58.7	540.4	522.2	151.1
77327	53034.38885	-114.5321	86.2387	4.0	36.5	167.91	35.7	8.6	-0.88040	38.2	147.8	144.8	48.5
77327	53109.25209	-120.2164	87.6006	8.9	125.1	5.71	124.5	15.3	0.80954	48.7	214.6	213.6	52.9
77327	53123.17148	-121.0349	87.8155	5.2	103.4	175.66	103.1	9.4	-0.83267	40.2	194.1	193.6	42.7
77327	53285.53887	-132.4920	90.3807	4.8	120.0	3.60	119.7	8.9	0.84170	39.5	209.6	209.2	41.5
77327	53333.56349	-135.5142	90.8606	10.6	328.6	167.60	321.0	71.3	-0.98844	53.4	449.5	439.2	109.7
77327	53334.56941	-136.1269	90.9579	10.0	202.5	169.67	199.2	37.6	-0.96248	51.7	298.2	293.5	73.8
77327	53340.57025	-136.4403	91.0411	11.2	241.3	173.55	239.7	29.3	-0.92269	55.1	343.5	341.4	67.0
77327	53341.55502	-136.6624	91.1231	16.9	147.5	170.45	145.5	29.6	-0.81530	73.1	237.4	234.4	82.2
77327	53466.23066	-145.0282	92.6659	9.3	59.2	174.15	58.9	11.1	-0.53277	49.7	159.8	159.0	52.1
77327	53467.22246	-144.8811	92.5945	17.5	202.4	172.63	200.7	31.3	-0.82461	75.1	298.0	295.7	83.8
77327	53473.												

**Table 5**  
PHASES Astrometry Measurements

77327	53732.49665	-161.8307	95.4057	4.5	45.1	172.21	44.7	7.5	-0.80147	39.0	151.8	150.5	43.7
77327	53734.47257	-161.9759	95.4596	3.3	30.1	167.83	29.4	7.1	-0.88005	37.2	145.4	142.3	47.5
77327	53746.46960	-162.8842	95.5801	8.0	94.0	174.54	93.6	12.0	-0.73969	46.4	185.8	185.0	49.4
77327	53753.43625	-162.8057	95.5909	20.8	813.3	171.92	805.2	116.1	-0.98349	86.4	1066.5	1056.0	172.6
77327	53777.36184	-164.5512	95.8050	9.5	188.7	170.04	185.8	33.9	-0.95855	50.3	282.4	278.3	69.6
77327	53779.35888	-164.2439	95.7494	20.4	437.0	170.37	430.9	75.8	-0.96220	85.1	585.1	577.0	128.9
77327	53789.23747	-165.3090	96.0722	30.6	827.4	21.45	770.2	303.9	0.99413	121.4	1084.7	1010.5	412.4
77327	53790.24516	-165.4556	95.9622	7.6	157.5	23.84	144.1	64.0	0.99165	45.4	248.0	227.6	108.5
77327	53818.32093	-167.2428	96.1559	14.4	296.3	7.09	294.1	39.3	0.92959	65.0	409.8	406.8	81.9
77327	53865.18143	-170.1031	96.5281	9.6	294.3	5.53	292.9	30.0	0.94621	50.6	407.4	405.5	63.8
77327	53866.15364	-170.3111	96.5471	12.5	373.2	179.72	373.2	12.6	-0.14192	59.0	505.0	504.9	59.1
77327	54070.54943	-181.8796	97.9328	8.4	124.1	167.85	121.4	27.4	-0.94951	36.0	213.6	209.0	57.1
77327	54075.56122	-182.0574	97.9003	11.6	190.4	173.89	189.3	23.3	-0.86658	36.9	284.4	282.8	47.5
77327	54083.56093	-182.6256	97.9823	15.1	249.6	178.94	249.6	15.8	-0.29046	38.1	353.4	353.3	38.7
77327	54084.53031	-183.5955	98.1133	23.7	930.5	171.99	921.5	131.8	-0.98339	42.3	1217.7	1205.9	174.8
77327	54090.54319	-183.0315	98.0199	13.3	160.1	179.08	160.1	13.5	-0.18942	37.4	250.8	250.8	37.7
77327	54138.39563	-185.2061	98.2216	18.1	405.1	174.88	403.5	40.3	-0.89333	39.4	544.9	542.8	62.5
77327	54174.33117	-187.4601	98.3954	5.8	118.7	3.34	118.5	9.0	0.76319	35.5	208.4	208.0	37.4
77327	54175.31402	-187.4958	98.4070	5.5	104.1	0.04	104.1	5.5	0.01440	35.4	194.7	194.7	35.4
77327	54196.22624	-188.4392	98.4568	7.6	167.2	173.34	166.0	20.8	-0.93001	35.8	255.8	256.8	46.5
77327	54215.17245	-189.6068	98.5838	3.8	55.4	172.53	54.9	8.1	-0.88042	35.2	157.4	156.2	40.5
77327	54216.18008	-189.4611	98.5665	17.4	138.1	175.19	137.6	20.8	-0.54686	39.1	227.7	226.9	43.4
77327	54229.17768	-190.3568	98.6330	14.4	298.9	4.01	298.2	25.4	0.82180	37.8	413.0	412.0	47.5
77327	54231.17091	-190.2099	98.6405	8.5	170.5	3.56	170.1	13.5	0.77952	36.0	262.2	261.7	39.5
77327	54237.17798	-190.3349	98.7236	19.8	921.7	9.21	909.8	148.8	0.99091	40.2	1206.4	1190.8	197.1
77327	54454.51102	-200.4767	99.2497	33.8	2453.1	171.18	2424.1	377.6	-0.99588	48.7	3192.1	3154.4	491.8
77327	54502.41055	-204.0323	99.4837	30.9	831.4	177.59	830.7	46.6	-0.74872	46.7	1089.8	1088.9	65.4
77327	54538.28712	-205.6761	99.5105	4.9	50.3	171.51	49.8	8.9	-0.82745	35.3	154.5	152.9	41.7
77327	54544.28725	-205.8363	99.4961	8.2	95.6	175.75	95.4	10.8	-0.64870	35.9	187.2	186.7	38.4
79096	54056.53627	0.2350	49.9778	27.6	312.7	157.07	288.2	124.5	-0.97070	44.6	429.9	396.3	172.5
79096	54075.43903	-15.0197	53.2484	22.3	350.3	147.35	295.2	189.9	-0.99025	41.5	476.4	401.8	259.4
81858	53467.16912	657.2324	-60.1448	25.7	433.9	155.97	396.4	178.3	-0.98749	103.7	581.2	532.5	254.9
81858	53705.49000	667.1219	-75.1289	25.6	186.3	157.18	172.0	76.0	-0.93123	103.4	279.7	260.9	144.4
81858	53746.41422	668.7353	-77.5370	20.0	194.3	157.92	180.2	75.4	-0.95801	83.7	288.8	269.5	133.4
81858	54061.55491	680.2136	-95.9792	10.1	193.6	159.13	181.0	69.6	-0.98791	36.4	288.0	269.4	108.1
81858	54063.55814	681.5987	-96.5756	29.5	574.6	160.99	543.3	189.3	-0.98630	45.8	760.0	718.7	251.3
81858	54083.48145	681.1639	-97.3074	17.1	130.8	154.57	118.4	58.2	-0.94606	39.0	220.3	199.6	100.9
81858	54090.48497	681.5160	-97.7666	24.3	659.0	160.67	621.9	219.3	-0.99309	42.6	868.1	819.3	290.1
81858	54138.34899	683.4584	-100.9094	31.2	537.2	158.58	500.2	198.3	-0.98562	46.9	712.3	663.3	263.8
81858	54425.54595	694.1319	-118.0261	31.2	325.1	156.94	299.3	130.5	-0.96579	123.6	445.2	412.5	208.2
81858	54426.56538	693.3936	-117.6748	27.6	635.2	161.30	601.7	205.3	-0.98989	110.6	837.5	794.1	288.2
81858	54526.25977	696.7234	-123.7262	13.7	252.0	153.11	224.8	114.6	-0.99099	37.6	356.3	318.2	164.6
81858	54529.24852	696.8410	-123.9198	20.2	311.0	151.96	274.6	147.3	-0.98781	40.4	427.9	378.1	204.3
90537	53474.19167	-248.2523	-281.1256	15.5	96.8	35.60	79.2	57.7	0.94492	68.5	188.2	158.2	122.9
90537	53494.18377	-243.6561	-292.1790	8.3	83.3	167.45	81.4	19.8	-0.90263	47.1	177.0	173.1	60.0
90537	53732.54966	-280.0714	-306.5021	25.5	170.0	169.62	167.3	39.6	-0.75545	103.0	261.6	258.0	111.8
90537	53746.45718	-278.8953	-305.0878	17.7	117.9	160.65	111.4	42.5	-0.89713	75.8	207.6	197.5	99.2
90537	53780.35698	-269.8591	-314.5219	14.2	161.9	157.59	149.8	63.1	-0.96977	64.3	252.8	235.0	113.2
90537	53789.33201	-271.4384	-315.2977	18.5	346.2	27.99	305.9	163.3	0.99177	78.5	471.3	417.8	231.8
90537	53790.34191	-271.6737	-315.4991	10.6	233.9	31.61	199.3	122.9	0.99484	53.4	334.8	286.5	181.2
90537	54201.28297	-302.9398	-340.5600	26.4	515.6	175.95	514.3	44.9	-0.80805	43.8	684.7	683.0	65.2
90537	54217.26207	-304.0353	-341.4965	14.8	319.5	1.04	319.4	15.9	0.36270	38.0	438.3	438.2	38.8
114378	53034.46586	75.1692	344.7686	12.7	304.2	149.79	263.0	153.5	-0.99543	59.6	419.5	363.8	217.3
114378	53109.37898	78.8911	361.2198	13.9	291.6	173.75	289.8	34.6	-0.91458	63.4	404.1	401.8	76.8
114378	53123.26130	79.5777	364.3108	16.6	424.6	156.62	389.8	169.2	-0.99428	72.1	569.5	523.5	235.5
114378	53131.27830	81.3717	366.6307	28.3	1269.6	35.71	1031.0	741.3	0.99890	113.1	1656.4	1346.6	971.2
114378	53145.18418	80.9790	368.8005	13.1	378.8	153.39	338.8	170.1	-0.99627	60.9	512.0	458.5	235.7
114378	53466.31699	94.9611	435.0800	7.1	208.4	155.35	189.4	87.1	-0.99598	44.2	305.0	277.8	133.4
114378	53467.28332	94.6993	435.3575	25.9	370.5	150.67	323.3	182.9	-0.98673	104.5	501.6	440.3	262.0
114378	53473.31290	95.8321	436.1674	17.2	609.2	158.06	565.1	228.1	-0.99669	74.1	804.2	746.5	308.3
114378	53494.26544	96.5771	440.3152	8.4	154.3	160.79	145.7	51.4	-0.98487	47.4	244.6	231.5	92.1
114378	53753.46614	107.0280	488.4115	23.3	2917.1	145.75	2411.3	1641.9	-0.99985	95.2	3794.8	3137.2	2137.2
114378	53777.43726	107.3061	492.9796	6.8	199.4	150.50	173.6	98.3	-0.99682	43.5	294.6	257.3	149.9
114378	53779.45201	107.7889	493.0071	20.0	214.4	154.51	193.7	94.0	-0.97185	83.7	311.9	283.8	154.0
114378	53790.38787	107.7252	495.0434	27.9	535.5	18.70	507.3	173.7	0.98557	111.6	710.1	673.6	251.0
114378	53832.30416	109.5871	502.1805	29.6	643.7	153.23	574.8	291.2	-0.99349	117.8	848.4	759.4	396.4
114378	53874.20324	111.2474	509.1821	10.3	144.1	155.99	131.7	59.4	-0.98187	52.5	233.9	214.7	106.6
114378	53895.19690	111.8346	512.6873	20.5	333.0	167.66	325.3	74.0	-0.95880	85.4	455.0	444.8	128.1
114378	54196.35212	121.5222	558.2313	18.8	87.9	165.19	85.1	28.9	-0.74147	39.7	180.7	175.0	60.1
114378	54230.18384	121.4432	563.5820	15.0	934.8	148.46	796.7	489.1	-0.99935	38.1	1223.3	1042.8	640.7
114378	54236.23439	123.8259	563.4369	4.5	26.9	159.38							

**Table 5**  
PHASES Astrometry Measurements

129246	53467.34466	-608.9232	322.0589	23.3	273.1	149.40	235.4	140.5	-0.98135	95.2	381.6	332.0	210.8
129246	53495.31448	-594.5117	312.5408	29.4	2687.1	157.23	2477.7	1040.3	-0.99953	117.1	3496.0	3223.9	1357.4
129246	53746.57095	-583.5150	302.9204	18.1	654.1	148.56	558.2	341.5	-0.99807	77.2	861.8	736.4	454.3
129246	53775.51962	-581.6762	301.1655	18.1	130.6	154.18	117.9	59.2	-0.94088	77.2	220.1	200.9	118.4
129246	53779.46998	-582.0267	301.4209	11.5	273.7	147.06	229.8	149.1	-0.99574	56.0	382.4	322.3	213.2
129246	53790.42751	-579.2605	301.0463	26.9	543.9	13.05	529.9	125.6	0.97549	108.0	720.8	702.6	193.8
129246	53865.22737	-576.7113	296.8973	22.2	1648.0	145.48	1357.9	934.0	-0.99958	91.3	2147.0	1769.7	1219.0
129246	53874.23660	-577.5548	297.2315	23.2	266.4	150.60	232.4	132.3	-0.97967	94.9	373.5	328.8	201.1
129246	53915.20514	-575.6900	295.4207	6.5	265.9	166.73	258.8	61.3	-0.99410	42.8	372.9	363.1	95.2
129246	53929.19040	-575.5811	295.0325	25.7	860.8	172.99	854.4	108.2	-0.97083	43.4	1127.8	1119.3	144.2
129246	53930.19601	-573.8361	294.7560	20.3	1199.8	174.81	1194.9	110.3	-0.98285	84.7	1566.0	1559.6	164.9
129246	54196.38310	-562.3833	283.7157	8.8	56.8	157.83	52.7	22.9	-0.91043	36.1	158.3	147.2	68.4
129246	54229.25332	-560.6448	282.2014	10.9	84.8	147.87	72.1	46.1	-0.96040	36.7	178.2	152.2	99.7
129246	54231.24985	-560.5548	282.1606	9.7	64.4	149.61	55.8	33.6	-0.94290	36.3	163.1	141.9	88.3
129246	54236.30029	-559.8066	281.7239	4.8	78.4	160.75	74.0	26.2	-0.98100	35.3	173.2	163.9	66.1
129246	54252.31015	-559.7136	281.2778	16.7	311.7	172.97	309.3	41.6	-0.91488	38.8	428.7	425.5	65.1
129246	54544.40795	-545.2344	268.7590	6.7	49.4	151.70	43.6	24.1	-0.94938	35.6	154.0	136.7	79.5
137107	53109.32634	531.1642	-89.1492	15.3	876.0	145.87	725.2	491.6	-0.99929	67.9	1147.4	950.5	646.2
137107	53110.37376	531.1031	-89.5071	10.2	280.7	154.52	253.4	121.1	-0.99565	52.2	390.8	353.5	174.6
137107	53123.30637	529.9131	-93.3526	7.3	214.7	148.93	183.9	111.0	-0.99701	44.7	312.3	268.4	165.6
137107	53145.28003	526.5734	-99.0990	16.4	319.8	155.46	291.0	133.6	-0.99090	71.5	438.7	400.2	193.5
137107	53168.30554	523.4366	-105.1787	10.1	403.7	173.33	400.9	48.0	-0.97727	51.9	543.2	539.5	81.5
137107	53172.29417	522.8037	-106.1552	5.2	90.8	174.05	90.3	10.7	-0.87251	40.2	183.1	182.2	44.3
137107	53181.19635	521.2515	-108.5494	5.8	179.4	158.19	166.6	66.9	-0.99567	41.4	272.0	253.0	108.1
137107	53182.18871	521.3702	-108.9539	8.1	208.5	156.63	191.4	83.0	-0.99432	46.6	305.1	280.7	128.4
137107	53199.23352	519.9659	-113.5036	12.4	507.7	176.77	506.9	31.2	-0.91759	58.7	674.7	673.6	69.9
137107	53466.40129	480.0686	-185.3656	4.9	26.6	155.85	24.4	11.8	-0.89233	39.6	144.2	132.6	69.2
137107	53473.42045	478.5369	-187.0777	13.8	131.0	163.22	125.5	40.1	-0.93290	63.0	220.5	211.9	87.7
137107	53481.36211	476.7500	-189.9505	20.4	766.1	25.41	692.0	329.3	0.99765	85.1	1005.7	909.2	438.3
137107	53508.34722	473.2721	-196.3472	17.7	549.5	167.15	535.8	123.4	-0.98908	75.8	727.9	709.9	178.0
137107	53552.22505	466.1191	-207.9214	4.6	80.4	166.75	78.2	19.0	-0.96812	39.1	174.7	170.3	55.3
137107	53586.18646	459.4907	-216.7858	22.6	607.1	0.14	607.1	22.7	0.06354	92.7	801.6	801.5	92.8
137107	53777.55293	428.7597	-266.5016	11.1	227.5	155.96	207.8	93.2	-0.99144	54.8	327.2	299.7	142.4
137107	53789.50370	426.9384	-269.7364	12.3	85.2	26.36	76.6	39.4	0.93727	58.4	178.5	162.0	95.0
137107	53838.38366	418.4371	-282.1850	9.7	121.5	154.68	109.9	52.7	-0.97913	50.8	211.1	192.0	101.3
137107	53858.35734	414.3501	-287.0404	26.1	366.1	160.61	345.4	124.0	-0.97483	105.2	496.1	469.3	192.3
137107	53873.30193	412.1842	-290.9649	24.6	310.9	158.28	288.9	117.3	-0.97418	99.8	427.7	399.1	183.5
137107	53894.25519	408.3143	-296.1528	7.2	74.8	160.73	70.6	25.6	-0.95457	44.4	170.5	161.6	70.2
137107	53895.28364	409.1704	-296.7199	23.4	419.8	166.29	407.9	102.1	-0.97171	95.6	563.4	547.8	162.6
137107	53915.24189	404.9289	-301.6093	7.9	93.3	168.46	91.4	20.2	-0.91757	46.1	185.2	181.7	58.4
137107	53921.21028	402.7064	-302.8913	9.6	623.6	166.23	605.7	148.8	-0.99777	50.6	822.7	799.1	201.9
137107	53922.19931	403.0928	-303.1740	9.1	258.3	164.14	248.5	71.1	-0.99106	49.2	363.8	350.2	110.1
137107	53929.21811	403.7722	-305.4077	14.4	619.4	173.02	614.8	76.6	-0.98190	37.8	817.3	811.3	106.2
137107	53930.21680	402.1173	-305.3839	11.9	400.4	173.32	397.6	48.1	-0.96867	57.2	539.0	535.4	84.6
137107	54173.43915	356.7275	-365.0582	12.5	101.1	151.00	88.6	50.2	-0.95881	37.2	192.0	168.9	98.6
137107	54175.43150	356.4653	-365.5890	5.3	147.4	149.89	127.5	74.1	-0.99663	35.4	237.3	206.1	122.9
137107	54194.37929	352.9816	-370.1861	21.2	141.3	153.57	126.9	65.7	-0.93305	40.9	231.0	207.6	109.1
137107	54216.31478	348.8051	-375.4462	35.3	349.1	150.26	303.6	175.9	-0.97306	49.7	474.9	413.1	239.5
137107	54222.37677	347.3641	-376.7105	23.4	208.4	164.45	200.9	60.2	-0.91539	42.1	305.0	294.0	91.3
137107	54229.26040	346.2828	-378.5544	9.6	240.5	145.70	198.7	135.7	-0.99632	36.3	342.6	283.7	195.4
137107	54230.28549	346.1827	-378.8516	9.8	101.8	152.18	90.2	48.3	-0.97366	36.3	192.6	171.2	95.5
137107	54231.27738	345.7634	-378.9567	8.7	121.5	151.31	106.7	58.8	-0.98565	36.1	211.1	186.0	106.2
137107	54236.27062	344.7011	-380.0427	4.9	37.2	151.41	32.7	18.3	-0.95174	35.3	148.1	131.2	77.4
137107	54238.28216	343.8738	-380.3467	19.8	177.1	153.66	158.9	80.5	-0.96178	40.2	269.5	242.1	124.9
137107	54245.21340	342.7419	-381.9826	17.5	127.8	146.82	107.4	71.5	-0.95684	39.1	217.3	183.1	123.3
137107	54250.23538	341.8321	-383.2984	19.6	114.8	157.74	106.5	47.1	-0.89401	40.1	204.6	190.0	85.9
137107	54266.21481	338.7509	-387.0380	23.8	112.1	158.79	104.0	45.9	-0.83318	42.3	201.2	188.2	82.8
137107	54272.23057	337.7686	-388.5211	12.2	153.8	162.01	146.4	48.9	-0.96490	37.1	244.1	232.4	83.2
137107	54273.26744	337.4026	-388.7903	12.7	344.5	170.30	339.6	59.4	-0.97616	37.2	469.2	462.6	87.2
137107	54279.21881	336.2489	-390.1061	15.1	137.7	162.78	131.6	43.2	-0.93069	38.1	227.3	217.4	76.5
137107	54280.20686	335.9651	-390.3342	14.8	158.9	161.97	151.2	51.2	-0.95270	38.0	249.5	237.6	85.3
137107	54524.47585	286.5216	-445.8906	20.4	216.4	151.08	189.7	106.1	-0.97560	40.5	314.2	275.7	156.0
137107	54529.45024	285.2266	-446.7797	23.7	221.8	149.55	191.6	114.2	-0.97065	42.3	320.5	277.1	166.5
137107	54544.45168	282.3985	-450.1820	23.9	241.4	155.39	219.7	102.9	-0.96690	42.4	343.6	312.9	148.2
137107	54627.23049	264.4019	-467.7278	7.4	83.8	155.20	76.2	35.8	-0.97369	35.8	177.4	161.7	81.2
137107	54629.29341	264.1297	-468.1424	18.5	127.7	172.48	126.6	24.8	-0.66005	39.6	217.2	215.4	48.5
137107	54643.20045	262.0685	-471.4366	34.5	766.1	159.00	715.3	276.5	-0.99102	49.1	1005.7	939.1	363.3
137107	54653.20544	258.8288	-473.2275	16.8	153.1	166.25	148.8	39.9	-0.90105	38.8	243.3	236.5	69.0
137391	53131.33397	-111.6255	23.7186	26.4	1609.9	28.08	1420.5	758.1	0.99922	106.3	2097.5	1851.3	991.8
137391	53173.23068	-105.2831	14.4002	5.1	111.4	31.21	95.3	57.9	0.99463	40.0	201.4	17	

**Table 5**  
PHASES Astrometry Measurements

137391	53790.50296	62.2247	-37.8414	15.8	75.5	22.03	70.3	31.9	0.84562	69.5	171.0	160.6	90.9
137391	54173.51167	-57.7890	80.3098	7.6	43.5	162.74	41.6	14.8	-0.84403	35.8	151.0	144.6	56.4
137391	54215.42046	-71.1760	78.9631	6.5	58.8	168.93	57.7	13.0	-0.85973	35.6	159.5	156.7	46.5
137391	54217.39168	-71.4893	78.7647	5.4	94.4	163.41	90.5	27.4	-0.97880	35.4	186.2	178.7	63.1
137391	54222.44236	-72.5317	78.4764	14.6	476.8	178.47	476.6	19.4	-0.65658	37.9	635.5	635.2	41.5
137391	54237.34357	-77.2901	77.3107	11.9	144.1	164.32	138.8	40.6	-0.95244	37.0	233.9	225.4	72.5
137391	54250.33246	-80.8381	76.1257	5.1	22.2	169.86	21.8	6.3	-0.58246	35.4	142.9	140.8	43.0
137391	54265.29221	-84.3822	74.4217	10.0	166.7	170.40	164.3	29.5	-0.93922	36.4	258.0	254.5	56.0
137391	54273.26986	-86.4135	73.5150	2.6	21.0	168.88	20.6	4.8	-0.82956	35.1	142.6	140.1	44.1
137391	54280.24357	-87.9096	72.5765	4.6	41.1	169.30	40.4	8.9	-0.85006	35.3	149.8	147.4	44.5
137391	54285.27988	-89.3442	71.9258	4.6	131.5	0.79	131.5	5.0	0.36354	35.3	221.0	220.9	35.4
137391	54300.23692	-92.1669	69.7310	4.5	111.7	0.54	111.7	4.6	0.22779	35.3	201.7	201.7	35.3
137391	54628.22039	-93.8692	-9.7530	9.2	230.9	155.39	210.0	96.5	-0.99448	36.2	331.2	301.5	141.8
137391	54630.20547	-93.1860	-10.5046	4.7	111.4	153.12	99.4	50.5	-0.99446	35.3	201.4	180.4	96.4
137909	53034.51366	53.5645	-194.5843	23.8	1438.6	143.37	1154.5	858.6	-0.99940	97.0	1875.4	1506.1	1121.7
137909	53109.41620	66.9564	-209.5610	7.1	163.8	161.51	155.4	52.4	-0.98960	44.2	254.8	242.1	91.0
137909	53110.33506	68.4221	-210.5182	27.4	1240.9	146.99	1040.7	676.4	-0.99883	109.8	1619.2	1359.2	886.9
137909	53116.44145	68.9445	-210.9433	15.9	360.4	171.28	356.2	56.9	-0.95913	69.8	489.0	483.5	101.3
137909	53123.35186	69.0323	-211.8662	10.4	277.1	156.18	253.5	112.3	-0.99486	52.8	386.5	354.2	163.4
137909	53131.35817	72.1608	-212.0850	25.4	1113.7	32.39	940.5	596.9	0.99873	102.7	1454.6	1229.5	784.0
137909	53137.25597	71.0095	-214.0018	20.8	164.9	148.57	141.1	87.8	-0.96110	86.4	256.0	223.1	152.5
137909	53144.25226	72.3729	-215.2859	18.8	591.4	149.75	511.0	298.4	-0.99733	79.6	781.5	676.2	399.6
137909	53145.25716	72.6629	-215.5332	14.1	62.5	154.89	56.9	29.4	-0.85085	64.0	161.9	149.1	89.9
137909	53168.22207	76.1372	-219.1702	11.7	101.5	154.17	91.5	45.5	-0.95813	56.6	192.4	174.9	98.1
137909	53172.32119	76.7569	-219.7537	10.8	439.1	178.90	439.0	13.7	-0.61406	53.9	587.7	587.6	55.1
137909	53173.27098	76.2659	-220.1791	12.8	473.9	37.09	378.1	285.9	0.99842	59.9	631.8	505.3	384.0
137909	53181.26233	78.2354	-221.1312	7.6	53.8	170.61	53.0	11.5	-0.74656	45.4	156.5	154.6	51.5
137909	53182.26133	78.4083	-221.2440	8.5	62.3	169.83	61.3	13.8	-0.78226	47.6	161.7	159.4	54.9
137909	53187.23910	79.1434	-222.0794	18.9	161.2	170.72	159.1	32.0	-0.80182	79.9	252.0	249.1	88.7
137909	53198.21815	80.7524	-223.6743	4.2	36.5	172.04	36.1	6.6	-0.75801	38.5	147.8	146.5	43.2
137909	53199.21988	80.8510	-223.8461	7.4	43.5	169.45	42.7	10.7	-0.71852	44.9	151.0	148.7	52.1
137909	53208.19574	81.3807	-225.4354	4.4	98.4	40.49	74.9	64.0	0.99582	38.8	189.6	146.4	126.6
137909	53214.19010	82.8394	-225.9509	7.7	107.2	176.79	107.0	9.7	-0.61289	45.6	197.5	197.2	46.9
137909	53228.16998	84.8381	-227.8406	8.4	243.2	0.01	243.2	8.4	0.00464	47.4	345.8	345.8	47.4
137909	53467.43736	116.5069	-254.1639	15.0	92.7	162.71	88.6	31.1	-0.86317	66.9	184.7	177.5	84.2
137909	53473.39997	117.0549	-254.6189	9.1	42.9	160.51	40.6	16.7	-0.81754	49.2	150.7	143.0	68.4
137909	53474.37831	116.7379	-254.8786	24.4	262.9	24.46	239.5	111.1	0.97044	99.1	369.3	338.7	177.6
137909	53487.43377	118.9563	-255.3060	35.3	3552.5	40.93	2684.1	2327.5	0.99980	138.6	4620.4	3491.9	3028.8
137909	53494.32489	119.5240	-256.2291	4.5	37.1	153.62	33.3	17.0	-0.95559	39.0	148.1	133.8	74.5
137909	53495.27147	117.5046	-254.8422	26.4	2313.6	145.58	1908.6	1307.9	-0.99970	106.3	3010.9	2484.5	1704.2
137909	53508.37081	120.8718	-257.3319	16.6	491.2	171.53	485.9	74.2	-0.97412	72.1	653.7	646.7	119.8
137909	53509.37190	120.5678	-257.3634	24.4	1039.8	172.70	1031.4	134.3	-0.98314	99.1	1359.0	1348.0	198.7
137909	53550.22220	126.2598	-260.2868	20.0	294.2	162.93	281.3	88.5	-0.97152	83.7	407.3	390.1	143.8
137909	53552.22051	126.0813	-260.2757	6.1	67.4	163.60	64.7	19.9	-0.94827	42.0	165.2	158.9	61.6
137909	53571.22733	128.1939	-261.4554	5.1	92.0	178.85	92.0	5.4	-0.34165	40.0	184.1	184.1	40.2
137909	53585.20008	129.7290	-262.1885	8.4	168.2	1.29	168.1	9.3	0.40776	47.4	259.6	259.6	47.7
137909	53747.53761	145.7598	-268.5562	24.5	642.3	145.69	530.7	362.6	-0.99664	99.5	846.6	701.6	484.2
137909	53748.56579	145.8894	-268.3788	21.1	334.9	11.49	328.2	69.8	0.95125	87.5	457.3	448.5	125.1
137909	53755.57238	146.9995	-269.0019	19.9	443.1	148.55	378.2	231.8	-0.99492	83.3	592.8	507.6	317.4
137909	53769.54876	147.4389	-268.6635	22.2	338.7	150.13	293.9	169.7	-0.98856	91.3	462.0	403.2	243.4
137909	53774.52483	147.7766	-268.7643	23.4	443.3	148.64	378.7	231.6	-0.99301	95.6	593.1	508.9	319.2
137909	53775.53474	148.0964	-268.9414	14.4	266.7	150.97	233.3	130.0	-0.99193	65.0	373.9	328.4	190.1
137909	53778.54697	149.1976	-269.3447	19.2	254.8	155.16	231.3	108.4	-0.98079	80.9	359.6	328.1	168.0
137909	53789.51750	149.3117	-269.1943	6.9	39.2	27.70	34.9	19.2	0.91372	43.7	149.0	133.5	79.3
137909	53817.37249	152.2839	-269.7881	38.2	2074.0	143.36	1664.4	1238.1	-0.99926	149.3	2699.8	2168.2	1615.7
137909	53818.39216	151.7108	-269.4217	9.7	96.7	146.36	80.7	54.2	-0.97671	50.8	188.2	159.2	112.5
137909	53838.39716	153.2793	-269.4958	12.9	146.1	157.47	135.1	57.2	-0.96978	60.2	236.0	219.2	106.2
137909	53865.31336	155.4860	-269.5653	14.1	62.6	158.88	58.6	26.1	-0.81719	64.0	161.9	152.8	83.5
137909	53874.31771	156.2805	-269.5344	9.1	60.6	163.98	58.3	18.9	-0.86421	49.2	160.6	155.0	64.8
137909	53894.27169	157.4676	-269.2663	7.0	77.5	162.01	73.8	24.8	-0.95536	44.0	172.5	164.6	67.7
137909	53895.33336	158.1374	-269.3299	14.7	199.9	176.75	199.5	18.5	-0.60708	65.9	295.2	294.7	67.9
137909	54174.51072	173.2814	-259.3431	4.7	37.1	163.07	35.5	11.7	-0.90640	35.3	148.1	142.0	54.8
137909	54196.35398	173.8172	-257.7037	18.5	140.2	147.30	118.4	77.3	-0.95920	39.6	229.8	194.6	128.6
137909	54201.42990	174.0685	-257.5548	13.6	81.2	161.50	77.1	28.8	-0.86791	37.5	175.3	166.7	66.1
137909	54215.33362	174.7108	-256.5834	8.0	93.3	151.65	82.2	44.9	-0.97930	35.9	185.2	163.9	93.5
137909	54217.33404	174.8460	-256.4839	4.7	56.6	152.93	50.5	26.1	-0.97947	35.3	158.2	141.7	78.5
137909	54222.39790	175.0331	-256.1332	9.0	60.6	167.56	59.2	15.7	-0.81238	36.1	160.6	157.1	49.4
137909	54229.33268	175.1202	-255.5651	6.3	52.9	156.30	48.5	22.0	-0.95045	35.6	156.0	143.5	70.6
137909	54237.25545	175.3859	-254.9517	5.6	55.8	146.46	46.6	31.2	-0.97622	35.4	157.7	132.9	92.0
137909	54245.26139	175.3279	-254.2065	9.5	285.4	151.94	251.9	134.5	-0.99682	36.3	396.6	350.4	189.3
137909	54250.30278	175.8783	-254.0458	5.7	27.6	169.63	27.2	7.5	-				

**Table 5**  
PHASES Astrometry Measurements

137909	54301.23328	177.0013	-249.8160	10.2	234.1	0.11	234.1	10.2	0.04578	36.5	335.0	335.0	36.5
137909	54481.59273	179.0538	-231.1182	9.4	316.0	150.26	274.4	157.0	-0.99763	36.2	434.0	377.3	217.6
137909	54515.53384	178.4511	-226.7391	14.3	138.6	156.86	127.6	56.0	-0.96057	37.8	228.2	210.3	96.2
137909	54546.42115	178.6146	-223.0048	27.3	179.7	148.17	153.4	97.6	-0.94471	44.4	272.3	232.6	148.5
137909	54627.28557	176.7394	-211.3458	4.3	26.0	164.92	25.1	7.9	-0.82781	35.3	144.0	139.4	50.6
137909	54628.32452	176.8688	-211.1799	11.3	105.1	178.34	105.1	11.7	-0.25711	36.8	195.6	195.5	37.2
137909	54630.29708	176.4618	-210.7976	9.3	88.1	169.86	86.7	18.0	-0.85225	36.2	180.9	178.2	47.8
137909	54643.21607	177.3337	-209.2726	11.4	485.1	161.47	460.0	154.5	-0.99698	36.8	646.0	612.6	208.2
137909	54652.20867	175.6355	-207.4353	9.7	236.6	165.11	228.7	61.5	-0.98660	36.3	337.9	326.7	93.7
137909	54653.20993	175.6903	-207.3676	4.9	126.5	166.21	122.9	30.5	-0.98642	35.3	216.0	209.9	61.9
138629	53909.23586	23.5841	47.8180	10.4	412.7	163.33	395.3	118.8	-0.99580	52.8	555.4	531.4	166.9
140159	53110.41886	173.2006	54.5009	14.9	420.9	159.96	395.4	144.9	-0.99396	66.6	564.8	531.1	203.4
140159	53123.41078	171.7168	54.1016	14.8	297.5	165.86	288.5	74.1	-0.97862	66.2	411.3	399.2	119.3
140159	53181.26600	167.5849	51.3957	11.9	248.8	169.02	244.2	48.8	-0.96886	57.2	352.4	346.2	87.5
140159	53182.26697	167.5830	51.2650	21.9	584.5	169.77	575.2	106.1	-0.97771	90.3	772.6	760.5	163.5
140159	53199.21014	167.6260	50.2550	14.9	602.4	167.75	588.6	128.7	-0.99296	66.6	795.5	777.6	180.9
140159	53215.18210	164.4576	49.8117	11.6	242.2	171.71	239.6	36.8	-0.94788	56.3	344.6	341.1	74.6
140159	53221.18430	164.1972	48.9769	39.7	2476.7	41.94	1842.4	1655.6	0.99948	154.9	3222.8	2399.5	2157.0
140159	53551.26199	130.1927	31.4453	7.0	171.2	171.33	169.2	26.7	-0.96431	44.0	262.9	260.0	58.8
140159	54524.53447	-21.0858	-30.5862	12.0	111.8	157.94	103.7	43.5	-0.95456	37.0	201.8	187.5	83.2
140159	54529.52522	-22.1019	-30.8333	12.6	119.7	159.60	112.3	43.3	-0.95109	37.2	209.3	196.6	80.9
140159	54630.26695	-39.3695	-36.5049	9.7	97.6	160.71	92.1	33.5	-0.95231	36.3	188.9	178.7	71.2
140159	54635.30502	-40.7530	-36.7617	11.7	299.2	173.35	297.2	36.5	-0.94679	36.9	413.4	410.6	60.3
140159	54636.28083	-40.7402	-36.8224	25.1	218.0	167.94	213.3	51.8	-0.86812	43.1	316.1	309.2	78.3
140159	54657.19365	-40.9334	-38.9513	23.0	997.2	162.29	950.0	304.1	-0.99684	41.9	1303.9	1242.2	398.6
140159	54671.21541	-45.3294	-38.8512	21.4	708.5	176.24	707.0	51.1	-0.90812	41.0	931.6	929.6	73.5
140436	53109.45226	664.3435	-294.4134	7.7	256.9	166.88	250.2	58.8	-0.99098	45.6	362.1	352.8	93.4
140436	53110.45365	664.9826	-294.5821	6.9	206.7	167.54	201.8	45.1	-0.98758	43.7	303.0	296.0	78.1
140436	53145.33169	664.2835	-293.9576	12.5	267.8	161.81	254.4	84.4	-0.98778	59.0	375.2	357.0	129.9
140436	53168.25220	663.9125	-293.5786	10.4	94.5	160.74	89.3	32.7	-0.94109	52.8	186.3	176.7	79.1
140436	53187.22658	663.4442	-293.3415	14.3	324.4	164.08	312.0	90.0	-0.98624	64.6	444.4	427.7	136.8
140436	53199.18576	664.6341	-293.4290	7.8	369.0	162.49	351.9	111.3	-0.99728	45.9	499.7	476.8	156.6
140436	53229.18064	664.7532	-292.6397	20.3	658.6	0.57	658.6	21.3	0.30773	84.7	867.6	867.5	85.1
140436	53466.42563	661.2097	-289.5648	7.2	37.5	160.03	35.3	14.5	-0.84895	44.4	148.2	140.2	65.6
140436	53494.34069	660.4979	-288.9465	6.6	58.1	154.64	52.6	25.6	-0.95883	43.1	159.1	144.9	78.5
140436	53777.49192	654.9326	-283.3120	27.2	653.9	143.52	526.0	389.4	-0.99622	109.1	861.5	695.8	519.7
140436	53818.41258	655.4666	-283.6246	13.3	378.4	148.20	321.7	199.7	-0.99692	61.5	511.5	435.9	274.5
140436	53858.42205	654.2191	-282.6916	21.7	608.1	171.06	600.7	96.9	-0.97404	89.6	802.8	793.2	153.0
140436	53872.26085	654.0747	-282.4653	24.7	283.9	147.12	238.8	155.5	-0.98206	100.2	394.7	335.9	230.2
140436	53916.19326	653.2698	-281.6721	5.2	85.2	155.93	77.9	35.1	-0.98660	40.2	178.5	163.8	81.5
140436	53921.23061	652.4034	-281.4666	9.0	521.8	167.32	509.1	114.9	-0.99674	48.9	692.6	675.8	159.4
140436	53922.23305	652.5061	-281.3333	16.5	977.7	168.64	958.6	193.2	-0.99620	71.8	1278.7	1253.7	261.5
140436	53957.17243	652.0252	-280.8090	8.7	148.9	176.88	148.7	11.9	-0.67980	36.1	238.9	238.5	38.3
140436	53965.16468	652.0843	-280.5933	12.7	395.2	0.51	395.1	13.2	0.26534	37.2	532.5	532.5	37.5
140436	54173.49376	672.3551	-288.1985	31.0	200.7	153.93	180.8	92.5	-0.92809	46.8	296.1	266.8	136.7
140436	54194.39957	658.7929	-283.7464	19.6	201.9	150.29	175.7	101.5	-0.97497	40.1	297.5	259.1	151.5
140436	54201.38883	645.6054	-275.5323	23.7	188.2	151.87	166.4	91.2	-0.95563	42.3	281.9	249.4	138.0
140436	54215.37171	671.2683	-285.4691	23.6	148.8	159.02	139.2	57.6	-0.89913	42.2	238.8	223.5	94.1
140436	54217.34740	658.2211	-282.5661	9.3	102.8	151.69	90.6	49.5	-0.97710	36.2	193.5	171.3	97.2
140436	54229.30007	644.8058	-274.7562	11.1	120.0	150.01	104.0	60.7	-0.97752	36.7	209.6	182.5	109.5
140436	54230.32399	670.5271	-285.4471	25.6	262.1	150.95	229.4	129.2	-0.97398	43.4	368.4	322.7	182.8
140436	54231.28180	644.9348	-274.9056	10.1	188.8	147.58	159.5	101.6	-0.99307	36.4	282.6	239.3	154.6
140436	54237.28511	645.0730	-274.8959	14.0	113.1	150.72	98.9	56.6	-0.95909	37.7	203.0	178.0	104.6
140436	54238.36791	644.6951	-274.7607	16.6	435.9	168.12	426.6	91.2	-0.98250	38.7	583.7	571.3	126.0
140436	54245.24557	644.9259	-274.7434	21.9	256.2	147.36	216.1	139.4	-0.98256	41.3	361.3	305.0	197.9
140436	54250.30133	644.4289	-274.4704	7.6	58.6	166.08	56.9	15.9	-0.86938	35.8	159.4	154.9	51.8
140436	54251.30630	644.4088	-274.4683	18.6	348.3	162.59	332.4	105.7	-0.98288	39.6	473.9	452.4	146.8
140436	54272.29098	644.0494	-273.9947	15.4	389.7	171.33	385.3	60.7	-0.96654	38.2	525.6	519.6	87.8
140436	54279.25251	643.5091	-273.8182	8.2	181.0	167.37	176.6	40.4	-0.97820	35.9	273.8	267.3	69.4
140436	54285.24771	643.6299	-273.8924	11.0	388.3	170.31	382.7	66.2	-0.98566	36.7	523.8	516.4	95.3
140436	54294.23032	641.4189	-273.2504	20.6	464.1	172.31	459.9	65.4	-0.94831	40.6	619.4	613.8	92.1
140436	54300.18894	671.0123	-281.5017	23.5	314.5	165.38	304.3	82.6	-0.95566	42.2	432.2	418.3	116.5
140436	54320.17781	641.9314	-272.6939	24.3	611.5	176.50	610.4	44.5	-0.83778	98.8	807.2	805.7	110.2
140436	54525.53453	635.6122	-267.9561	12.2	75.4	159.51	70.7	28.8	-0.89179	37.1	170.9	160.6	69.2
140436	54544.48538	635.0145	-267.4932	8.0	40.1	161.82	38.1	14.6	-0.81809	35.9	149.4	142.4	57.8
140436	54627.22639	632.2443	-265.5922	6.1	47.6	151.41	41.9	23.4	-0.95574	35.5	153.1	135.5	79.6
140436	54629.25668	631.7883	-265.3466	13.2	52.6	164.94	50.9	18.7	-0.68433	37.4	155.8	150.8	54.3
140436	54670.20834	630.7171	-264.2290	9.1	207.4	173.78	206.2	24.2	-0.92566	36.2	303.8	302.0	48.7
140436	54671.19106	629.5806	-264.2138	11.4	171.2	170.65	168.9	30.0	-0.92305	36.8	262.9	259.5	56.1
149630	54279.23100	33.9523	93.2975	19.0	256.5	154.72	232.1	110.9	-0.98189	39.8	361.6	327.5	158.6
149630	54286.26316												

**Table 5**  
PHASES Astrometry Measurements

155103	53958.17528	3.0330	65.7742	9.0	169.5	164.61	163.5	45.8	-0.97895	36.1	261.1	251.9	77.6
155103	53978.18708	0.0185	65.9289	25.2	550.8	179.45	550.8	25.8	-0.20511	43.1	729.6	729.6	43.7
155103	54174.52214	-30.8860	59.4502	14.0	431.2	152.71	383.2	198.1	-0.99682	37.7	577.8	513.8	267.0
155103	54215.49147	-36.5327	55.5474	29.2	427.7	167.55	417.6	96.5	-0.95076	45.6	573.4	560.0	131.4
155103	54252.37253	-41.0015	50.9033	29.8	850.3	164.26	818.4	232.5	-0.99107	46.0	1114.2	1072.5	305.5
155103	54300.28308	-44.3879	42.8265	21.4	458.5	174.08	456.0	51.8	-0.90995	41.0	612.3	609.0	75.2
155103	54315.23535	-45.0469	39.8706	11.3	228.7	172.65	226.8	31.3	-0.93204	55.4	328.6	326.0	69.2
155103	54349.15893	-46.2630	32.3331	12.2	264.3	176.56	263.9	20.0	-0.79098	58.1	371.0	370.4	62.1
155103	54670.26295	20.6203	-51.4981	16.5	455.7	172.80	452.1	59.4	-0.96020	38.7	608.7	603.9	85.4
157482	53109.48025	49.6406	-84.4966	7.3	282.5	158.77	263.4	102.5	-0.99707	44.7	393.0	366.7	148.3
157482	53110.48257	48.0945	-84.1334	11.9	600.3	159.53	562.4	210.3	-0.99818	57.2	792.8	743.1	282.4
157482	53123.45846	49.1860	-85.9318	18.1	507.8	162.47	484.3	153.9	-0.99240	77.2	674.8	643.9	216.2
157482	53130.44282	48.4777	-86.4134	6.6	205.8	162.94	196.7	60.7	-0.99360	43.1	302.0	288.9	97.7
157482	53137.43118	48.3928	-87.1396	14.0	280.2	164.34	269.9	76.8	-0.98202	63.7	390.2	376.1	121.9
157482	53144.42500	47.7018	-87.6613	25.1	1039.7	167.13	1013.5	232.9	-0.99386	101.6	1358.8	1324.9	318.5
157482	53145.39616	48.3082	-87.8014	13.7	316.5	161.59	300.4	100.8	-0.98963	62.7	434.6	412.8	149.6
157482	53168.34023	47.0275	-89.7513	15.0	340.0	162.93	325.0	100.8	-0.98777	66.9	463.6	443.7	150.4
157482	53172.35295	47.3440	-90.1337	6.3	170.0	168.29	166.5	35.1	-0.98309	42.4	261.6	256.3	67.4
157482	53173.33276	47.1603	-90.3599	8.0	77.4	33.97	64.4	43.8	0.97548	46.4	172.4	145.3	103.7
157482	53181.33465	46.4333	-90.7858	7.5	174.6	169.71	171.8	32.1	-0.97114	45.1	266.7	262.5	65.1
157482	53182.33238	46.5646	-91.0137	13.9	333.2	169.62	327.7	61.6	-0.97328	63.4	455.2	447.9	103.0
157482	53186.30522	45.6585	-91.1213	18.2	426.5	166.80	415.2	99.0	-0.98196	77.5	571.9	557.0	150.8
157482	53187.30536	46.1426	-91.2225	13.0	441.4	166.94	430.0	100.6	-0.99110	60.5	590.7	575.5	145.9
157482	53197.26925	46.1852	-92.1523	4.8	117.1	164.87	113.0	30.9	-0.98714	39.5	206.8	199.9	66.1
157482	53198.24332	46.2937	-92.2555	5.7	54.6	160.36	51.5	19.1	-0.94837	41.2	157.0	148.5	65.5
157482	53199.29260	44.0251	-91.9446	24.7	1645.4	171.42	1627.0	246.7	-0.99488	100.2	2143.6	2119.7	334.8
157482	53208.25310	46.4304	-92.4901	6.6	181.7	37.67	143.9	111.1	0.99718	43.1	274.6	218.9	171.2
157482	53214.24152	45.6336	-93.3429	5.5	125.9	169.45	123.8	23.7	-0.97194	40.8	215.4	211.9	56.2
157482	53215.23168	45.6364	-93.5172	4.8	110.7	167.53	108.1	24.3	-0.97962	39.5	200.8	196.2	58.0
157482	53221.22283	46.2560	-92.9726	8.8	342.3	38.91	266.4	215.1	0.99860	48.4	466.5	364.3	295.4
157482	53228.21020	45.0884	-94.3310	7.2	100.6	169.45	98.9	19.7	-0.92813	44.4	191.6	188.5	56.0
157482	53229.22147	45.2196	-94.5160	6.4	80.0	172.84	79.4	11.8	-0.83913	42.6	174.4	173.1	47.5
157482	53233.18369	45.0993	-94.8458	6.0	64.7	167.67	63.2	15.0	-0.91188	41.8	163.3	159.8	53.7
157482	53234.20226	44.8269	-94.7637	7.6	37.8	172.74	37.5	8.9	-0.51350	45.4	148.4	147.3	48.8
157482	53235.21839	45.2153	-94.9183	8.5	107.1	176.57	106.9	10.6	-0.60012	47.6	197.4	197.1	49.0
157482	53236.16808	44.4598	-94.8862	4.7	78.1	166.59	76.0	18.7	-0.96551	39.3	172.9	168.5	55.4
157482	53249.16080	44.2467	-95.8032	4.3	87.9	172.71	87.2	12.0	-0.93122	38.6	180.7	179.3	44.7
157482	53466.52339	31.4133	-102.8882	9.9	204.2	163.01	195.3	60.4	-0.98523	51.4	300.1	287.4	100.5
157482	53481.50702	30.4443	-103.3347	11.1	311.1	38.18	244.7	192.5	0.99731	54.8	428.0	338.1	268.0
157482	53494.45379	29.5257	-103.1672	18.6	251.9	163.98	242.2	71.8	-0.96315	78.9	356.1	343.0	124.1
157482	53585.25004	23.9817	-102.6116	10.1	114.7	174.02	114.0	15.6	-0.76046	51.9	204.5	203.5	55.9
157482	53874.42903	1.2460	-88.7776	6.8	99.5	168.07	97.4	21.6	-0.94661	43.5	190.6	186.7	58.0
157482	53956.21473	-5.0781	-81.9131	9.2	341.7	170.23	336.8	58.7	-0.98729	36.2	465.7	459.0	86.7
157482	54216.50608	-22.1555	-45.7120	8.7	202.1	171.22	199.7	32.0	-0.96157	36.1	297.7	294.3	57.8
157482	54217.49399	-23.6355	-49.4281	9.6	162.5	169.30	159.7	31.6	-0.95109	36.3	253.4	249.1	59.0
157482	54222.50033	-28.3453	-48.1186	15.6	453.9	172.74	450.3	59.4	-0.96421	38.3	606.5	601.6	85.5
163840	54229.48700	32.9814	-47.2685	17.1	267.9	168.21	262.2	57.2	-0.95254	39.0	375.4	367.5	85.7
163840	54336.19699	29.6432	-81.4727	17.6	163.5	168.93	160.5	35.8	-0.86590	75.5	254.5	250.2	88.7
163840	54350.16298	28.9940	-84.8398	20.4	327.5	170.79	323.3	56.2	-0.92952	85.1	448.2	442.6	110.4
171779	52808.35348	222.2909	-118.7665	31.3	424.5	105.79	119.4	408.6	-0.96212	124.0	569.3	195.5	548.9
171779	52834.36024	225.6783	-119.4033	20.4	1868.3	175.56	1862.7	145.9	-0.99015	85.1	2432.8	2425.5	206.5
171779	52862.30296	221.9964	-119.4218	5.7	100.4	179.91	100.4	5.7	-0.02887	41.2	191.4	191.4	41.2
171779	52863.28434	222.1970	-119.4295	9.8	127.3	175.62	126.9	13.8	-0.69960	51.1	216.8	216.2	53.6
171779	52864.31303	222.32126	-119.3997	9.5	180.2	4.43	179.6	16.8	0.82539	50.3	272.9	272.1	54.4
171779	52865.30141	221.9020	-119.4603	10.4	117.0	1.66	116.9	11.0	0.30652	52.8	206.7	206.6	53.1
171779	52891.21310	221.9119	-119.7123	13.9	417.5	177.49	417.1	23.0	-0.79584	63.4	560.5	560.0	67.9
171779	52894.23156	221.9503	-119.7423	7.8	234.7	3.92	234.1	17.8	0.89999	45.9	335.7	334.9	51.2
171779	52896.20046	221.6371	-119.6784	6.0	62.7	177.22	62.6	6.7	-0.45030	41.8	162.0	161.8	42.5
171779	52897.22741	222.9335	-119.6507	11.7	348.7	5.15	347.3	33.4	0.93643	56.6	474.4	472.5	70.6
171779	52917.13191	221.1082	-119.9472	4.9	147.1	175.12	146.6	13.4	-0.93027	39.6	237.0	236.2	44.3
171779	52918.16098	221.2135	-119.9961	15.7	937.9	2.98	936.6	51.2	0.95168	69.2	1227.3	1225.6	94.0
171779	52920.14902	221.2713	-120.0294	12.3	408.3	1.61	408.2	16.8	0.68297	58.4	548.9	548.7	60.4
171779	52929.11933	221.3020	-120.0970	4.5	137.1	0.23	137.1	4.6	0.12035	39.0	226.6	226.6	39.0
171779	52930.10995	221.1524	-120.0815	7.2	185.5	178.74	185.5	8.3	-0.49262	44.4	278.8	278.8	44.8
171779	53131.44662	219.4510	-122.5100	19.0	403.5	25.15	365.3	172.4	0.99258	80.2	542.9	492.6	241.9
171779	53168.47198	219.4481	-122.6406	4.1	70.4	1.94	70.3	4.7	0.50092	38.3	167.3	167.2	38.7
171779	53173.33134	219.3735	-122.8492	4.8	116.6	24.98	105.8	49.5	0.99416	39.5	206.3	187.8	94.2
171779	53199.36474	219.6117	-123.0555	9.7	328.0	176.46	327.4	22.5	-0.90134	50.8	448.8	447.9	57.8
171779	53207.24884	219.5253	-123.0926	13.3	462.9	27.06	412.3	210.9	0.99749	61.5	617.8	550.9	286.4
171779	53214.34597	219.1263	-123.1707	3.1	77.3	1.40	77.2	3.7	0.51293	36.9	172.3	172.3	37.2
171779	53236.26985	218.8993	-123.4054	2.5	81.0	177.98	80.9	3.8	-0.75752	36.3	175.2	175.1	

**Table 5**  
PHASES Astrometry Measurements

171779	53930.37774	213.1329	-130.3739	3.2	71.6	0.08	71.6	3.2	0.03067	37.1	168.1	168.1	37.1
171779	53936.35814	213.1750	-130.4222	4.5	110.2	178.59	110.1	5.2	-0.51567	35.3	200.3	200.2	35.6
171779	53937.35615	213.2334	-130.4124	3.6	82.9	178.86	82.9	4.0	-0.41030	37.6	176.7	176.6	37.7
171779	53942.33879	212.8086	-130.4947	9.8	455.0	178.07	454.7	18.2	-0.84189	36.3	607.8	607.5	41.7
171779	53949.32378	213.4291	-130.5064	17.8	1009.2	179.18	1009.1	23.0	-0.62961	39.3	1319.4	1319.3	43.6
171779	53951.31374	212.7836	-130.5483	2.8	47.5	178.39	47.5	3.1	-0.42651	35.1	153.0	153.0	35.4
171779	53956.31011	212.9765	-130.6239	4.9	123.4	0.78	123.4	5.1	0.32578	35.3	212.9	212.9	35.5
171779	53957.28590	212.6294	-130.6101	6.4	398.4	175.46	397.2	32.2	-0.97984	35.6	536.5	534.8	55.3
171779	53958.29026	212.9650	-130.5947	5.2	59.5	176.45	59.4	6.3	-0.57588	35.4	159.9	159.7	36.7
171779	53963.26954	212.7146	-130.6330	24.5	686.3	175.85	684.5	55.4	-0.89612	42.7	903.1	900.7	78.0
171779	53964.26536	213.2967	-130.7210	17.1	480.8	175.35	479.2	42.6	-0.91533	39.0	640.5	638.4	64.8
171779	53965.26415	212.6975	-130.6755	3.2	86.8	175.73	86.6	7.2	-0.89600	35.1	179.8	179.3	37.5
171779	53970.26381	212.9056	-130.7631	3.3	112.3	178.66	112.3	4.2	-0.62001	35.2	202.3	202.2	35.5
171779	53971.25825	212.8738	-130.7368	4.1	110.2	178.54	110.2	5.0	-0.56223	35.2	200.3	200.2	35.6
171779	53979.25553	212.8052	-130.7791	6.5	206.8	2.34	206.6	10.6	0.79376	35.6	303.1	302.9	37.7
171779	53992.19426	212.8410	-130.9400	7.1	89.4	175.99	89.2	9.5	-0.65598	35.7	182.0	181.5	37.8
171779	53993.17934	211.6802	-130.8416	19.3	1407.9	173.68	1399.3	156.3	-0.99225	40.0	1835.6	1824.5	205.9
171779	54003.17235	212.6577	-131.0548	16.8	165.0	177.52	164.8	18.2	-0.38794	38.8	256.1	255.9	40.3
171779	54006.17808	212.6724	-131.1255	3.4	96.4	1.81	96.3	4.6	0.66686	35.2	187.9	187.8	35.6
171779	54007.18032	212.5338	-131.1279	4.4	141.7	2.92	141.5	8.4	0.85380	35.3	231.4	231.1	37.1
171779	54251.49209	210.5304	-133.4152	8.0	209.9	178.19	209.8	10.4	-0.63936	35.9	306.7	306.5	37.2
171779	54252.48964	209.8767	-133.4837	9.2	259.3	178.18	259.1	12.4	-0.66493	36.2	365.0	364.8	38.0
171779	54376.17462	210.2435	-134.6941	9.8	303.1	4.02	302.4	23.4	0.90812	51.1	418.2	417.1	58.8
171779	54728.18950	206.8926	-138.0488	21.6	862.4	179.21	862.3	24.7	-0.48004	41.1	1129.8	1129.7	44.0
171779	54741.17373	205.9022	-138.2655	7.3	172.2	3.69	171.9	13.3	0.83253	35.8	264.0	263.5	39.5
171779	54748.15753	206.6104	-138.2506	9.4	309.9	4.61	308.9	26.6	0.93500	36.2	426.5	425.1	49.8
176051	52865.18946	-716.3549	217.1509	33.2	3587.6	153.57	3212.7	1597.0	-0.99973	130.9	4666.0	4178.7	2080.2
176051	52891.15205	-725.7708	214.5872	38.3	2736.4	160.45	2578.8	916.2	-0.99902	149.7	3560.1	3355.2	1199.6
176051	53109.51640	-764.3662	172.3603	9.2	274.0	153.10	244.4	124.3	-0.99654	49.5	382.7	342.0	178.7
176051	53110.52340	-763.8966	171.9603	20.2	787.2	155.34	715.5	329.0	-0.99772	84.4	1032.9	939.4	437.7
176051	53123.50203	-766.5383	169.5217	13.7	337.0	157.50	311.4	129.6	-0.99348	62.7	459.9	425.6	185.3
176051	53145.43757	-770.5581	165.2904	30.1	1532.4	156.75	1408.0	605.5	-0.99853	119.6	1997.0	1835.5	795.9
176051	53168.38529	-773.5629	160.5122	24.5	609.6	158.86	568.7	221.1	-0.99292	99.5	804.8	751.4	304.7
176051	53172.39036	-774.8076	159.7908	9.3	294.8	161.87	280.2	92.1	-0.99433	49.7	408.0	388.1	135.5
176051	53187.34070	-777.2660	156.8094	8.9	248.8	160.08	233.9	85.2	-0.99387	48.7	352.4	331.8	128.5
176051	53197.36964	-779.0516	154.9404	5.0	36.4	171.53	36.0	7.3	-0.72343	39.8	147.8	146.3	45.0
176051	53198.38049	-779.4953	154.7126	5.6	224.0	175.37	223.2	18.9	-0.95426	41.0	323.1	322.1	48.4
176051	53215.29575	-782.3349	151.3896	3.3	28.7	165.72	27.9	7.8	-0.89815	37.2	144.9	140.7	50.7
176051	53222.32431	-783.3567	149.9677	7.8	395.9	177.60	395.5	18.3	-0.90375	45.9	533.4	532.9	51.0
176051	53228.28183	-784.3775	148.7425	4.9	31.3	170.87	30.9	6.9	-0.69885	39.6	145.8	144.1	45.5
176051	53233.19737	-784.9444	147.7408	13.5	535.9	156.45	491.3	214.5	-0.99764	62.1	710.6	651.9	289.6
176051	53235.29812	-784.4927	147.5957	14.1	627.5	179.93	627.5	14.2	-0.05756	64.0	827.7	827.7	64.0
176051	53242.16492	-786.6680	146.5146	18.0	357.0	25.76	321.6	156.0	0.99173	76.8	484.8	437.9	221.7
176051	53250.20055	-788.5477	144.6414	5.3	33.4	167.11	32.6	9.1	-0.79918	40.4	146.6	143.2	51.2
176051	53251.16205	-788.1705	144.2936	13.6	748.1	159.65	701.4	260.4	-0.99844	62.4	982.6	921.5	346.7
176051	53263.19272	-790.7290	142.0380	7.9	62.7	172.83	62.2	11.1	-0.69416	46.1	162.0	160.8	50.0
176051	53271.17385	-791.8338	140.3757	5.8	59.3	173.45	59.0	8.9	-0.75487	41.4	159.8	158.8	45.0
176051	53481.42532	-824.7575	100.0525	19.6	172.2	6.55	171.1	27.7	0.70016	82.3	264.0	262.5	87.1
176051	53544.44519	-836.0487	86.2634	13.8	106.8	178.40	106.7	14.1	-0.20740	63.0	197.2	197.1	63.3
176051	53551.33624	-837.0295	85.0116	6.8	57.0	157.72	52.8	22.5	-0.94589	43.5	158.4	147.5	72.3
176051	53565.34142	-839.7999	82.3298	29.3	1014.0	167.65	990.6	218.7	-0.99058	116.7	1325.6	1295.2	305.6
176051	53585.30412	-841.6259	78.3693	7.0	41.6	168.17	40.7	10.9	-0.75737	44.0	150.1	147.2	52.9
176051	53599.23162	-844.0472	75.5130	15.9	822.8	164.08	791.3	226.2	-0.99733	69.8	1078.8	1037.6	303.4
176051	53600.24883	-844.2410	75.2877	6.2	39.8	167.20	38.9	10.7	-0.80367	42.2	149.3	145.8	52.8
176051	53607.17364	-845.4474	73.9736	4.5	77.1	156.57	70.8	30.9	-0.98763	39.0	172.2	158.7	77.2
176051	53613.18114	-846.0260	72.6663	12.1	362.8	161.82	344.7	113.8	-0.99374	57.8	492.0	467.8	163.0
176051	53614.17295	-846.2973	72.5875	6.7	182.5	160.40	171.9	61.5	-0.99328	43.3	275.5	259.9	101.0
176051	53639.15941	-850.7464	67.6243	11.0	129.4	170.33	127.6	24.3	-0.88789	54.5	218.9	215.9	65.1
176051	53858.50224	-884.1126	24.0259	12.8	202.7	161.15	191.9	66.6	-0.97934	59.9	298.4	283.1	111.9
176051	53872.43887	-885.9335	21.1953	13.6	244.8	155.54	222.9	102.1	-0.98925	62.4	347.7	317.5	154.8
176051	53873.46821	-885.9209	20.8900	23.2	168.6	162.71	161.1	54.8	-0.89612	94.9	260.1	249.9	119.1
176051	53895.43043	-889.0916	16.3485	10.7	100.8	165.33	97.6	27.5	-0.91632	53.6	191.8	186.0	71.1
176051	53915.38557	-892.7212	12.5358	13.7	114.1	166.41	110.9	29.9	-0.88184	62.7	204.0	198.8	77.6
176051	53922.36301	-893.3954	11.0379	8.3	87.2	168.77	85.6	18.9	-0.89263	47.1	180.1	176.9	58.0
176051	53923.36821	-892.8996	10.8388	25.6	286.8	169.75	282.3	56.9	-0.88924	43.4	398.3	392.0	82.7
176051	53942.29756	-895.8330	7.1329	7.6	179.7	164.73	173.4	47.9	-0.98651	35.8	272.3	262.9	79.6
176051	53956.26896	-897.8470	4.2030	11.3	302.7	166.90	294.8	69.5	-0.98584	36.8	417.7	406.9	101.2
176051	53970.18199	-900.4581	1.4808	11.6	441.3	157.30	407.2	170.6	-0.99727	36.9	590.5	545.0	230.4
176051	53971.17568	-899.9728	1.0645	14.3	435.3	156.27	398.6	175.7	-0.99603	37.8	583.0	533.9	237.1
176051	53977.17968	-901.3281	0.0533	7.2	165.7	160.31	156.0	56.2	-0.99060	35.7	256.9	242.2	92.9
176051	53995.17191	-903.8195	-3.4528	23.0	219.8	168.21</td							

**Table 5**  
PHASES Astrometry Measurements

176051	54300.34759	-945.6096	-64.3333	12.4	263.2	171.49	260.3	40.8	-0.95148	37.1	369.7	365.7	65.9
176051	54315.30463	-946.8404	-67.5020	16.5	314.6	170.89	310.6	52.4	-0.94785	71.8	432.3	427.0	98.5
176051	54320.30936	-948.1228	-68.3782	8.5	149.5	175.48	149.0	14.5	-0.80962	47.6	239.5	238.8	51.1
176051	54336.27158	-950.2820	-71.6059	6.6	127.1	176.69	126.9	9.9	-0.74162	43.1	216.6	216.2	44.8
176051	54343.25058	-950.7254	-73.0148	7.1	157.2	176.16	156.9	12.7	-0.82899	44.2	247.7	247.2	47.1
176051	54348.23686	-951.5093	-74.1000	8.2	154.6	175.66	154.2	14.3	-0.81731	46.9	244.9	244.3	50.3
176051	54350.22324	-951.8030	-74.3261	9.3	154.1	174.08	153.3	18.4	-0.86105	49.7	244.4	243.2	55.5
176051	54357.21302	-952.8741	-75.8207	8.0	187.2	176.55	186.8	13.8	-0.81357	46.4	280.8	280.3	49.3
176051	54376.14606	-954.9497	-79.6896	16.2	480.6	173.99	478.0	52.8	-0.95099	70.8	640.3	636.8	97.2
176051	54377.14482	-955.1633	-79.7522	7.0	121.7	173.41	120.9	15.6	-0.89110	44.0	211.3	209.9	49.9
176051	54383.13838	-955.5471	-80.9643	10.9	289.2	176.14	288.6	22.3	-0.87166	54.2	401.2	400.3	60.5
176051	54671.37080	-991.1354	-137.7092	12.9	223.4	0.29	223.4	13.0	0.08820	37.3	322.4	322.4	37.3
176051	54685.33104	-993.4281	-140.4674	15.4	328.6	179.70	328.6	15.5	-0.11255	38.2	449.5	449.5	38.3
176051	54698.29734	-994.6124	-143.2756	21.0	471.1	0.96	471.1	22.4	0.35095	40.8	628.2	628.1	42.1
176051	54706.27220	-994.4562	-144.6023	16.0	225.3	179.41	225.3	16.2	-0.14317	38.5	324.6	324.6	38.6
187362	53909.36616	-20.1136	-131.3605	10.8	107.6	153.40	96.3	49.2	-0.96914	53.9	197.9	178.6	100.9
187362	53930.34694	-18.6589	-133.4846	15.3	559.1	159.72	524.5	194.3	-0.99649	67.9	740.2	694.7	264.3
187362	53958.21750	-21.2649	-134.0831	32.2	995.3	150.17	863.5	495.9	-0.99720	47.6	1301.4	1129.3	648.7
187362	53964.18964	-18.4896	-136.0483	27.0	662.2	148.42	564.4	347.5	-0.99584	44.2	872.2	743.4	458.3
187362	53972.17329	-18.5223	-136.5315	13.0	343.0	149.56	295.8	174.2	-0.99623	37.3	467.4	403.4	239.0
187362	54006.14033	-17.4188	-139.4907	9.0	194.7	160.75	183.9	64.8	-0.98920	36.1	289.2	273.3	101.3
187362	54008.14292	-17.8290	-139.4114	14.5	387.7	162.47	369.8	117.6	-0.99158	37.9	523.1	498.9	161.6
187362	54336.22798	-7.2546	-163.6643	20.8	121.6	157.15	112.3	51.0	-0.89703	86.4	211.2	197.5	114.3
187362	54341.24525	-7.3695	-163.9836	30.6	987.2	164.92	953.3	258.5	-0.99246	121.4	1291.0	1246.9	355.7
187362	54356.19475	-6.7854	-164.9968	20.7	228.9	163.69	219.8	67.3	-0.94715	86.1	328.9	316.5	123.9
196524	52919.15033	-52.7322	586.2133	15.7	526.6	160.79	497.3	173.9	-0.99544	69.2	698.7	660.2	239.0
196524	53200.34646	-25.0494	585.6767	33.2	568.9	25.92	511.9	250.5	0.98910	130.9	752.7	679.4	349.5
196524	53207.32515	-25.0499	585.3716	14.0	238.4	27.77	211.1	111.8	0.98988	63.7	340.1	302.4	168.2
196524	53214.28543	-24.9518	585.1530	10.9	371.2	149.74	320.7	187.3	-0.99772	54.2	502.5	434.9	257.5
196524	53221.31357	-23.5277	584.9481	6.4	162.6	31.14	139.2	84.2	0.99606	42.6	253.5	218.1	136.1
196524	53234.20413	-22.8423	584.6511	6.8	111.1	146.51	92.7	61.5	-0.99113	43.5	201.1	169.5	116.8
196524	53242.26045	-21.4859	584.4005	12.7	125.2	34.15	103.9	71.1	0.97667	59.6	214.7	180.8	130.2
196524	53250.19842	-21.8239	584.4826	13.1	377.7	151.42	331.7	181.0	-0.99659	60.9	510.6	449.3	250.0
196524	53263.18972	-20.6518	584.1074	8.8	545.8	156.11	499.1	221.2	-0.99905	48.4	723.2	661.5	296.2
196524	53271.15653	-18.4303	583.2751	8.0	286.3	154.14	257.7	125.1	-0.99746	46.4	397.6	358.4	178.4
196524	53284.15401	-17.3960	583.3073	9.1	141.1	33.76	117.4	78.8	0.99034	49.2	230.8	193.8	134.6
196524	53294.15110	-17.0894	582.9895	12.3	286.9	166.14	278.5	69.7	-0.98348	58.4	398.4	387.0	111.0
196524	53508.45604	3.3893	574.5971	17.7	814.7	146.57	680.0	449.1	-0.99888	75.8	1068.3	892.6	591.9
196524	53509.45813	2.4331	575.3321	13.4	488.2	147.44	411.5	263.0	-0.99817	61.8	649.9	548.8	353.6
196524	53551.39533	7.5489	572.2611	7.3	40.0	153.01	35.8	19.3	-0.90692	44.7	149.3	134.6	78.6
196524	53565.33746	9.1612	571.3476	25.4	345.7	148.61	295.4	181.4	-0.98643	102.7	470.7	405.4	260.4
196524	53572.43002	10.2995	571.4202	25.3	591.3	42.84	434.0	402.5	0.99632	102.3	781.3	577.1	536.5
196524	53584.35475	10.9113	570.1280	12.8	87.1	162.71	83.2	28.6	-0.88391	59.9	180.1	172.8	78.3
196524	53586.26593	10.3136	570.4053	7.7	61.4	154.46	55.5	27.4	-0.94981	45.6	161.2	146.7	80.8
196524	53599.20180	13.2131	568.6734	10.1	542.5	145.53	447.3	307.1	-0.99920	51.9	719.0	593.5	409.2
196524	53600.22267	12.5157	569.0969	6.2	64.0	148.22	54.5	34.1	-0.97694	42.2	162.9	140.2	93.0
196524	53606.34340	13.3513	569.0109	7.1	122.4	176.93	122.3	9.6	-0.67791	44.2	211.9	211.7	45.6
196524	53607.34297	13.1690	568.9778	5.9	140.2	177.63	140.1	8.3	-0.69693	41.6	229.8	229.6	42.6
196524	53613.32596	13.4970	568.6135	13.7	281.8	177.57	281.6	18.2	-0.65715	62.7	392.2	391.8	64.8
196524	53614.32379	13.8057	568.5047	10.7	237.1	177.41	236.9	15.1	-0.70819	53.6	338.5	338.2	55.7
196524	53621.20009	14.3445	568.0796	42.6	232.6	30.11	202.3	122.4	0.91643	165.6	333.2	300.0	220.2
196524	53639.21868	16.1788	566.7894	5.3	29.0	169.26	28.5	7.5	-0.69481	40.4	145.0	142.6	48.0
196524	53649.19784	17.2474	566.1405	8.7	53.6	171.31	53.0	11.8	-0.66896	48.1	156.4	154.8	53.1
196524	53655.15772	18.0352	565.7046	12.2	124.4	163.42	119.3	37.4	-0.93988	58.1	213.9	205.7	82.6
196524	53676.11652	19.0929	564.5358	11.6	106.5	167.66	104.1	25.4	-0.88469	56.3	196.9	192.7	69.2
196524	53957.25341	46.1307	541.1888	6.0	212.2	149.99	183.8	106.3	-0.99787	35.5	309.4	268.5	157.7
196524	53972.24316	47.8343	539.5585	5.9	61.4	153.88	55.2	27.5	-0.97100	35.5	161.2	145.5	77.8
196524	53978.26170	47.9166	539.0539	5.3	50.2	161.93	47.7	16.3	-0.94110	35.4	154.5	147.3	58.5
196524	53996.19517	49.3756	537.4114	6.1	179.1	158.12	166.2	67.0	-0.99518	35.5	271.7	252.5	106.5
196524	54004.19705	50.5316	536.5239	9.0	123.1	163.02	117.8	37.0	-0.96727	36.1	212.6	203.6	71.1
196524	54008.20254	50.9299	536.2051	4.7	47.6	166.28	46.2	12.2	-0.91753	35.3	153.1	148.9	49.9
196524	54032.12437	53.3578	533.5132	13.8	86.1	164.70	83.1	26.3	-0.83963	37.6	179.2	173.2	59.6
196524	54037.14931	54.0282	532.9612	9.3	250.6	174.23	249.3	26.9	-0.93734	36.2	354.6	352.8	50.7
196524	54245.44853	72.1388	508.7330	8.9	283.7	147.81	240.2	151.3	-0.99760	36.1	394.5	334.4	212.4
196524	54250.43334	72.6182	508.1093	7.8	336.1	147.64	284.0	180.0	-0.99867	35.9	458.8	388.0	247.4
196524	54251.43698	73.5329	507.3488	9.4	140.3	149.45	120.9	71.8	-0.98827	36.2	229.9	198.9	121.0
196524	54252.42277	73.6944	507.3307	16.0	219.3	147.26	184.7	119.4	-0.98723	38.5	317.6	268.0	174.8
196524	54266.41214	74.9599	505.4144	8.5	108.9	152.83	97.0	50.3	-0.98168	36.0	199.1	177.9	96.4
196524	54272.37663	74.8844	505.0680	6.4	238.9	148.02	202.7	126.6	-0.99825	35.6	340.7	289.6	182.9
196524	54278.34417	75.5951	504.2017	21.2	1711.5	145.35	1408.1	973.1	-0.99965	40.9	2229.4	1834.1	1268.0
196524	54279.42309	75.8577	503.7161	7.6	80.9	163.23							

**Table 5**  
PHASES Astrometry Measurements

196524	54308.28913	77.8873	500.3942	7.8	328.6	149.35	282.7	167.6	-0.99852	35.9	449.5	387.2	231.2
196524	54320.24118	79.0568	498.6158	5.8	196.0	147.34	165.1	105.9	-0.99790	41.4	290.7	245.8	160.7
196524	54341.25708	81.6521	495.3649	4.6	17.6	158.90	16.5	7.7	-0.76593	39.1	141.9	133.1	62.8
196524	54348.24998	82.2682	494.3164	3.9	22.9	160.61	21.6	8.4	-0.87375	38.0	143.1	135.6	59.5
196524	54356.23181	82.7031	493.3491	3.9	24.2	163.29	23.2	7.9	-0.85949	38.0	143.5	137.9	55.0
196524	54363.21162	83.4030	492.4233	17.8	402.7	162.64	384.4	121.3	-0.98811	76.2	541.9	517.7	177.3
196524	54377.20906	84.5719	490.3751	4.9	41.6	170.78	41.1	8.2	-0.79676	39.6	150.1	148.3	45.9
196524	54384.16336	85.2876	489.4183	7.3	51.2	165.73	49.6	14.5	-0.85221	44.7	155.0	150.6	57.7
196524	54385.15314	85.2516	489.2226	6.5	57.8	161.55	54.9	19.3	-0.93502	42.8	158.9	151.3	64.7
196524	54627.40783	105.8214	450.9476	10.1	281.6	148.74	240.7	146.4	-0.99672	36.4	391.9	335.6	205.8
196524	54629.40264	105.5982	450.8387	6.9	230.4	148.83	197.2	119.4	-0.99773	35.7	330.6	283.5	173.8
196524	54653.33660	107.9257	446.4978	8.6	135.0	147.77	114.2	72.3	-0.99007	36.0	224.5	190.9	123.6
196524	54678.25808	109.9239	442.0530	7.1	263.9	147.02	221.5	143.8	-0.99826	35.7	370.5	311.4	203.9
196524	54685.23690	110.1886	440.9976	6.3	255.9	146.54	213.5	141.2	-0.99857	35.6	360.9	301.7	201.2
196524	54695.32872	111.2543	438.7978	14.0	145.7	167.64	142.3	34.0	-0.90750	37.7	235.5	230.2	62.4
196524	54696.23641	111.2657	438.8904	9.4	236.4	150.86	206.6	115.4	-0.99567	36.2	337.7	295.5	167.5
196524	54707.32334	112.5222	436.7090	12.0	232.5	175.65	231.8	21.3	-0.82495	37.0	333.1	332.2	44.7
196524	54713.25461	113.0873	435.5313	5.5	56.7	162.68	54.2	17.7	-0.94600	35.4	158.2	151.4	58.0
196524	54740.14335	114.4883	431.0694	10.8	419.4	155.84	382.7	171.9	-0.99763	36.6	562.9	513.8	232.8
196524	54742.14085	114.5775	430.6359	21.2	1055.0	156.14	964.9	427.1	-0.99853	40.9	1378.6	1260.9	558.9
196524	54749.13151	116.4486	428.8318	37.0	1987.4	158.68	1851.4	723.4	-0.99849	50.9	2587.4	2410.4	941.9
202275	52896.18633	43.1322	28.3062	7.3	73.4	150.12	63.8	37.1	-0.97374	44.7	169.4	148.6	92.9
202275	52897.16089	42.9726	29.2560	6.4	99.7	146.48	83.2	55.3	-0.99049	42.6	190.8	160.8	111.2
202275	52915.20668	46.9137	41.1243	9.2	122.4	163.69	117.5	35.5	-0.96301	49.5	211.9	203.9	76.1
202275	52917.18635	46.8907	42.6174	4.0	71.9	160.61	67.8	24.2	-0.98482	38.2	168.3	159.3	66.5
202275	52918.17605	46.9123	43.3930	6.9	80.3	158.50	74.7	30.1	-0.96946	43.7	174.6	163.3	75.8
202275	52920.20175	46.8784	44.7321	9.7	403.8	166.02	391.9	98.0	-0.99474	50.8	543.3	527.3	140.2
202275	52929.16173	49.5693	50.3719	4.7	87.8	162.42	83.7	26.9	-0.98301	39.3	180.6	172.6	66.2
202275	52930.16500	49.3717	51.1594	14.0	353.4	163.85	339.5	99.2	-0.98921	63.7	480.3	461.7	146.9
202275	52951.10502	53.1315	64.3282	31.5	890.9	163.63	854.8	252.9	-0.99154	124.7	1166.6	1119.9	349.9
202275	53172.44864	30.9086	105.4061	7.1	223.4	153.00	199.0	101.6	-0.99695	44.2	322.4	288.0	151.6
202275	53173.40524	30.6928	104.8851	9.1	165.6	17.94	157.5	51.7	0.98293	49.2	256.8	244.8	91.9
202275	53181.40299	28.0314	101.4540	9.5	413.7	149.29	355.7	211.4	-0.99865	50.3	555.7	478.5	287.1
202275	53182.40362	27.4784	101.1195	7.7	352.2	149.87	304.6	176.9	-0.99874	45.6	478.8	414.7	243.6
202275	53186.40418	25.5096	99.5865	18.2	733.9	151.54	645.2	350.1	-0.99825	77.5	964.3	848.6	464.6
202275	53187.40064	26.2103	98.5359	6.0	214.8	151.72	189.2	101.9	-0.99778	41.8	312.4	275.8	152.5
202275	53197.39934	21.9937	93.8954	4.1	33.4	155.89	30.5	14.1	-0.94769	38.3	146.6	134.7	69.3
202275	53198.37488	21.8510	93.2834	3.9	36.0	152.64	32.0	16.9	-0.96512	38.0	147.6	132.3	75.8
202275	53199.39640	22.2859	92.4201	17.5	782.0	156.61	717.8	310.8	-0.99812	75.1	1026.2	942.3	413.2
202275	53208.32346	17.7858	87.9997	5.2	51.9	20.76	48.6	19.0	0.95683	40.2	155.4	146.0	66.7
202275	53214.34527	15.9121	84.5147	5.9	55.4	154.04	49.9	24.8	-0.96434	41.6	157.4	142.7	78.4
202275	53215.34493	15.4419	83.9798	3.6	34.8	153.85	31.3	15.7	-0.96757	37.6	147.1	133.1	73.1
202275	53221.26852	14.0157	80.9109	3.3	63.3	15.60	61.0	17.3	0.98013	37.2	162.4	156.7	56.5
202275	53222.34771	12.6374	79.9100	4.3	206.5	159.11	192.9	73.7	-0.99806	38.6	302.8	283.2	113.8
202275	53229.30700	10.0093	75.6266	4.4	108.0	154.99	97.9	45.8	-0.99442	38.8	198.3	180.4	90.9
202275	53236.24325	8.2332	70.6560	25.8	960.6	147.94	814.3	510.4	-0.99822	104.1	1256.6	1066.4	672.8
202275	53249.24609	1.7949	62.9850	3.9	50.8	153.48	45.5	22.9	-0.98154	38.0	154.8	139.5	77.0
202275	53251.20507	2.4740	60.8709	14.3	1217.5	148.21	1034.9	641.5	-0.99966	64.6	1588.9	1351.0	838.9
202275	53508.51014	-86.2661	-117.6466	25.7	1872.8	150.49	1630.0	922.7	-0.99949	103.7	2438.7	2122.9	1204.6
202275	53550.41476	-94.5634	-143.7430	33.6	248.4	151.98	219.8	120.4	-0.94901	132.4	352.0	316.9	202.5
202275	53552.39070	-95.1314	-144.7394	10.0	85.5	150.13	74.3	43.5	-0.96433	51.7	178.8	157.1	99.7
202275	53571.33708	-99.1014	-155.5406	9.8	68.1	149.71	59.0	35.4	-0.94763	51.1	165.6	145.3	94.5
202275	53584.32209	-101.4808	-162.5820	10.4	104.4	151.49	91.9	50.7	-0.97257	52.8	195.0	173.2	104.0
202275	53586.30551	-102.0699	-163.5724	13.2	831.4	150.94	726.8	404.0	-0.99930	61.2	1089.8	953.1	532.1
202275	53607.23153	-105.7110	-174.9132	3.2	80.6	148.50	68.8	42.2	-0.99616	37.1	174.9	150.4	96.7
202275	53613.22656	-107.1689	-177.7122	6.7	243.9	150.28	211.8	121.0	-0.99794	43.3	346.6	301.8	175.9
202275	53614.22404	-106.8640	-178.5237	5.9	174.7	150.30	151.8	86.7	-0.99697	41.6	266.8	232.7	137.0
202275	53637.20260	-111.2011	-189.7810	12.3	357.4	157.38	330.0	137.9	-0.99532	58.4	485.3	448.5	194.3
202275	53656.13119	-114.1212	-198.7176	16.3	215.2	154.15	193.8	95.0	-0.98163	71.1	312.8	283.2	150.7
202275	53874.48740	-133.8872	-275.5346	12.3	424.1	147.53	357.9	227.9	-0.99794	58.4	568.8	480.9	309.3
202275	53909.42929	-133.9992	-283.9042	6.1	58.2	152.62	51.8	27.3	-0.96784	42.0	159.1	142.6	82.1
202275	53957.31225	-133.5951	-293.0314	9.0	405.4	154.61	366.3	174.0	-0.99836	36.1	545.3	492.9	236.1
202275	53970.25687	-133.8277	-294.8670	5.7	50.6	153.56	45.3	23.1	-0.96133	35.5	154.7	139.4	75.8
202275	53971.25697	-133.8720	-294.9994	7.3	62.3	152.11	55.1	29.8	-0.96094	35.8	161.7	143.9	82.0
202275	53977.26568	-133.7452	-295.9258	5.3	39.3	157.55	36.4	15.8	-0.93150	35.4	149.0	138.4	65.6
202275	54003.21436	-132.9971	-299.3500	16.7	206.3	161.12	195.3	68.6	-0.96619	38.8	302.5	286.5	104.5
202275	54005.19256	-133.0756	-299.4872	11.6	115.3	157.22	106.4	45.9	-0.96173	36.9	205.1	189.6	86.4
202275	54028.10997	-132.3819	-301.8684	13.3	406.8	153.38	363.7	182.7	-0.99667	37.4	547.1	489.4	247.4
202275	54037.11371	-132.9331	-302.3088	11.0	319.6	159.14	298.7	114.3	-0.99468	36.7	438.4	409.9	159.8
202275	54230.50430	-116.0750	-301.5447	13.1	508.3	146.70	424.9	279.3	-0.99843	37.4	675.5	564.9	372.2
202275	54266.47312	-111.8958	-297.2173	13.2	112.0	158.12	1						

**Table 5**  
PHASES Astrometry Measurements

202275	54383.17856	-95.1820	-275.3360	12.0	337.7	161.87	321.0	105.7	-0.99284	57.5	460.8	438.3	153.4
202275	54389.15740	-93.5380	-274.1005	26.4	260.9	161.04	246.9	88.4	-0.94900	106.3	366.9	348.7	155.9
202275	54627.48303	-43.9409	-188.7326	8.4	227.8	156.57	209.0	90.9	-0.99497	36.0	327.6	300.9	134.4
202275	54629.47795	-43.8838	-187.6002	31.0	797.2	156.50	731.2	319.2	-0.99439	46.8	1045.8	959.2	419.2
202275	54670.36488	-33.8286	-167.4185	16.9	198.7	156.05	181.7	82.1	-0.97445	38.9	293.8	269.0	124.4
202275	54678.29381	-32.6938	-162.8598	15.7	1030.4	147.67	870.7	551.2	-0.99943	38.4	1346.8	1138.2	721.0
202275	54695.22568	-26.8923	-154.9510	17.4	1442.8	144.99	1181.8	827.8	-0.99967	39.1	1880.9	1540.7	1079.6
202275	54698.21273	-27.6502	-152.2701	20.1	1342.1	144.43	1091.8	780.8	-0.99950	40.4	1750.3	1423.9	1018.7
202275	54706.19610	-26.6969	-147.2190	11.1	853.0	145.08	699.4	488.4	-0.99962	36.7	1117.7	916.7	640.5
202275	54707.19017	-25.8258	-147.1529	10.3	663.8	144.75	542.1	383.2	-0.99946	36.5	874.2	714.2	505.4
202275	54741.22082	-15.9349	-128.7799	20.8	2031.7	166.92	1979.0	460.2	-0.99892	40.7	2644.9	2576.3	599.9
202275	54748.19278	-14.0966	-124.6952	9.9	315.6	164.78	304.6	83.4	-0.99238	36.4	433.5	418.4	119.1
202275	54762.15379	-8.3398	-117.0524	29.0	1281.7	164.98	1237.9	333.5	-0.99593	45.5	1672.1	1615.0	435.5
202444	53234.35595	-753.9975	31.7802	12.3	588.3	170.69	580.5	96.0	-0.99147	58.4	777.5	767.3	138.4
202444	53243.26521	-754.0677	29.5872	33.0	1259.1	26.66	1125.4	565.7	0.99786	130.2	1642.8	1469.3	746.2
202444	53250.31241	-753.8386	27.5376	9.5	59.1	165.11	57.2	17.7	-0.83399	50.3	159.7	154.9	63.6
202444	53270.26350	-754.7529	22.3568	14.6	556.6	172.09	551.3	77.9	-0.98183	65.6	737.0	730.0	120.5
202444	53272.24593	-753.7950	21.7361	27.4	1011.7	169.23	993.9	190.9	-0.98926	109.8	1322.6	1299.5	269.7
202444	53285.14592	-753.7582	19.1240	8.4	96.3	25.96	86.6	42.8	0.97592	47.4	187.8	170.1	92.6
202444	53291.15886	-753.7914	16.7714	10.6	82.2	159.82	77.3	30.1	-0.92649	53.4	176.1	166.3	78.7
202444	53312.11074	-753.8118	11.3891	6.3	137.8	164.09	132.6	38.3	-0.98535	42.4	227.4	219.0	74.5
202444	53551.46586	-750.7528	-50.6872	11.0	70.7	165.49	68.5	20.7	-0.83534	54.5	167.5	162.7	67.4
202444	53571.40917	-750.2907	-56.0105	8.8	70.1	171.09	69.3	13.9	-0.76967	48.4	167.0	165.2	54.4
202444	53583.41831	-749.7614	-58.9536	13.6	134.6	175.82	134.3	16.7	-0.58190	62.4	224.1	223.5	64.4
202444	53600.31206	-749.6416	-63.3621	15.3	97.0	162.16	92.4	33.1	-0.87508	67.9	188.4	180.6	86.6
202444	53606.34868	-749.3081	-64.9009	8.0	59.9	171.55	59.3	11.8	-0.73237	46.4	160.2	158.6	51.5
202444	53607.32867	-749.1312	-65.1141	12.6	123.2	167.84	120.5	28.7	-0.89315	59.3	212.7	208.3	73.3
202444	53613.34066	-748.7877	-66.6577	9.3	80.6	175.46	80.4	11.3	-0.55833	49.7	174.9	174.4	51.5
202444	53614.32504	-749.2825	-67.1063	10.7	82.5	171.36	81.6	16.3	-0.74708	53.6	176.4	174.5	59.3
202444	53621.20519	-748.6727	-68.8551	21.0	156.3	18.03	148.8	52.3	0.90666	87.1	246.8	236.2	112.7
202444	53639.26290	-748.5259	-73.6027	11.7	108.9	172.25	107.9	18.7	-0.77459	56.6	199.1	197.4	62.2
202444	53649.23303	-748.0584	-76.2148	13.2	123.3	172.68	122.3	20.4	-0.76012	61.2	212.8	211.2	66.4
202444	53656.17565	-748.0981	-77.9192	22.5	144.2	164.51	139.1	44.2	-0.84924	92.4	234.0	226.8	108.8
202444	53670.19052	-749.2667	-81.3797	14.3	655.5	177.12	654.7	35.9	-0.91688	64.6	863.6	862.5	77.8
202444	53676.17822	-747.4412	-83.1706	14.4	177.5	179.35	177.5	14.6	-0.13800	65.0	269.9	269.9	65.0
202444	53965.36823	-738.0858	-157.9427	12.0	155.3	171.90	153.8	24.9	-0.87269	37.0	245.7	243.3	50.4
202444	53992.32268	-736.9830	-164.7958	22.8	243.0	178.61	242.9	23.5	-0.24912	41.8	345.5	345.4	42.6
202444	54003.28908	-736.6610	-167.7696	11.3	124.8	176.37	124.5	13.8	-0.56853	36.8	214.3	213.9	39.1
202444	54005.28445	-736.4926	-168.3373	22.4	200.9	175.26	200.2	27.8	-0.58950	41.6	296.3	295.3	48.1
202444	54007.24802	-737.9458	-168.5377	25.6	713.1	172.02	706.2	102.2	-0.96750	43.4	937.5	928.5	137.1
202444	54292.47998	-721.5522	-241.3831	17.8	247.0	174.08	245.7	31.0	-0.81763	39.3	350.3	348.4	53.2
202444	54294.48070	-721.1221	-241.8132	19.2	196.6	174.28	195.7	27.3	-0.70958	39.9	291.4	290.0	49.2
202444	54308.47445	-720.7922	-245.4270	19.4	508.3	3.32	507.4	35.3	0.83420	40.0	675.5	674.3	55.9
202444	54320.44499	-719.6565	-248.4346	8.9	207.2	4.73	206.5	19.2	0.88543	48.7	303.6	302.6	54.6
202444	54336.38361	-718.4807	-252.4435	9.5	206.3	0.39	206.3	9.6	0.14705	50.3	296.3	295.3	50.3
202444	54343.39071	-720.3947	-254.5731	20.6	1194.3	6.81	1185.9	143.1	0.98948	85.7	1558.9	1547.9	203.5
202444	54348.35784	-717.7994	-255.5873	12.7	133.4	1.40	133.4	13.1	0.24680	59.6	222.9	222.8	59.8
202444	54356.34408	-716.9435	-257.4669	10.8	229.5	3.71	229.0	18.3	0.80799	53.9	329.6	328.9	57.9
202444	54370.30092	-716.1909	-260.9870	9.3	172.8	2.93	172.6	12.8	0.68784	49.7	264.7	264.4	51.5
202444	54389.24995	-715.2299	-265.7632	13.3	243.4	2.83	243.1	17.9	0.66939	61.5	346.0	345.6	63.7
202444	54685.40356	-693.9389	-338.7618	12.2	270.4	174.93	269.4	26.8	-0.88884	37.1	378.4	376.9	49.8
202444	54748.27591	-690.0880	-354.5028	24.5	731.1	6.05	727.1	80.8	0.95232	42.7	960.7	955.3	109.8
206901	52591.15779	139.4206	-68.9506	22.4	338.6	174.63	337.1	38.7	-0.81429	92.0	461.9	460.0	101.3
206901	52809.42396	176.3281	-52.8096	8.6	357.0	148.20	303.5	188.3	-0.99855	47.9	484.8	412.8	258.7
206901	52834.42978	178.7631	-49.4983	8.3	38.1	158.25	35.5	16.1	-0.83208	47.1	148.5	139.0	70.3
206901	52836.48099	178.2378	-48.6333	13.4	379.5	173.84	377.4	42.8	-0.94915	61.8	512.8	509.9	82.5
206901	52862.26859	179.1249	-46.6475	5.2	49.4	144.90	40.5	28.7	-0.97540	40.2	154.0	128.1	94.5
206901	52864.44008	180.0358	-45.8584	4.9	95.7	1.42	95.7	5.4	0.43467	39.6	187.3	187.2	39.9
206901	52865.26284	180.3062	-45.0074	7.5	116.2	146.66	97.2	64.2	-0.99022	45.1	206.0	173.8	119.3
206901	52868.43221	179.3846	-45.8721	3.5	89.2	2.24	89.1	5.0	0.70400	37.4	181.8	181.7	38.1
206901	52891.31479	180.2397	-42.5409	5.0	18.6	172.30	18.5	5.6	-0.41389	39.8	142.1	140.9	43.8
206901	52893.35685	180.8687	-42.7415	9.0	313.4	0.77	313.4	9.9	0.42163	48.9	430.8	430.8	49.3
206901	52894.34291	181.2303	-42.0470	4.3	37.8	0.66	37.8	4.3	0.10017	38.6	148.4	148.4	38.7
206901	52895.31557	181.5077	-41.4499	5.8	21.5	173.23	21.4	6.3	-0.37133	41.4	142.8	141.9	44.4
206901	52896.29588	180.7689	-41.3583	3.3	11.5	172.05	11.4	3.7	-0.39838	37.2	140.8	139.5	41.7
206901	52897.29256	180.3940	-41.7392	2.9	9.7	171.46	9.6	3.2	-0.41204	36.7	140.6	139.1	41.9
206901	52915.28773	180.4714	-39.4499	5.7	26.1	179.52	26.1	5.7	-0.03695	41.2	144.1	144.0	41.2
206901	52916.29801	179.8881	-39.7949	8.1	329.1	1.79	329.0	13.1	0.78564	46.6	450.2	449.9	48.7
206901	52918.12279	181.2809	-38.7867	9.6	569.7	147.06	478.1	309.9	-0.99931	50.6	753.7	633.2	412.0
206901	52919.29319	181.3655	-38.3084	3.6	91.3	2.52	91.2	5.4	0.74137	37.6	183.5	183.4	38.4
206901	52920.12509	180.8836	-38.2825	11.0	768.0	148.32	653.6	403.					

**Table 5**  
PHASES Astrometry Measurements

206901	53145.46573	168.9519	-7.4875	29.9	2133.0	143.09	1705.5	1281.3	-0.99958	118.9	2776.4	2221.1	1670.1
206901	53152.47126	166.1403	-4.9520	7.3	136.4	146.80	114.2	74.9	-0.99313	44.7	225.9	190.6	129.2
206901	53168.42498	164.7522	-3.8657	14.3	637.2	145.84	527.3	358.0	-0.99884	64.6	840.1	696.1	474.7
206901	53172.46956	162.4897	-2.9051	2.8	27.6	155.52	25.2	11.7	-0.96478	36.6	144.5	132.4	68.5
206901	53173.44613	162.7452	-3.3452	4.3	108.4	21.10	101.1	39.2	0.99311	38.6	198.6	185.8	80.1
206901	53181.41429	162.9372	-0.9773	4.4	55.9	150.65	48.7	27.6	-0.98325	38.8	157.7	138.8	84.4
206901	53182.41243	162.5235	-0.6682	5.5	73.1	150.81	63.9	36.0	-0.98450	40.8	169.2	149.1	89.9
206901	53186.42249	161.7314	-0.6717	6.8	88.9	153.55	79.6	40.1	-0.98173	43.5	181.5	163.7	89.8
206901	53187.40438	162.1818	-0.1174	5.2	75.5	154.17	68.0	33.2	-0.98451	40.2	171.0	154.9	82.8
206901	53197.36675	159.6345	0.5089	3.0	29.9	149.29	25.7	15.5	-0.97505	36.8	145.3	126.3	80.7
206901	53198.39543	160.0522	1.0916	2.4	21.2	156.02	19.4	8.9	-0.95641	36.2	142.7	131.2	66.7
206901	53199.40686	160.6159	1.6193	9.4	177.6	157.43	164.0	68.7	-0.98902	50.0	270.0	250.1	113.5
206901	53200.41612	159.4855	1.7590	7.0	439.9	29.74	382.0	218.3	0.99931	44.0	588.8	511.7	294.5
206901	53207.41539	157.6357	2.4066	7.4	101.4	33.07	85.1	55.7	0.98740	44.9	192.3	163.0	111.5
206901	53208.36952	157.5620	2.1611	5.7	248.5	24.63	225.9	103.7	0.99817	41.2	352.1	320.5	151.4
206901	53215.32976	156.9976	3.2389	3.0	32.1	151.09	28.1	15.7	-0.97571	36.8	146.1	129.1	77.6
206901	53221.39324	156.3876	3.9671	3.2	46.3	35.67	37.7	27.1	0.98965	37.1	152.4	125.7	93.8
206901	53228.30457	155.6000	5.6295	2.7	17.1	155.62	15.6	7.5	-0.91724	36.5	141.8	130.0	67.3
206901	53229.29698	156.0966	6.1881	3.1	22.7	152.91	20.3	10.7	-0.94425	36.9	143.1	128.5	73.0
206901	53233.24583	154.8587	5.5452	9.5	804.5	145.13	660.0	460.0	-0.99969	50.3	1055.2	866.2	604.7
206901	53234.27318	154.9429	6.3996	3.1	20.8	152.93	18.6	9.9	-0.93637	36.9	142.6	128.1	72.7
206901	53235.28320	155.2381	7.0259	3.1	23.5	154.23	21.2	10.6	-0.94743	36.9	143.3	130.0	70.6
206901	53236.24527	154.6529	7.2612	6.2	42.6	150.03	37.1	22.0	-0.94661	42.2	150.6	132.1	83.6
206901	53249.22827	151.8697	8.8392	2.9	42.4	148.88	36.4	22.1	-0.98827	36.7	150.5	130.2	83.9
206901	53270.23356	148.9027	11.8985	7.5	254.2	160.31	239.3	86.0	-0.99575	45.1	358.9	338.2	128.2
206901	53285.23902	145.3551	13.9452	5.0	79.9	37.54	63.4	48.8	0.99161	39.8	174.3	140.3	110.8
206901	53313.11002	142.2376	18.5970	4.1	96.9	159.77	91.0	33.7	-0.99156	38.3	188.3	177.2	74.4
206901	53494.50860	104.6070	43.3686	13.6	645.9	143.23	517.4	386.8	-0.99904	62.4	851.3	682.9	512.0
206901	53586.36546	83.9661	55.9065	2.2	11.5	166.51	11.2	3.4	-0.75101	36.0	140.8	137.2	48.0
206901	53637.29660	71.2325	62.9288	6.3	53.5	173.82	53.2	8.5	-0.66479	42.4	156.3	155.5	45.4
206901	53921.45247	24.8756	86.0577	43.2	10260.1	160.72	9684.6	3388.1	-0.99991	167.8	13338.9	12590.9	4407.1
206901	53963.35933	-9.1868	98.3657	6.2	79.3	165.54	76.8	20.7	-0.95158	35.5	173.9	168.6	55.4
206901	53978.32784	-14.0826	99.4668	2.7	17.6	162.84	16.8	5.8	-0.87053	35.1	141.9	135.9	53.6
206901	53995.24459	-17.0642	101.1075	11.5	514.3	159.38	481.4	181.5	-0.99770	36.8	683.1	639.5	243.0
206901	54003.32693	-22.4853	101.1584	10.9	849.6	3.09	848.3	47.1	0.97274	36.7	1113.3	1111.7	70.3
206901	54008.31169	-21.6045	102.0985	4.6	114.0	2.48	113.9	6.7	0.73343	35.3	203.9	203.7	36.4
206901	54075.12742	-38.5877	107.2121	7.0	183.8	3.06	183.5	12.0	0.81544	35.7	276.9	276.5	38.6
206901	54265.40042	-84.8151	119.9655	8.2	390.0	142.94	311.2	235.1	-0.99904	35.9	526.0	420.3	318.3
206901	54300.44689	-92.7572	122.5645	6.4	195.8	167.80	191.4	41.9	-0.98783	35.6	290.5	284.0	70.6
206901	54350.31082	-104.3619	124.6444	4.1	121.5	167.58	118.7	26.5	-0.98705	38.3	211.1	206.3	58.8
206901	54357.29056	-106.1244	125.6022	6.5	163.6	167.26	159.5	36.6	-0.98337	42.8	254.6	248.5	70.0
206901	54383.21418	-111.9102	126.9752	4.6	113.3	166.17	110.0	27.4	-0.98521	39.1	203.2	197.5	61.7
206901	54679.41161	-172.8035	133.2679	11.4	57.9	168.80	56.8	15.9	-0.68026	36.8	159.0	156.1	47.5
206901	54696.35516	-176.7584	132.9610	11.1	244.3	165.65	236.7	61.5	-0.98236	36.7	347.1	336.4	93.1
206901	54741.24018	-184.2790	134.0046	8.5	307.9	167.71	300.8	66.1	-0.99128	36.0	424.0	414.4	96.9
206901	54748.22201	-186.2535	133.4596	8.3	333.1	168.07	325.9	69.3	-0.99255	36.0	455.1	445.3	100.4
206901	54762.18297	-187.3707	132.5954	15.6	576.8	168.19	564.6	119.1	-0.99100	38.3	762.8	746.7	160.6
207652	53197.45645	-133.8768	81.2102	8.5	381.2	164.04	366.5	105.1	-0.99644	47.6	515.0	495.3	148.8
207652	53208.37830	-132.0981	82.5773	14.0	78.5	25.57	71.0	36.2	0.90366	63.7	173.2	158.7	94.3
207652	53221.37388	-130.3666	84.1157	8.0	123.3	32.79	103.8	67.1	0.99003	46.4	212.8	180.7	121.7
207652	53222.43753	-130.3333	84.2283	6.8	213.4	175.50	212.7	18.1	-0.92544	43.5	310.7	309.8	49.8
207652	53235.38748	-128.1930	85.8001	12.1	241.3	171.68	238.7	36.9	-0.94315	57.8	343.5	340.0	75.8
207652	53242.29037	-127.3840	86.6003	22.3	130.9	24.69	119.3	58.3	0.90756	91.7	220.4	203.8	124.1
207652	53249.33920	-125.9704	87.4362	8.2	198.0	169.28	194.5	37.7	-0.97529	46.9	293.0	288.0	71.3
207652	53263.30482	-124.0721	89.1354	4.1	87.0	170.16	85.8	15.4	-0.96361	38.3	180.0	177.4	48.7
207652	53271.28256	-123.2069	90.1595	8.0	177.9	170.13	175.3	31.5	-0.96623	46.4	270.3	266.5	65.1
207652	53272.27909	-122.4090	90.1623	20.7	479.4	170.13	472.3	84.7	-0.96884	86.1	638.8	629.5	138.5
207652	53284.17716	-121.1109	91.7648	16.9	142.3	26.99	127.0	66.3	0.95840	73.1	232.0	209.4	123.8
207652	53285.17291	-120.8239	91.9257	10.7	117.8	27.12	104.9	54.5	0.97529	53.6	207.5	186.3	106.0
207652	53312.18733	-116.7492	95.0140	4.4	73.2	174.05	72.8	8.8	-0.86435	38.8	169.3	168.4	42.4
207652	53313.18134	-116.8817	95.1509	11.5	220.6	174.15	219.4	25.2	-0.88879	56.0	319.1	317.5	64.5
207652	53340.10789	-113.0726	98.4038	8.9	312.1	174.65	310.7	30.4	-0.95618	48.7	429.2	427.4	62.8
207652	53344.49033	-81.9289	122.1372	9.1	170.7	161.30	161.7	55.4	-0.98479	49.2	262.4	249.0	96.2
207652	53552.42931	-80.9221	123.1689	12.2	72.5	152.49	64.6	35.2	-0.92074	58.1	168.8	152.1	93.4
207652	53578.44813	-77.2454	126.1175	22.5	466.7	171.70	461.8	71.0	-0.94719	92.4	622.7	616.3	128.2
207652	53586.41630	-75.7361	126.9855	6.5	73.2	167.25	71.4	17.4	-0.92283	42.8	169.3	165.4	56.0
207652	53606.31027	-72.4123	129.1602	5.8	39.9	155.80	36.4	17.2	-0.92833	41.4	149.3	137.2	71.9
207652	53607.34935	-72.3787	129.3258	9.9	46.8	164.01	45.1	16.0	-0.76585	51.4	152.6	147.4	64.9
207652	53613.28991	-71.5268	129.9927	15.6	89.2	156.91	82.3	37.8	-0.89401	68.8	181.8	169.4	95.4
207652	53614.27712	-71.1540	130.0019	10.2	87.0	154.18	78.4	39.0	-0.95665	52.2	180.0	163.6	91.4
207652	53620.24356	-70.6217	130.8757	16.1	189.3	153.20	169.2	86.6	-0.97802	70.5	283.1	254.7	142.3
207652	53639.3167												

**Table 5**  
PHASES Astrometry Measurements

207652	53965.26136	-16.5547	167.1254	5.6	74.4	147.81	63.0	39.9	-0.98621	35.4	170.2	145.2	95.5
207652	53970.28910	-15.7220	167.5639	6.7	60.0	155.38	54.6	25.7	-0.95825	35.6	160.3	146.4	74.2
207652	53971.27626	-15.6794	167.7189	12.1	101.1	153.62	90.7	46.2	-0.95635	37.0	192.0	172.8	91.5
207652	53977.27336	-14.5286	168.2311	8.7	427.1	154.19	384.5	186.1	-0.99866	36.1	572.6	515.7	251.4
207652	53979.26824	-13.8536	168.2328	22.9	269.6	153.21	240.9	123.2	-0.97814	41.8	377.4	337.4	174.2
207652	54004.25001	-9.9478	170.7274	16.5	97.8	162.39	93.4	33.5	-0.85688	38.7	189.1	180.6	68.1
207652	54006.21622	-9.3107	170.7578	8.7	242.5	158.12	225.1	90.7	-0.99459	36.1	344.9	320.4	132.8
207652	54055.10631	-2.4938	175.7309	34.6	656.3	164.26	631.7	181.1	-0.98007	49.2	864.6	832.3	239.3
207652	54250.48384	28.5977	193.1474	19.0	563.7	148.52	480.8	294.8	-0.99715	39.8	746.1	636.6	391.1
207652	54273.48711	32.2170	195.0610	14.2	239.3	159.58	224.4	84.6	-0.98380	37.8	341.1	320.0	124.2
207652	54285.42022	33.8562	196.2516	25.5	191.3	153.97	172.3	87.0	-0.94539	43.3	285.4	257.1	131.1
207652	54320.37597	39.5862	198.8974	11.8	282.0	162.62	269.2	85.0	-0.98930	56.9	392.4	374.9	129.2
207652	54321.35550	40.0575	198.8870	8.9	93.2	159.03	87.1	34.4	-0.96069	48.7	185.1	173.8	80.3
207652	54336.36273	42.3585	200.1153	12.0	133.4	167.80	130.5	30.5	-0.91564	57.5	222.9	218.2	73.3
207652	54341.27437	42.9497	200.5359	17.4	133.0	154.87	120.7	58.7	-0.94493	74.8	222.5	203.9	116.2
207652	54349.26104	44.1403	201.2312	16.3	193.1	156.63	177.4	78.0	-0.97378	71.1	287.4	265.4	131.4
207652	54356.27856	45.6029	201.6078	12.8	113.6	162.34	108.3	36.5	-0.93059	59.9	203.5	194.8	84.1
207652	54370.24774	47.9721	202.6525	32.0	824.9	164.25	793.9	226.0	-0.98912	126.5	1081.5	1041.4	317.8
207652	54763.15991	107.5791	228.2302	27.8	212.8	161.68	202.2	71.9	-0.91341	44.7	310.0	294.7	106.3
207652	54769.15275	108.1681	228.6971	11.0	101.6	163.39	97.4	30.9	-0.92795	36.7	192.5	184.7	65.3
214850	52929.30989	-85.7984	40.6140	14.1	313.2	4.20	312.3	26.9	0.85015	64.0	430.6	429.4	71.2
214850	53199.43265	-34.1236	-60.9225	18.3	1390.8	152.99	1239.2	631.8	-0.99947	77.9	1813.5	1616.0	826.5
214850	53214.45293	-28.1837	-63.4211	18.2	87.0	167.02	84.8	26.4	-0.70618	77.5	180.0	176.2	85.7
214850	53222.34762	-26.2844	-68.8409	5.5	74.3	149.26	63.9	38.3	-0.98572	40.8	170.1	147.7	93.7
214850	53228.38604	-21.7678	-65.8955	7.4	36.1	158.04	33.6	15.1	-0.85052	44.9	147.7	138.0	69.2
214850	53234.28734	-18.8760	-66.9964	13.2	441.4	145.20	362.6	252.2	-0.99797	61.2	590.7	486.3	340.8
214850	53249.34575	-11.1521	-69.3863	4.9	28.3	161.40	26.8	10.1	-0.86155	39.6	144.8	137.8	59.5
214850	53251.36251	-9.1149	-65.3152	21.0	417.5	166.81	406.5	97.4	-0.97516	87.1	560.5	546.1	153.5
214850	53263.28708	-4.6554	-70.9525	3.3	18.7	158.58	17.4	7.5	-0.88220	37.2	142.1	133.0	62.4
214850	53271.28405	0.1596	-67.3104	5.0	29.0	162.41	27.7	10.0	-0.85313	39.8	145.0	138.7	58.0
214850	53272.33767	-1.5094	-67.2046	27.1	1013.9	175.25	1010.4	88.2	-0.95126	108.8	1325.5	1321.0	154.3
214850	53284.25772	4.5993	-67.2050	8.7	102.7	36.94	82.3	62.1	0.98459	48.1	193.5	157.3	122.5
214850	53291.23760	9.3687	-73.4842	12.5	103.0	162.27	98.2	33.6	-0.92004	59.0	193.7	185.4	81.5
214850	53313.17667	19.9534	-74.7293	5.7	43.9	163.11	42.1	13.9	-0.90357	41.2	151.2	145.2	59.0
214850	53558.47353	124.7631	-63.1929	30.2	204.3	31.24	175.4	109.1	0.94663	120.0	300.2	264.1	186.5
214850	53572.47237	129.4358	-62.0761	13.5	405.5	37.43	322.1	246.7	0.99762	62.1	545.4	434.8	335.2
214850	53699.12563	171.5710	-47.4356	36.3	1209.6	36.35	974.5	717.5	0.99802	142.3	1578.7	1274.3	942.7
214850	53915.46401	230.5831	-19.3065	8.3	90.2	152.95	80.5	41.7	-0.97488	47.1	182.6	164.0	93.0
214850	53921.47505	231.3387	-18.2154	14.1	142.2	160.22	133.9	49.9	-0.95419	64.0	231.9	219.3	98.9
214850	53922.45053	231.9841	-18.1996	7.8	68.8	154.68	62.3	30.3	-0.95840	45.9	166.1	151.4	82.3
214850	53923.45395	232.2589	-18.0692	14.1	127.2	155.28	115.7	54.7	-0.95888	37.7	216.7	197.4	96.9
214850	53928.45512	234.2969	-17.7839	35.4	428.4	157.15	395.0	169.5	-0.97397	49.8	574.2	529.5	227.7
214850	53972.29694	243.6457	-11.5526	6.4	89.4	150.49	77.8	44.4	-0.98604	35.6	182.0	159.3	94.8
214850	53977.29227	244.6056	-10.7498	4.7	43.1	151.56	37.9	20.9	-0.96752	35.3	150.8	133.7	78.2
214850	53986.25515	246.4636	-9.4808	11.1	218.5	149.77	188.9	110.4	-0.99322	36.7	316.7	274.2	162.6
214850	53991.23821	247.7312	-8.9313	22.0	243.8	150.06	211.6	123.2	-0.97861	41.3	346.5	301.0	176.6
214850	53992.23683	248.4780	-9.1510	33.0	529.7	147.74	448.3	284.1	-0.99056	48.1	702.7	594.8	377.3
214850	53996.23681	248.6310	-8.1911	6.7	233.9	150.67	203.9	114.7	-0.99777	35.6	334.8	292.4	166.9
214850	54004.25476	250.8699	-7.2371	11.0	162.8	157.93	150.9	62.0	-0.98141	36.7	253.8	235.6	101.2
214850	54006.24651	251.4713	-7.0401	6.4	212.7	156.90	195.6	83.6	-0.99650	35.6	309.9	285.4	125.9
214850	54008.22793	251.2939	-6.4971	4.6	60.2	154.51	54.3	26.2	-0.98062	35.3	160.4	145.6	76.0
214850	54009.24001	250.7240	-6.0639	9.6	398.2	157.25	367.3	154.3	-0.99774	36.3	536.3	494.7	210.1
214850	54272.47261	301.4287	29.1132	17.7	474.6	149.76	410.1	239.5	-0.99634	39.2	632.7	546.9	320.4
214850	54278.46198	302.2981	30.0087	30.9	1252.5	150.91	1094.6	609.6	-0.99831	46.7	1634.3	1428.3	795.6
214850	54280.45627	302.5046	30.3333	20.3	870.7	150.78	760.0	425.4	-0.99850	40.5	1140.5	995.6	557.9
214850	54286.48156	303.8200	30.9290	9.3	90.9	157.57	84.1	35.8	-0.95951	36.2	183.2	169.9	77.5
214850	54287.49296	304.8060	30.7331	23.0	359.3	162.08	342.0	112.7	-0.97671	41.9	487.6	464.1	155.2
214850	54299.43856	306.0079	32.5123	27.8	400.2	156.73	367.8	160.1	-0.98201	44.7	538.8	495.3	216.8
214850	54301.41509	306.0451	32.9879	20.3	208.5	153.13	186.2	96.0	-0.97140	40.5	305.1	272.7	142.5
214850	54308.40973	307.0107	34.0340	13.7	244.9	155.35	222.7	102.9	-0.98928	37.6	347.8	316.5	149.0
214850	54315.38540	308.4879	34.7380	15.6	157.0	154.61	142.0	68.8	-0.96822	68.8	247.5	225.5	123.0
214850	54320.38497	309.2132	35.4745	7.1	62.3	156.94	57.4	25.3	-0.95222	44.2	161.7	149.8	75.3
214850	54341.35276	312.6661	38.1674	9.4	86.8	162.07	82.6	28.2	-0.93639	50.0	179.8	171.8	73.0
214850	54349.34561	313.8073	39.2502	7.7	42.1	166.16	40.9	12.5	-0.77680	45.6	150.3	146.4	57.1
214850	54357.29628	315.1705	40.2712	10.0	80.8	159.10	75.6	30.3	-0.93593	51.7	175.0	164.5	78.9
214850	54376.25470	318.2691	42.6486	11.0	85.8	160.95	81.2	29.9	-0.92161	54.5	179.0	170.1	77.9
214850	54385.20924	319.2450	43.9520	18.7	287.0	155.37	261.0	120.8	-0.98546	79.2	398.5	363.7	181.0
214850	54426.10562	324.5429	49.5298	29.4	1245.5	159.16	1164.1	443.9	-0.99748	117.1	1625.2	1519.4	588.4
214850	54713.31324	360.3687	85.7081	29.3	714.0	156.75	656.1	283.2	-0.99366	45.6	938.7	862.7	372.9
214850	54740.27892	362.9611	89.1431	26.8	238.9	167.11	233.0	59.3	-0.88665	44.1	340.7	332.2	87.3
214850	54763.18334	365.2987	91.9101	12.4	89.2	158.63	83.2	34.5					

**Table 5**  
PHASES Astrometry Measurements

221673	52862.41340	549.4289	-59.1585	12.9	714.5	158.14	663.2	266.3	-0.99864	60.2	939.3	872.1	354.2
221673	52863.47102	549.2919	-59.1185	8.6	62.9	169.96	62.0	13.8	-0.77782	47.9	162.1	159.9	55.0
221673	52864.44442	549.2326	-59.0766	2.9	11.3	166.02	11.0	3.9	-0.65394	36.7	140.8	136.9	49.2
221673	52865.38748	548.9158	-58.9585	14.1	147.0	155.01	133.4	63.4	-0.96962	64.0	236.9	216.4	115.7
221673	52867.46329	549.6920	-60.0242	28.4	729.9	120.82	374.7	627.0	-0.99611	113.5	959.1	501.0	825.7
221673	52868.50300	549.1984	-59.2133	4.3	99.4	1.65	99.3	5.1	0.55474	38.6	190.5	190.4	39.0
221673	52891.30989	549.5545	-59.7791	10.7	125.4	154.89	113.6	54.1	-0.97577	53.6	214.9	195.9	103.3
221673	52893.38611	549.5980	-59.6624	5.3	19.6	172.98	19.4	5.8	-0.38275	40.4	142.3	141.3	43.7
221673	52894.33540	548.9453	-59.6509	8.3	29.2	160.27	27.7	12.6	-0.71937	47.1	145.1	137.5	66.1
221673	52895.35912	549.2563	-59.6784	7.6	25.4	173.18	25.2	8.1	-0.33554	45.4	143.8	142.9	48.2
221673	52896.38533	549.3331	-59.6550	3.6	16.6	174.46	16.5	3.9	-0.38760	37.6	141.7	141.0	39.8
221673	52897.34630	549.3711	-59.6767	6.4	23.2	167.02	22.7	8.1	-0.59109	42.6	143.2	139.9	52.5
221673	52915.26425	549.0868	-59.9704	8.0	121.2	157.33	111.9	47.3	-0.98303	46.4	210.8	195.3	91.8
221673	52916.28479	549.2595	-60.0644	4.5	20.7	159.65	19.5	8.3	-0.82134	39.0	142.6	134.3	61.6
221673	52918.35122	549.2852	-60.1093	2.7	17.6	178.08	17.6	2.7	-0.21085	36.5	141.9	141.8	36.8
221673	52919.27980	549.3843	-60.0741	3.6	17.7	162.79	16.9	6.3	-0.79874	37.6	141.9	136.0	55.2
221673	52929.30328	549.3110	-60.3371	5.8	23.7	172.35	23.5	6.6	-0.45239	41.4	143.4	142.2	45.2
221673	52930.29591	549.5447	-60.1763	4.3	21.8	174.57	21.7	4.8	-0.41521	38.6	142.8	142.2	40.8
221673	52951.29151	549.5450	-60.7551	9.4	513.2	4.93	511.3	45.1	0.97768	50.0	681.7	679.2	76.9
221673	52952.18546	549.6621	-60.9652	9.3	351.4	161.84	333.9	109.9	-0.99598	49.7	477.8	454.3	156.2
221673	52979.20973	549.3397	-61.3501	7.1	253.4	4.62	252.6	21.6	0.94347	44.2	357.9	356.8	52.6
221673	52983.09470	549.0704	-61.2782	12.5	352.7	160.94	333.4	115.8	-0.99344	59.0	479.4	453.5	166.2
221673	53173.48472	550.0843	-65.6975	5.1	104.1	12.56	101.6	23.2	0.97442	40.0	194.7	190.3	57.6
221673	53181.47785	550.4844	-65.2139	4.2	92.8	148.47	79.1	48.7	-0.99477	38.5	184.8	158.8	102.1
221673	53182.47712	550.1318	-65.0467	9.8	226.9	148.55	193.6	118.7	-0.99527	51.1	326.5	279.8	175.8
221673	53186.46492	550.5223	-65.2587	11.0	296.4	147.39	249.8	160.0	-0.99669	54.5	410.0	346.6	225.7
221673	53187.47920	550.5175	-65.4077	8.3	171.2	150.63	149.2	84.3	-0.99355	47.1	262.9	230.3	135.3
221673	53197.49019	550.1753	-65.3980	2.0	44.9	157.62	41.6	17.2	-0.99174	35.8	151.7	140.9	66.6
221673	53198.50084	550.1909	-65.4282	2.4	49.6	159.84	46.5	17.2	-0.98895	36.2	154.1	145.2	63.0
221673	53200.43538	550.1017	-66.0207	2.7	11.4	24.06	10.5	5.2	0.83198	36.5	140.8	129.4	66.4
221673	53207.47422	549.9007	-66.2948	6.4	67.2	33.40	56.2	37.4	0.97868	42.6	165.0	139.8	97.6
221673	53208.42692	550.1943	-66.0788	5.4	38.9	22.72	35.9	15.8	0.92842	40.6	148.9	138.2	68.6
221673	53214.47246	550.4298	-65.6234	9.2	290.6	162.94	277.8	85.7	-0.99370	49.5	402.9	385.4	127.3
221673	53215.44040	550.1716	-65.6325	4.2	42.7	157.36	39.5	16.9	-0.96245	38.5	150.6	139.8	68.0
221673	53221.48070	550.0917	-66.5736	5.8	227.5	38.06	179.1	140.3	0.99863	41.4	327.2	258.9	204.3
221673	53228.38579	550.6584	-66.1699	4.6	224.7	152.99	200.2	102.1	-0.99875	39.1	323.9	289.1	151.2
221673	53229.42358	550.2706	-65.9502	3.9	70.7	162.59	67.5	21.5	-0.98183	38.0	167.5	160.2	61.9
221673	53234.46422	550.6167	-66.1891	3.2	14.9	179.37	14.9	3.2	-0.04800	37.1	141.3	141.3	37.1
221673	53235.42219	550.3449	-66.1579	3.8	13.1	161.46	12.4	5.5	-0.68764	37.9	141.0	134.3	57.4
221673	53236.43069	550.4971	-66.2728	6.4	23.9	169.38	23.5	7.7	-0.53396	42.6	143.4	141.2	49.5
221673	53242.31297	550.0230	-66.6882	4.8	23.4	14.35	22.7	7.5	0.74431	39.5	143.3	139.1	52.2
221673	53243.31094	549.7876	-66.7023	6.3	45.9	13.02	44.8	12.0	0.84520	42.4	152.2	148.6	53.7
221673	53249.42642	550.4547	-66.4007	2.2	10.7	171.04	10.6	2.7	-0.58625	36.0	140.7	139.1	41.8
221673	53250.38253	550.5730	-66.5028	4.5	15.3	167.50	14.9	5.5	-0.55162	39.0	141.4	138.3	48.8
221673	53251.45045	549.1802	-66.5891	18.7	812.1	0.52	812.1	20.1	0.36563	79.2	1065.0	1064.9	79.8
221673	53263.35701	550.4810	-66.6103	2.4	9.0	167.99	8.8	3.0	-0.58360	36.2	140.5	137.6	45.9
221673	53270.31676	550.6152	-66.7473	13.8	125.6	157.48	116.2	49.8	-0.95375	63.0	215.1	200.1	100.9
221673	53271.34096	550.6568	-66.7652	2.4	9.8	171.28	9.7	2.8	-0.49347	36.2	140.6	139.1	41.6
221673	53272.35697	550.7969	-66.8644	7.6	55.2	166.25	53.7	15.0	-0.85560	45.4	157.3	153.2	57.8
221673	53284.29576	550.0727	-67.6204	7.6	80.6	34.68	66.4	46.3	0.97970	45.4	174.9	146.1	106.3
221673	53294.19718	551.3057	-67.7952	15.1	899.1	151.47	789.9	429.7	-0.99919	67.2	1177.2	1034.7	565.3
221673	53312.24114	550.4505	-67.4818	1.7	7.9	175.41	7.9	1.8	-0.32459	35.6	140.4	140.0	37.2
221673	53341.16609	551.1716	-68.1655	3.2	19.4	170.58	19.2	4.5	-0.68551	37.1	142.3	140.5	43.3
221673	53557.50429	548.8653	-70.9760	34.7	2311.5	157.60	2137.1	881.4	-0.99909	136.4	3008.2	2781.7	1153.3
221673	53571.46204	551.0010	-72.2548	3.8	22.2	162.32	21.1	7.7	-0.85188	37.9	142.9	136.7	56.4
221673	53605.48331	550.8475	-73.1599	2.3	60.1	0.80	60.1	2.4	0.34815	36.1	160.3	160.3	36.1
221673	53606.47795	550.9714	-73.1236	2.5	68.3	0.20	68.3	2.5	0.09257	36.3	165.8	165.8	36.3
221673	53607.46900	550.7180	-73.1690	2.5	128.8	179.12	128.8	3.2	-0.61707	36.3	218.3	218.2	36.4
221673	53613.46276	550.8423	-73.2931	3.2	81.0	1.08	81.0	3.6	0.42838	37.1	175.2	175.2	37.2
221673	53614.46039	551.1958	-73.2973	4.8	126.8	0.96	126.8	5.3	0.40252	39.5	216.3	216.2	39.6
221673	53620.41852	551.2319	-73.3194	3.2	27.5	177.10	27.4	3.5	-0.39330	37.1	144.5	144.3	37.7
221673	53621.41100	551.3038	-72.9044	29.5	1209.0	41.57	904.7	802.5	0.99879	117.4	1577.9	1183.1	1050.7
221673	53632.28961	551.2917	-73.6416	8.6	155.4	154.09	139.8	68.3	-0.99016	47.9	245.8	222.1	115.7
221673	53636.27235	551.1164	-73.6035	2.6	29.0	152.96	25.8	13.4	-0.97649	36.4	145.0	130.2	73.4
221673	53637.29322	551.2846	-73.6352	5.4	24.2	163.61	23.3	8.6	-0.75819	40.6	143.5	138.1	56.2
221673	53638.33555	551.2646	-73.3866	16.2	808.2	36.98	645.7	486.4	0.99913	70.8	1059.9	847.8	640.1
221673	53648.31722	551.4661	-73.9306	15.7	77.9	171.44	77.0	19.4	-0.57355	69.2	172.8	171.2	73.1
221673	53655.33875	550.7180	-73.9970	5.0	121.1	178.77	121.0	5.7	-0.45936	39.8	210.7	210.6	40.1
221673	53656.33367	552.0201	-74.0009	12.7	386.1	179.79	386.1	12.8	-0.11179	59.6	521.1	521.1	59.6
221673	53712.13247	551.9463	-74.2856	32.7	876.9	37.57	695.2	535.3	0.99703	129.1	1148.5	913.7	707.7
221673	53914.48372	551.8130	-78.5447	3.1	59.6	150.39	51.9	29.6	-0.99269	36.9	160.0	140.3	85.3
221673	53929.43482	551.8314	-78.8102	6.4	84.9	147.91							

**Table 5**  
PHASES Astrometry Measurements

221673	53951.38665	551.7626	-79.1717	4.7	64.3	150.67	56.1	31.7	-0.98519	35.3	163.1	143.2	85.6	
221673	53956.35084	551.7124	-79.1795	5.6	190.3	146.46	158.7	105.3	-0.99795	35.4	284.3	237.7	159.8	
221673	53957.34458	551.6692	-79.1902	5.5	254.3	145.98	210.8	142.3	-0.99890	35.4	359.0	298.2	203.0	
221673	53958.38759	551.8129	-79.2895	3.6	27.8	156.17	25.5	11.7	-0.94184	35.2	144.6	133.0	66.7	
221673	53964.33245	552.1755	-79.5331	19.2	820.2	146.70	685.6	450.7	-0.99870	39.9	1075.4	899.1	591.4	
221673	53965.32670	551.4894	-79.1123	4.9	201.2	146.25	167.3	111.8	-0.99863	35.3	296.7	247.5	167.4	
221673	53986.27129	552.1597	-79.8650	6.3	109.4	146.83	91.6	60.1	-0.99205	35.6	199.6	168.2	113.2	
221673	53991.28888	551.8293	-79.7872	13.9	217.3	151.89	191.7	103.1	-0.98825	37.7	315.3	278.7	152.2	
221673	54005.20826	552.7337	-80.5138	17.9	1173.3	144.70	957.7	678.1	-0.99948	39.3	1531.7	1250.3	885.7	
221673	54007.21609	552.3667	-80.2662	4.8	235.0	146.27	195.5	130.6	-0.99900	35.3	336.1	280.2	188.9	
221673	54029.19479	552.4126	-80.5909	15.0	131.5	152.99	117.3	61.2	-0.96157	38.1	221.0	197.6	105.9	
221673	54279.48952	552.4951	-85.0218	3.8	87.2	151.03	76.3	42.4	-0.99471	35.2	180.1	158.5	92.5	
221673	54285.49505	552.9978	-85.3929	14.1	372.7	154.55	336.6	160.7	-0.99526	37.7	504.3	455.7	219.4	
221673	54300.41432	552.1334	-85.1757	6.4	256.8	147.43	216.4	138.4	-0.99849	35.6	362.0	305.7	197.2	
221673	54350.34574	552.8836	-86.3918	4.3	131.5	159.08	122.8	47.1	-0.99530	38.6	221.0	206.9	86.8	
221673	54376.24276	552.5559	-86.5712	5.1	215.2	153.05	191.8	97.6	-0.99828	40.0	312.8	279.5	146.2	
221673	54653.45217	553.6985	-92.1632	24.0	2079.0	148.10	1765.2	1098.8	-0.99967	42.4	2706.3	2297.7	1430.6	
221673	54678.38762	553.0523	-92.2873	13.4	732.2	148.58	624.9	381.9	-0.99915	37.5	962.1	821.3	502.6	
221673	54741.26504	553.9814	-93.8159	9.9	539.5	157.03	496.7	210.7	-0.99870	36.4	715.2	658.6	281.1	
221673	54748.24700	552.7592	-93.2839	19.0	1071.7	157.43	989.6	411.8	-0.99875	39.8	1400.2	1293.1	538.7	
221673	54762.20752	553.1224	-93.7379	25.2	1864.2	156.99	1715.9	729.1	-0.99929	43.1	2427.5	2234.4	949.7	
221673	54776.17063	554.0054	-94.3155	36.5	391.2	157.92	362.8	150.9	-0.96536	50.6	527.5	489.2	203.7	
222842	54343.42036	-770.8249	139.0081	42.7	1642.4	169.94	1617.2	289.9	-0.98874	166.0	2139.7	2107.0	407.9	
224930	53243.35715	-615.0169	-480.7104	26.0	885.7	21.70	823.0	328.3	0.99637	104.8	1159.9	1078.4	439.8	
224930	53687.21451	-732.3355	-366.6561	22.2	130.1	33.37	109.3	73.9	0.93384	91.3	219.6	190.1	142.8	
224930	53699.10666	-745.6906	-368.9391	18.0	224.3	19.70	211.3	77.5	0.96910	76.8	323.5	305.6	130.8	
224930	54376.37317	-840.3871	-218.3862	26.2	419.5	175.80	418.4	40.3	-0.75862	105.5	563.0	561.6	113.0	

**Note.** — All quantities are in the ICRS 2000.0 reference frame. The uncertainty values presented in Columns 5–10 have not been rescaled, whereas the values in Columns 11–15 have been scaled according to the correction formula presented in Section 4. Column 1 is the star’s HD catalog number. Column 2 is the heliocentric modified Julian date. Columns 3 and 4 is the differential right ascension and declination between A and B, in milli-arcseconds. Columns 5 and 6 are the formal  $1\sigma$  uncertainties in the minor and major axes of the measurement uncertainty ellipse, in micro-arcseconds. Column 7,  $\phi_e$ , is the angle between the major axis of the uncertainty ellipse and the right ascension axis, measured from increasing differential right ascension through increasing differential declination (the position angle of the uncertainty ellipse’s orientation is  $90 - \phi_e$ ); this is to be used with either Columns 5 and 6 or Columns 11 and 12—the uncertainty scaling operates on the ellipse major and minor axes, and thus does not change the ellipse’s rotation angle. Columns 8 and 9 are the projected formal uncertainties in the right ascension and declination axes, in micro-arcseconds, while Column 10 is the covariance between these. Columns 11 and 12 are the rescaled  $1\sigma$  uncertainties in the minor and major axes of the measurement uncertainty ellipse, in micro-arcseconds. Columns 13 and 14 are the projected rescaled uncertainties in the right ascension and declination axes, in micro-arcseconds, while Column 15 is the covariance between these. Column 16 is the number of scans taken during a given night. Column 17 is 1 if the longitudinal dispersion compensator was in use, 0 otherwise. Column 18 is 1 if the autoaligner was in use, 0 otherwise. Column 19 represents the tracking frequency of the phase-referencing camera. Column 20 is 0 if the measurement is consistent with the other measures, 1 if a fringe ambiguity is suspected (the measurement is in error by  $\sim 4$  mas), and 2 if it is a significant outlier but not of the fringe ambiguity variety.